

Augmented balancing weights as linear regression*

David Bruns-Smith Oliver Dukes Avi Feller Elizabeth L. Ogburn
UC Berkeley Ghent Univ. UC Berkeley Johns Hopkins Univ.

June 7, 2024

Abstract

We provide a novel characterization of augmented balancing weights, also known as automatic debiased machine learning (AutoDML). These popular *doubly robust* or *de-biased machine learning* estimators combine outcome modeling with balancing weights — weights that achieve covariate balance directly in lieu of estimating and inverting the propensity score. When the outcome and weighting models are both linear in some (possibly infinite) basis, we show that the augmented estimator is equivalent to a single linear model with coefficients that combine the coefficients from the original outcome model and coefficients from an unpenalized ordinary least squares (OLS) fit on the same data. We see that, under certain choices of regularization parameters, the augmented estimator often collapses to the OLS estimator alone; this occurs for example in a re-analysis of the [LaLonde \(1986\)](#) dataset. We then extend these results to specific choices of outcome and weighting models. We first show that the augmented estimator that uses (kernel) ridge regression for both outcome and weighting models is equivalent to a single, undersmoothed (kernel) ridge regression. This holds numerically in finite samples and lays the groundwork for a novel analysis of undersmoothing and asymptotic rates of convergence. When the weighting model is instead lasso-penalized regression, we give closed-form expressions for special cases and demonstrate a “double selection” property. Our framework opens the black box on this increasingly popular class of estimators, bridges the gap between existing results on the semiparametric efficiency of undersmoothed and doubly robust estimators, and provides new insights into the performance of augmented balancing weights.

*We would like to thank David Arbour, Eli Ben-Michael, Andreas Buja, Alex D’Amour, Skip Hirshberg, Guido Imbens, Apoorva Lal, Mark van der Laan, Whitney Newey, Rahul Singh, Jann Spiess, and Qingyuan Zhao for useful discussion and comments. A.F. and D.B-S. were supported in part by the Institute of Education Sciences, U.S. Department of Education, through Grant R305D200010. The opinions expressed are those of the authors and do not represent the views of the Institute or the U.S. Department of Education. O.D. was supported by NIH grant 579679 and by the FWO grant 1222522N. E.L.O. was supported by ONR grant N000142112820 and by the Simons Institute for Theoretical Computer Science.

1 Introduction

Combining outcome modeling and weighting, as in augmented inverse propensity score weighting (AIPW) and other doubly robust (DR) or double machine learning (DML) estimators, is a core strategy for estimating causal effects using observational data. A growing body of literature finds weights by solving a “balancing weights” optimization problem to estimate weights directly, rather than by first estimating the propensity score and then inverting. DR versions of these estimators are referred to by a number of terms, including *augmented balancing weights* (Athey et al., 2018; Hirshberg and Wager, 2021), *automatic debiased machine learning* (AutoDML; Chernozhukov et al., 2022d), and *generalized regression estimators* (GREG; Deville and Särndal, 1992); see Ben-Michael et al. (2021b) for a review. Moreover, this strategy has been applied to a wide range of linear estimands via the Riesz representation theorem (e.g., Hirshberg and Wager, 2021; Chernozhukov et al., 2022e). In this paper, we consider augmented balancing weights in which the estimators for both the outcome model and the balancing weights are based on penalized linear regressions in some possibly infinite basis; in addition to all high-dimensional linear models, this broad class includes popular nonparametric models such as kernel regression and certain forms of random forests and neural networks.

We first show that, somewhat surprisingly, augmenting any regularized linear outcome regression (the “base learner”) with linear balancing weights is numerically equivalent to a single linear outcome regression applied to the target covariate profile. The resulting coefficients are an affine (and often convex) combination of the base learner model coefficients and unregularized OLS coefficients; the hyperparameter for the balancing weights estimator directly controls the regularization path defining the affine combination. In the extreme case where the weighting hyperparameter is set to zero — which we show can easily occur in practice — the entire procedure is equivalent to estimating a single, unregularized OLS regression.

We specialize these results to ridge and lasso regularization (ℓ_2 and ℓ_∞ balancing, respectively) and show that augmenting an outcome regression estimator with balancing weights generally corresponds to a form of *undersmoothing*. Most notably, we show that an augmented balancing weight estimator that use (kernel) ridge regression for both outcome and weighting models — which we refer to as “double ridge” — collapses to a single, undersmoothed (kernel) ridge regression estimator.

We leverage these results to prove novel *statistical* results for double ridge estimators and to make progress towards practical hyperparameter tuning, which remains an open problem in this area. We first make explicit the connection between asymptotic results for double kernel ridge estimators (e.g., Singh et al., 2020) and prior results on optimal undersmoothing for a single kernel ridge outcome model (e.g., Mou et al., 2023), showing that the latter is also semiparametrically efficient. This generalizes the argument in Robins et al. (2007) that “OLS is doubly robust” to a much broader class of penalized parametric and non-parametric regression estimators. As a complementary analysis, we next adapt existing finite sample error analysis results for single ridge regression (Dobriban and Wager, 2018) to derive the finite-sample-exact bias and variance of double ridge estimators. Using these expressions, we can compute oracle hyperparameters for any given data-generating process.

Finally, we illustrate our results with several numerical examples. We first explore hyperparameter tuning for double ridge regression in an extensive simulation study on 36 data-generating processes, and compare three practical methods to the optimal hyperparameter computed using our finite sample analysis. Surprisingly, asymptotic theory and our simulation results suggest equating the hyperparameters for the outcome and weighting models. We caution against the naive application of hyperparameter tuning based solely on cross-validating the weighting model, forms of which have been suggested previously. This approach can lead to setting the weighting hyperparameter to exactly zero — and therefore recovering standard OLS — even in scenarios where OLS is far from optimal. We emphasize this point by applying our results to the canonical LaLonde (1986) study, highlighting that researchers can inadvertently recover OLS in practice.

Broadly, our results provide important insights into the nexus of causal inference and machine learning. First, these results open the black box on the growing number of methods based on augmented balancing weights and AutoDML — methods that can sometimes be difficult to taxonomize or understand. We show that, under

linearity, these estimators all share an underlying and very simple structure. Our results further highlight that estimation choices for augmented balancing weights can lead to potentially unexpected behavior. At a high level, as causal inference moves towards incorporating machine learning and automation, our work highlights how the traditional lines between weighting and regression-based approaches are becoming increasingly blurred.

Second, our results connect two approaches to “automate” semiparametric causal inference. AutoDML and related methods exploit the fact that we can estimate a Riesz representer without a closed form expression for a wide class of functionals. The estimated Riesz representer then augments a base learner by bias correcting a plug-in estimator of the functional. Older approaches, such as undersmoothing (Goldstein and Messer, 1992; Newey et al., 1998), twicing kernels (Newey et al., 2004), and sieve estimation (Newey, 1994; Shen, 1997), avoid estimation of the Riesz representer, tuning the base learner regression fit such that an additional bias correction is not required. Achieving this optimal tuning in practice has long been a hurdle for the implementation of these methods. Subject to certain conditions, both approaches can yield estimators that are asymptotically efficient. We show that if all required tuning parameters are defined in terms of an ℓ_2 -norm constraint, then these approaches can be numerically identical even in finite samples. We use these equivalences to make progress toward practical hyperparameter selection and find promising directions for new theoretical analysis.

In Section 2 we introduce the problem setup, identification assumptions, and common estimation methods; we also review balancing weights and previous results linking balancing weights to outcome regression models. In Section 3 we present our new numerical results, and in Sections 4 and 5 we cache out the implications for ℓ_2 and ℓ_∞ balancing weights specifically. Building on our numerical results, Section 6 explores both asymptotic and finite sample statistical results for kernel ridge regression. Section 7 illustrates our results with a simulation study and application to canonical data sets. Section 8 offers some other directions for future research. The appendix includes extensive additional technical discussion and extensions.

1.1 Related work

Balancing weights and AutoDML. With deep roots in survey calibration methods and the *generalized regression estimator* (GREG; see Deville and Särndal, 1992; Lumley et al., 2011; Gao et al., 2022), a large and growing causal inference literature uses balancing weights estimation in place of traditional inverse propensity score weighting (IPW). Ben-Michael et al. (2021b) provide a recent review; we discuss specific examples at length in Section 2.3 below. This approach typically balances features of the covariate distributions in the different treatment groups, with the aim of minimising the maximal design-conditional mean squared error of the treatment effect estimator. Of particular interest here are augmented balancing weights estimators that combine balancing weights with outcome regression; see, for example, Athey et al. (2018); Hirshberg and Wager (2021); Ben-Michael et al. (2021c).

A parallel literature in econometrics instead focuses on so-called *automatic* estimation of the Riesz representer, of which IPW are a special case, where “automatic” refers to the fact that we can estimate the Riesz representer without obtaining a closed form expression. Estimating the Riesz representer directly, under the assumption that it is linear in some basis, dates back at least to Robins et al. (2008); see also Robins et al. (2007). The corresponding augmented estimation framework has more recently come to be known as Automatic Debiased Machine Learning, or AutoDML; see, among others, Chernozhukov et al. (2022a), Chernozhukov et al. (2022b), Chernozhukov et al. (2022d), and Chernozhukov et al. (2022e). This approach has also been applied in a range of settings, including to corrupted data (Agarwal and Singh, 2021), to dynamic treatment regimes (Chernozhukov et al., 2022c), and to address noncompliance (Singh et al., 2022). As we discuss in Appendix C.3, the AutoDML approach nearly always employs cross-fitting and is typically motivated by asymptotic properties rather than achieving minimax design-conditional mean squared error.

Numerical equivalences for balancing weights. Many seminal papers highlight connections between weighting approaches, such as balancing weights and IPW, and outcome modeling; see Bruns-Smith and

Feller (2022) for discussion. Most relevant are a series of papers that show numerical equivalences between linear regression and (exact) balancing weights, especially Robins et al. (2007); Kline (2011); Chattopadhyay and Zubizarreta (2021), and between kernel ridge regression and forms of kernel weighting (Kallus, 2020; Hirshberg et al., 2019). We discuss these equivalences at length in Appendix A.4. Finally, as we discuss in Appendix D, there are close connections between balancing weights and Empirical Likelihood (Hellerstein and Imbens, 1999; Newey and Smith, 2004).

2 Problem setup and background

2.1 Setup and motivation

The core results in our paper are numeric equivalences for existing estimation procedures, and as such these results hold absent any causal assumptions or statistical model. Nonetheless, a primary motivation for this work is the task of estimating unobserved counterfactual means in causal inference, as well as estimating the broad class of linear functionals described in Chernozhukov et al. (2018b). We briefly review the corresponding setup, emphasizing that this is purely for interpretation.

2.1.1 Example: Estimating counterfactual means

Let X, Y, Z be random variables defined on $\mathcal{X}, \mathbb{R}, \mathcal{Z}$ with joint probability distribution p . To begin, consider the example of a binary treatment, $\mathcal{Z} = \{0, 1\}$ and covariates X . Define potential or counterfactual outcomes $Y(1)$ and $Y(0)$ under assignment to treatment and control, respectively. Under SUTVA (Rubin, 1980), we observe outcomes $Y = ZY(1) + (1 - Z)Y(0)$. To estimate the average treatment effect, $\mathbb{E}[Y(1) - Y(0)]$, we first estimate the means of the partially observed potential outcomes. We initially focus on estimating $\mathbb{E}[Y(1)]$; a symmetric argument holds for $\mathbb{E}[Y(0)]$.

Let $m(x, z) := \mathbb{E}[Y \mid X = x, Z = z]$ be the *outcome model*, $e(x) := \mathbb{P}[Z = 1 \mid X = x]$ be the *propensity score*, and $\alpha(x, z) = z/e(x)$ be the *inverse propensity score weights* (IPW). Under the additional assumptions of *conditional ignorability*, $Y(1) \perp\!\!\!\perp Z \mid X$, and *overlap*, $\mathbb{E}[\alpha(X, Z)^2] < \infty$, we have that $\mathbb{E}[Y(1)]$ is identified by $\mathbb{E}[m(X, 1)]$, a linear functional of the observed data distribution.

There are three broad strategies for estimating $\mathbb{E}[Y(1)]$. First, the identifying functional above suggests estimating the outcome model, $m(x, 1)$ among those units with $Z = 1$, and plugging this into the *regression functional*, $\mathbb{E}[m(X, 1)]$. Second, the equality $\mathbb{E}[m(X, 1)] = \mathbb{E}[Z/e(X)Y] = \mathbb{E}[\alpha(X, Z)Y]$ suggests estimating the inverse propensity score weights, $\alpha(x, z) = z/e(x)$, and plugging these into the *weighting functional*. Finally, we can combine these two via the *doubly robust functional* (Robins et al., 1994):

$$\mathbb{E}[m(X, 1) + \alpha(X, Z)(Y - m(X, 1))].$$

This functional has the attractive property of being equal to $\mathbb{E}[m(X, 1)]$ even if either one of α or m is replaced with an arbitrary function of X and Z , hence the term “doubly robust.” Doubly robust estimators have been studied extensively in semiparametric theory; note that $m(X, 1) + \alpha(X, Z)(Y - m(X, Z)) - \psi(m)$ coincides with the efficient influence function for $\psi(m)$ under a nonparametric model (see Kennedy, 2022 for a review of the relevant theory). See Chernozhukov et al. (2018a); Kennedy (2022) for recent overviews of the active literature in causal inference and machine learning focused on estimating versions of this functional.

2.1.2 General class of functionals via the Riesz representer

Our results apply well beyond the example above. In particular, they apply to any functional of the form

$$\psi(m) = \mathbb{E}[h(X_i, Z_i, m)], \tag{1}$$

where \mathcal{Z} is an arbitrary set; Z a random variable with support \mathcal{Z} ; and h is a real-valued, mean-squared continuous linear functional of m (Chernozhukov et al., 2018b; Hirshberg and Wager, 2021; Chernozhukov

et al., 2022d). Following Chernozhukov et al. (2022d,e), we can generalize the weighting functional to this general class of estimands via the *Riesz representer*, which is a function $\alpha(X, Z) \in L_2(p)$ such that, for all square-integrable functions $f \in L_2(p)$:

$$\mathbb{E}[h(X, Z, f)] = \mathbb{E}[\alpha(X, Z)f(X, Z)]. \quad (2)$$

As in the counterfactual mean example, we can identify the more general target functional in (2) via the outcome regression functional in (1), via the Riesz representer functional in (2) with $f = m$, or via the doubly robust functional

$$\mathbb{E}[h(X, Z, m) + \alpha(X, Z)(Y - m(X, Z))]. \quad (3)$$

Estimators of this DR functional are *augmented* in the sense that they augment the “plug-in,” “outcome regression,” or “base learner” estimator of $\mathbb{E}[h(X, Z, m)]$ with appropriately weighted residuals; or, equivalently, that augment the weighting estimator with an appropriate outcome regression. This is the class of estimators to which our results apply. Doubly robust estimators have been studied extensively in semiparametric theory. In particular, $h(X, Z, m) + \alpha(X, Z)(Y - m(X, Z)) - \psi(m)$ coincides with the efficient influence function for $\psi(m)$ under a nonparametric model (see Kennedy, 2022 for a review of the relevant theory). In future work we will explore whether we can extend our results to a different class of functionals that admit DR functional forms, first introduced by Robins et al. (2008), and to the superset of such functionals characterized by Rotnitzky et al. (2021).

2.2 Balancing weights: Background and general form

The core idea behind balancing weights is to estimate the Riesz representer directly — rather than via an analytic functional form (e.g., by estimating the propensity score and inverting it). As a result, balancing weights do not require a known analytic form for the Riesz representer (Chernozhukov et al., 2022e), are often much more stable (Zubizarreta, 2015), and offer improved control of finite sample covariate imbalance (Zhao, 2019). We briefly describe two primary motivations for this approach.

First, a central property of the Riesz representer is that the corresponding weights, $w(X, Z) = \alpha(X, Z)$, are the unique weights that satisfy the *population balance property* property in Equation (2) for all square-integrable functions $f \in L_2(p)$. For our target estimand $\psi(m)$ we only need to satisfy the condition in Equation (2) for the special case of $f = m$. If we are willing to assume that m lies in a model class $\mathcal{F} \subset L_2(p)$, then it suffices to balance functions in that class. This is achieved by minimizing the imbalance over \mathcal{F} :

$$\text{Imbalance}_{\mathcal{F}}(w) := \sup_{f \in \mathcal{F}} \left\{ \mathbb{E}[w(X, Z)f(X, Z)] - \mathbb{E}[h(X, Z, f)] \right\}. \quad (4)$$

As we discuss next, balancing weights minimize a (penalized) sample analog of Equation (4).

Alternatively, Chernozhukov et al. (2022d) consider finding weights f that minimize the mean-squared error for $\alpha(X, Z)$:

$$\min_{f \in \mathcal{F}} \left\{ \mathbb{E} \left[(f(X, Z) - \alpha(X, Z))^2 \right] \right\}. \quad (5)$$

Automatic estimation of the Riesz representer, also known as *Riesz regression* (Chernozhukov et al., 2024), minimizes a sample analog of Equation (5). When \mathcal{F} is convex, then up to choice of hyperparameters (see (6) below), the solutions to Equations (4) and (5) are equivalent.

2.3 Linear balancing weights

In this paper, we consider the special case in which the outcome models are linear in some basis expansion of X and Z . This is an extremely broad class that encompasses linear and polynomial models of arbitrary

functions of X and Z and with dimension possibly larger than the sample size, as well as non-parametric models such as reproducing kernel Hilbert spaces (RKHSs; [Gretton et al., 2012](#)), the Highly-Adaptive Lasso ([Benkeser and Van Der Laan, 2016](#)), the neural tangent kernel space of infinite-width neural networks ([Jacot et al., 2018](#)), and “honest” random forests ([Agarwal et al., 2022](#)). However, this class excludes models for m that are fundamentally non-linear in their parameters, like general neural networks or generalized linear models with a non-linear link function. We extend our results to arbitrary nonlinear balancing weights in [Appendix D](#).

Under linearity, the imbalance over all $f \in \mathcal{F}$ has a simple closed form. Because our results concern numeric equivalences, we will focus on the finite sample version of the linear balancing weights problem. Let $\mathcal{F} = \{f(x, z) = \theta^\top \phi(x, z) : \|\theta\| \leq 1\}$ where $\|\cdot\|$ can be any norm on \mathbb{R}^d . The general setup constrains $\|\theta\| \leq r$; we set $r = 1$ without loss of generality, which simplifies exposition below. Let $\|\cdot\|_*$ be the *dual norm* of $\|\cdot\|$; that is, $\|v\|_* := \sup_{\|u\| \leq 1} u^\top v$. Many common vector norms have familiar, closed-form, dual norms, e.g., the dual norm of the ℓ_2 -norm is the ℓ_2 -norm; and the dual norm of the ℓ_1 -norm is the ℓ_∞ -norm. Let X_p, Y_p, Z_p be n i.i.d. samples from the distribution p of the observed data. Define the feature map $\phi : \mathcal{X} \times \mathcal{Z} \rightarrow \mathbb{R}^d$ and let $\phi_j : \mathcal{X} \times \mathcal{Z} \rightarrow \mathbb{R}$ denote the mapping for the j th feature. Define $\Phi_p := \phi(X_p, Z_p)$ and let $\Phi_q := h(X_p, Z_p, \phi)$ denote the *target features*. We will write $\hat{\mathbb{E}}$ for sample averages; define $\bar{\Phi}_p := \hat{\mathbb{E}}[\Phi_p]$ and $\bar{\Phi}_q := \hat{\mathbb{E}}[\Phi_q]$. For exposition, we assume that $d < n$ and that Φ_p has rank d . We emphasize that this is not necessary for our results — one can replace \mathbb{R}^d with an infinite-dimensional Hilbert space \mathcal{H} and relax the rank restriction. See [Appendix B](#) for a formal presentation of the high-dimensional ($d > n$) setting.

In what follows we write w for the $1 \times n$ vector $w(\Phi_p)$, to highlight the fact that we will estimate w directly rather than as an explicit function of X or Φ_p . Using the derivation above, we can directly calculate the finite sample imbalance as:

$$\widehat{\text{Imbalance}}_{\mathcal{F}}(w) = \|\frac{1}{n}w\Phi_p - \bar{\Phi}_q\|_*.$$

Now we can write the penalized sample analog of balancing weights optimization problem in [\(4\)](#) equivalently as either:

$$\begin{aligned} \text{Penalized form:} \quad & \min_{w \in \mathbb{R}^n} \left\{ \|\frac{1}{n}w\Phi_p - \bar{\Phi}_q\|_*^2 + \delta_1 \|w\|_2^2 \right\} \\ \text{Constrained form:} \quad & \min_{w \in \mathbb{R}^n} \|w\|_2^2 \\ & \text{such that } \|\frac{1}{n}w\Phi_p - \bar{\Phi}_q\|_* \leq \delta_2. \end{aligned}$$

Furthermore, we can write the equivalent problem in [\(5\)](#) as:

$$\text{Riesz regression form:} \quad \min_{\theta \in \mathbb{R}^d} \left\{ \frac{1}{n}\theta^\top (\Phi_p^\top \Phi_p)\theta - \frac{1}{n}2\theta^\top \bar{\Phi}_q + \delta_3 \|\theta\| \right\}, \quad (6)$$

where we use the terminology “Riesz regression” from [Chernozhukov et al. \(2024\)](#). For any parameter $\delta_2 > 0$ and corresponding constrained problem solution \hat{w} , there exists a parameter $\delta_3 > 0$ such that $\hat{w} = \delta_3 \Phi_p \hat{\theta}$, where $\hat{\theta}$ is the solution to the Riesz regression form. As a result, for any norm $\|\cdot\|$, the penalized and constrained forms will always produce weights that are linear in Φ_p (see [Ben-Michael et al., 2021b](#), Section 9). Therefore, since the problems are equivalent, we typically use a generic δ to denote the regularization parameter, and will specify the particular form only if necessary. In [Appendix A.2](#) we illustrate several concrete examples for this problem and in [Appendix D](#) we consider alternative dispersion parameters and discuss popular forms of balancing that constrain the weights to be non-negative.

Remark 1 (Intercept). *An important constraint in practice is to normalize the weights, $\frac{1}{n} \sum_{i=1}^n w_i = 1$. This corresponds to replacing Φ_p and Φ_q with their centered forms, $\Phi_p - \bar{\Phi}_p$ and $\Phi_q - \bar{\Phi}_p$, in the dual form of the balancing weights problem. This is also equivalent to adding a column of 1s to Φ_p . Appropriately accounting for this normalization, however, unnecessarily complicates the notation. Therefore, without loss of generality, we will assume that the features are centered throughout, that is, $\bar{\Phi}_p = 0$.*

Remark 2 (Equivalence with kernel ridge regression). *For the special case of ℓ_2 balancing (as in Appendix A.2) the balancing weights problem is numerically equivalent to directly estimating the conditional expectation $\mathbb{E}[Y_p|\Phi_p]$ via (kernel) ridge regression and applying the estimated coefficients to $\bar{\Phi}_q$. Moreover, the solution to the balancing weights problem has a closed form that is always linear in $\bar{\Phi}_q$; we provide further details in Appendix A.4. For exact balance with $\delta = 0$, the balancing weights problem is equivalent to fitting unregularized OLS; see, for example, [Robins et al. \(2007\)](#), [Kline \(2011\)](#), and [Chattopadhyay et al. \(2020\)](#).*

3 Novel equivalence results for (augmented) balancing weights and outcome regression models

Our first main result demonstrates that *any* linear balancing weights estimator is equivalent to applying OLS to the re-weighted features. Our second result provides a novel analysis of augmented balancing weights, demonstrating that augmenting any linear balancing weights estimator with a linear outcome regression estimator is equivalent to a plug-in estimator of a new linear model with coefficients that are a weighted combination of estimated OLS coefficients and the coefficients of the original linear outcome model.

3.1 Weighting alone

Our first result is that estimating $\psi(m)$ with any linear balancing weights is equivalent to fitting OLS for the regression of Y_p on Φ_p and then applying those coefficients to the re-weighted target feature profile. The key idea for this result begins with the simple unregularized regression prediction for $\psi(m)$, $\bar{\Phi}_q \hat{\beta}_{ols}$.

Proposition 3.1. *Let $\hat{w}^\delta := \hat{\theta}^\delta \Phi_p^\top$, $\hat{\theta}^\delta \in \mathbb{R}^d$, be any linear balancing weights, with corresponding weighted features $\hat{\Phi}_q^\delta := \frac{1}{n} \hat{w}^\delta \Phi_p$. Let $\hat{\beta}_{ols} = (\Phi_p^\top \Phi_p)^\dagger \Phi_p^\top Y_p$ be the OLS coefficients of the regression of Y_p on Φ_p . Then:*

$$\begin{aligned} \hat{\mathbb{E}}[\hat{w}^\delta \circ Y_p] &= \hat{\Phi}_q^\delta \hat{\beta}_{ols} \\ &= (\bar{\Phi}_p + \hat{\Delta}^\delta) \hat{\beta}_{ols}, \end{aligned}$$

where $\hat{\Delta}^\delta = \hat{\Phi}_q^\delta - \bar{\Phi}_p$ is the mean feature shift implied by the balancing weights and where superscript δ indicates possible dependence on a hyperparameter. We have assumed without loss of generality that $\bar{\Phi}_p = 0$, but we sometimes use $\hat{\Delta}$ notation to demonstrate the role of mean feature shift in various expressions. We use the symbol \circ to denote element-wise multiplication.

Note that here we have written the OLS coefficients using the pseudo-inverse \dagger . For clarity in the main text, we focus on the full rank setting, where $(\Phi_p^\top \Phi_p)^\dagger = (\Phi_p^\top \Phi_p)^{-1}$; we provide a proof for the general setting in Appendix B.3. In Appendix D, we extend Proposition 3.1 to non-linear balancing weights, including those with a non-negativity constraint.

We can interpret this result via a contrast with standard regularization. Regularized regression models navigate a bias-variance trade-off by regularizing estimated coefficients $\hat{\beta}_{reg}$ relative to $\hat{\beta}_{ols}$, leading to $\bar{\Phi}_q \hat{\beta}_{reg}$. The balancing weights approach instead keeps $\hat{\beta}_{ols}$ fixed and regularizes the target feature distribution by penalizing the implied feature shift, $\hat{\Delta}^\delta = \hat{\Phi}_q^\delta - \bar{\Phi}_p$.

We emphasize that this is a new and quite general result. As we discuss in Appendix A.4, it has been shown previously that for exact balancing weights, $\hat{\mathbb{E}}[\hat{w}_{\text{exact}} Y_p] = \bar{\Phi}_q \hat{\beta}_{ols}$. However, Proposition 3.1 holds for any weights of the form $w = \theta \Phi_p^\top$ with arbitrary $\theta \in \mathbb{R}^d$. In Sections 4 and 5, we consider the particular form of $\hat{\Phi}_q^\delta$ for ℓ_2 and ℓ_∞ balancing, respectively.

3.2 Augmented balancing weights

We can immediately extend this to augmented balancing weights, which regularize *both* the coefficients and the feature shift. Let $\hat{\beta}_{\text{reg}}^\lambda$ be the coefficients of any regularized linear model for the relationship between Y_p and Φ_p , where the superscript λ indicates dependence on a hyperparameter (e.g., estimated by regularized least squares). We consider augmenting $\hat{\mathbb{E}}[\hat{w}^\delta \circ Y_p]$ with $\hat{\beta}_{\text{reg}}^\lambda$ using the doubly robust functional representation in Equation (3). The augmented estimator is:

$$\hat{\mathbb{E}}[\Phi_q \hat{\beta}_{\text{reg}}^\lambda] + \hat{\mathbb{E}}[\hat{w}^\delta \circ (Y_p - \Phi_p \hat{\beta}_{\text{reg}}^\lambda)] = \hat{\mathbb{E}}[\hat{w}^\delta \circ Y_p] + \hat{\mathbb{E}}\left[\left(\Phi_q - \hat{\Phi}_q^\delta\right) \hat{\beta}_{\text{reg}}^\lambda\right]. \quad (7)$$

Many recently proposed estimators have this form; see e.g., [Athey et al. \(2018\)](#); [Ben-Michael et al. \(2021b\)](#). If the weighting model and outcome model have different bases, our result applies to a shared basis by either combining the dictionaries as in [Chernozhukov et al. \(2022d\)](#) or by applying an appropriate projection as in [Hirshberg and Wager \(2021\)](#).

We apply Proposition 3.1 to the first term of the right-hand side of (7) to yield the following result. As this result is purely numerical, it applies to arbitrary vectors $\hat{\beta}_{\text{reg}}^\lambda \in \mathbb{R}^d$, but substantively we think of $\hat{\beta}_{\text{reg}}^\lambda$ as the estimated coefficients from an outcome model.

Proposition 3.2. *For any $\hat{\beta}_{\text{reg}}^\lambda \in \mathbb{R}^d$, and any linear balancing weights estimator with estimated coefficients $\hat{\theta}^\delta \in \mathbb{R}^d$, and with $\hat{w}^\delta := \hat{\theta}^\delta \Phi_p^\top$ and $\hat{\Phi}_q^\delta := \frac{1}{n} \hat{w}^\delta \Phi_p$, the resulting augmented estimator*

$$\begin{aligned} & \hat{\mathbb{E}}[\hat{w}^\delta \circ Y_p] + \hat{\mathbb{E}}\left[\left(\Phi_q - \hat{\Phi}_q^\delta\right) \hat{\beta}_{\text{reg}}^\lambda\right] \\ &= \hat{\mathbb{E}}\left[\hat{\Phi}_q^\delta \hat{\beta}_{\text{ols}} + \left(\Phi_q - \hat{\Phi}_q^\delta\right) \hat{\beta}_{\text{reg}}^\lambda\right] \\ &= \hat{\mathbb{E}}[\Phi_q \hat{\beta}_{\text{aug}}], \end{aligned}$$

where the j th element of $\hat{\beta}_{\text{aug}}$ is:

$$\begin{aligned} \hat{\beta}_{\text{aug},j} &:= (1 - a_j^\delta) \hat{\beta}_{\text{reg},j}^\lambda + a_j^\delta \hat{\beta}_{\text{ols},j} \\ a_j^\delta &:= \frac{\hat{\Delta}_j^\delta}{\Delta_j}, \end{aligned}$$

where $\Delta_j = \bar{\Phi}_{q,j} - \bar{\Phi}_{p,j}$ is the observed mean feature shift for feature j ; and $\hat{\Delta}_j^\delta = \hat{\Phi}_{q,j}^\delta - \bar{\Phi}_{p,j}$ is the feature shift for feature j implied by the balancing weights model. Finally, $a^\delta \in [0, 1]^d$ when the covariance matrix is diagonal, $(\Phi_p^\top \Phi_p) = \text{diag}(\sigma_1^2, \sigma_2^2, \dots, \sigma_d^2)$, with $\sigma_j^2 > 0$.

This is our central numerical result for augmented balancing weights: when both the outcome and weighting models are linear, the augmented estimator is equivalent to a linear model applied to the target features Φ_q , with coefficients that are element-wise affine combinations of the base learner coefficients, $\hat{\beta}_{\text{reg}}^\lambda$, and the coefficients $\hat{\beta}_{\text{ols}}$ from an OLS regression of Y_p on Φ_p . (The coefficients are additionally *convex* combinations of $\hat{\beta}_{\text{reg}}^\lambda$ and $\hat{\beta}_{\text{ols}}$ when the covariance matrix is diagonal.) In Sections 4 and 5 below, we analyze some of the properties of the augmented estimator for ℓ_2 and ℓ_∞ balancing weights problems respectively.

The regularization parameter for the balancing weights problem, δ , parameterizes the path between $\hat{\beta}_{\text{reg}}^\lambda$ and $\hat{\beta}_{\text{ols}}$. To see this, consider the cases where $\delta \rightarrow 0$ and $\delta \rightarrow \infty$. As $\delta \rightarrow 0$ the balancing weights problem prioritizes minimizing balance over controlling variance, and $\hat{\Delta}_j^\delta \rightarrow \Delta_j$ for all j . (Recall that we assume $\bar{\Phi}_{p,j} = 0$ for all j . Thus, $\Delta_j = \bar{\Phi}_{q,j}$ and $\hat{\Delta}_j^\delta = \hat{\Phi}_{q,j}^\delta$. So $\hat{\Delta}_j^\delta \rightarrow \Delta_j$ is equivalent to $\hat{\Phi}_q^\delta \rightarrow \bar{\Phi}_{q,j}$.) In this case, $a_j^\delta = \hat{\Delta}_j^\delta / \Delta_j \rightarrow 1$, and the weights fully “de-bias” the original outcome model by recovering unregularized regression, $\hat{\beta}_{\text{aug}} \rightarrow \hat{\beta}_{\text{ols}}$. In Section 7.2, we will see that when chosen by cross-validation, δ sometimes equals exactly 0 in applied problems; thus even when $\hat{\beta}_{\text{reg}}^\lambda$ is a sophisticated regularized estimator, the final

augmented point estimate can nonetheless be numerically equivalent to the simple OLS plug-in estimate. Conversely, as $\delta \rightarrow \infty$, the balancing weights problem prioritizes controlling variance, leading to uniform weights and $\hat{\Delta}_j \rightarrow 0$. In this case, $a_j^\delta = \hat{\Delta}_j^\delta / \Delta_j \rightarrow 0$, the weighting model does very little, and $\hat{\beta}_{\text{aug}} \rightarrow \hat{\beta}_{\text{reg}}^\lambda$.

It is also instructive to consider two other extremes: unregularized outcome model and unregularized balancing weights. First, consider the special case of fitting an unregularized linear regression outcome model, i.e., $\hat{\beta}_{\text{reg}}^\lambda = \hat{\beta}_{\text{ols}}$. Then Proposition 3.2 reproduces the result, originally due to Robins et al. (2007), that ‘‘OLS is doubly robust’’ (see also Kline, 2011). This is because $\hat{\beta}_{\text{aug}} = \hat{\beta}_{\text{ols}}$ for arbitrary linear weights $\hat{\theta}^\delta \in \mathbb{R}^d$. Thus, OLS augmented by *any* choice of linear balancing weights collapses to OLS alone. Equivalently, we can view OLS alone as an augmented estimator that combines an OLS base learner with linear balancing weights.

A similar result holds for unregularized balancing weights, i.e., exact balancing weights. Let \hat{w}_{exact} be the solution to a balancing weights problem in Section 2.3 with hyperparameter $\delta = 0$, and let $\hat{\beta}_{\text{reg}}^\lambda \in \mathbb{R}^d$ be arbitrary coefficients. Then from the balance condition, $\hat{\Phi}_q = \bar{\Phi}_q$, $a_j^\delta = 1$ for all j , and we have that $\hat{\beta}_{\text{aug}} = \hat{\beta}_{\text{ols}}$. Thus, the augmented exact balancing weights estimator also collapses to the OLS regression estimator. Equivalently, the augmented exact balancing weights estimator collapses to the *unaugmented* exact balancing weights estimator. Zhao and Percival (2017) use a very similar result to argue that entropy balancing, a form of exact balancing weights, is doubly robust.

Finally, before we turn to new results for ℓ_2 and ℓ_∞ balancing, we briefly comment on several points that are discussed in more detail in the Appendix.

Remark 3 (Sample splitting). *Sample splitting is a common technique in the AutoDML literature especially, in which we only apply the outcome and weighting models to data points not used for estimation; see, for example, Newey and Robins (2018); Chernozhukov et al. (2022d). Since Proposition 3.2 holds for arbitrary vectors $\hat{\beta}_{\text{reg}}^\lambda$ and $\hat{\theta}^\delta$, the results still hold under cross-fitting. See Appendix C for an extended discussion.*

Remark 4 (Infinite dimensional setting). *While we emphasize the linear, low-dimensional setting where $\Phi_p^\top \Phi_p$ is invertible, Proposition 3.2 holds far more broadly. The result remains true when the function class \mathcal{F} is a subset of any Hilbert space. This includes the high dimensional setting where $d > n$ and the infinite dimensional setting. See Appendix B for a formal statement.*

Remark 5 (Nonlinear balancing weights). *A rich tradition in survey statistics (e.g., Deville and Särndal, 1992), machine learning (e.g., Menon and Ong, 2016), and causal inference (e.g., Vermeulen and Vansteelandt, 2015; Zhao, 2019; Tan, 2020) focuses on non-linear balancing weights, such as when the weights correspond to a specific link function $g(\cdot)$ applied to the linear predictor, $\hat{w} = g(\hat{\theta}^\top \Phi_p^\top)$, or, equivalently, when the balancing weights problem penalizes an alternative dispersion penalty. In Appendix D, we briefly consider extending Proposition 3.1 to nonlinear weights and show that the nonlinearity introduces an additional approximation error. A more thorough extension is a promising direction for future research.*

Remark 6 (Non-negative weights). *A common modification of the (minimum variance) balancing weights problem is to constrain the estimated weights to be non-negative or on the simplex; examples include Stable Balancing Weights (Zubizarreta, 2015) and the Synthetic Control Method (Abadie et al., 2010), as well as their augmented analogues (Athey et al., 2018; Ben-Michael et al., 2021c). Such weights have a number of attractive practical properties: they limit extrapolation; they ensure that the final weighting estimator is sample bounded; and they are typically sparse, which can sometimes aid interpretability (Robins et al., 2007). In Appendix D.2, we extend Proposition 3.1 and show that restricting weights to be non-negative is equivalent to sample trimming. In particular, let \hat{w}_\pm^δ be the estimated non-negative weights and $\hat{\beta}_{\text{ols}}^+$ be the OLS coefficient of the regression of Y_p on Φ_p , but restricted to units with positive weight. Then, Proposition 3.1 continues to hold, but with $\hat{\beta}_{\text{ols}}^+$ in place of the unrestricted $\hat{\beta}_{\text{ols}}$: $\hat{\mathbb{E}}[\hat{w}_\pm^\delta \circ Y_p] = \Phi_q^\delta \hat{\beta}_{\text{ols}}^+$. See Arbour and Feller (2024) for additional discussion of the simplex constraint.*

Remark 7 (Bilinear form). *As pointed out by a reviewer, (many of) the functionals we consider can be*

written as a bilinear form $\alpha^T \Sigma \beta$ where β is the coefficient for the outcome model, α is the coefficient for the Riesz representer and Σ is the some weighted population Gram matrix (Robins et al., 2008); for $E[Y(1)]$, it would be $E[Z\phi(X)\phi(X)^T]$. Proposition 3.2 suggests that β can be estimated using the methods we discuss here, and moreover that the aggregation weights would then be entangled with Σ or α . Understanding whether this could be used to then motivate new estimators is an interesting topic for future work.

4 Augmented ℓ_2 Balancing Weights

In this section, we study ℓ_2 balancing weights estimators, which are commonly used in the context of kernel balancing (Gretton et al., 2012; Hirshberg et al., 2019; Kallus, 2020; Ben-Michael et al., 2021a) and for panel data methods (Abadie et al., 2010; Ben-Michael et al., 2021c). We first show that the regularization path a_j^δ from Proposition 3.2 follows typical ridge regression shrinkage, with a smooth decay. Moreover, augmenting with ℓ_2 balancing weights is equivalent to boosting with ridge regression, and always overfits relative to the unaugmented outcome model alone. We then show that when the outcome model used to augment ℓ_2 balancing weights is also a ridge regression (which we refer to as “double ridge”), the augmented estimator is itself equivalent to a single, generalized ridge regression, albeit undersmoothed relative to the base learner. These results extend immediately to the RKHS setting of “double kernel ridge” estimation, combining kernel balancing weights and kernel ridge regression. In Section 6, we show the implications of these numeric results for undersmoothing in the statistical sense.

While the following results hold for arbitrary covariance matrices, in the main text we simplify the presentation by assuming that $\Phi_p^\top \Phi_p$ is diagonal; that is, $(\Phi_p^\top \Phi_p) = \text{diag}(\sigma_1^2, \sigma_2^2, \dots, \sigma_d^2)$, with $\sigma_j^2 > 0$. We show that this is without loss of generality for ℓ_2 balancing in Appendix E.

4.1 General linear outcome model

Following Remark 2 above, ℓ_2 balancing weights, including kernel balancing weights, have a closed form that is always linear in $\bar{\Phi}_q$. Our next result applies this closed form to Proposition 3.2 to derive the regularization path that results from augmenting an arbitrary linear outcome model with ℓ_2 balancing weights. Although this is an immediate consequence of Proposition 3.2, the resulting form of the augmented estimator has unique structure that warrants a new result.

Proposition 4.1. *Let $\hat{w}_{\ell_2}^\delta$ be (penalized) linear balancing weights with regularization parameter δ and $\mathcal{F} = \{f(x) = \theta^\top \phi(x) : \|\theta\|_2 \leq 1\}$. Then $\frac{1}{n} \hat{w}_{\ell_2}^\delta = \bar{\Phi}_q (\Phi_p^\top \Phi_p + \delta I)^{-1} \Phi_p^\top$. Therefore, the augmented ℓ_2 balancing weights estimator with outcome model $\hat{\beta}_{reg}^\lambda \in \mathbb{R}^d$ has the form*

$$\hat{\mathbb{E}}[\Phi_q \hat{\beta}_{reg}^\lambda] + \hat{\mathbb{E}}[\hat{w}_{\ell_2}^\delta (Y_p - \Phi_p \hat{\beta}_{reg}^\lambda)] = \hat{\mathbb{E}}[\Phi_q \hat{\beta}_{\ell_2}],$$

where the j th coefficient of $\hat{\beta}_{\ell_2}$ is given by

$$\begin{aligned} \hat{\beta}_{\ell_2, j} &:= (1 - a_j^\delta) \hat{\beta}_{reg, j}^\lambda + a_j^\delta \hat{\beta}_{ols, j} \\ a_j^\delta &:= \frac{\sigma_j^2}{\sigma_j^2 + \delta}. \end{aligned} \tag{8}$$

In this case, the a_j^δ are exactly equal to the standard regularization path of ridge regression. To see this, recall that ridge regression with penalty δ shrinks the $\hat{\beta}_{ols}$ coefficients as follows:

$$\hat{\beta}_{ridge, j}^\delta = \left(\frac{\sigma_j^2}{\sigma_j^2 + \delta} \right) \hat{\beta}_{ols, j} = a_j^\delta \hat{\beta}_{ols, j}. \tag{9}$$

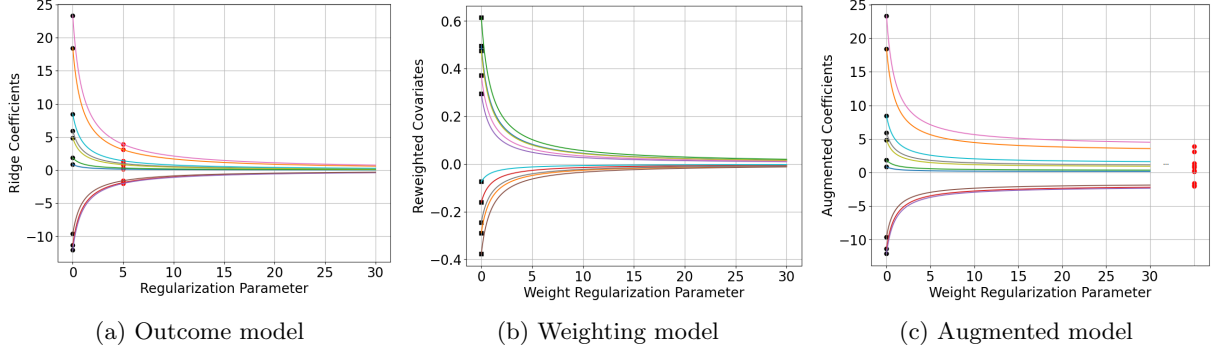


Figure 1: Regularization paths for “double ridge” augmented ℓ_2 balancing weights. Panel (a) shows the coefficients $\hat{\beta}_{\text{reg}}^\lambda$ of a ridge regression of Y_p on Φ_p with hyperparameter λ . The black dots on the left are the OLS coefficients, with $\lambda = 0$. The red dots at $\lambda = 5$ illustrate the coefficients at a plausible hyperparameter value, $\hat{\beta}_{\text{reg}}^5$. Panel (b) shows re-weighted covariates, $\hat{\Phi}_q^\delta$, for the ℓ_2 balancing weights problem with hyperparameter δ ; the black dots show exact balance, which corresponds to OLS. As δ increases, the weights converge to uniform weights and $\hat{\Phi}_q^\delta$ converges to $\bar{\Phi}_p$, which we have centered at zero. Panel (c) shows the augmented coefficients, $\hat{\beta}_{\ell_2}$ as a function of the weight regularization parameter δ . The black dots on the left are the OLS coefficients. As $\delta \rightarrow \infty$, the coefficients converge to $\hat{\beta}_{\text{reg}}^5$. All three regularization paths have essentially identical qualitative behavior.

This is identical to the expression in (8) but with $\hat{\beta}_{\text{reg}}^\lambda$ set to 0: Ridge regression shrinks $\hat{\beta}_{\text{ols}}$ towards 0 with regularization path a_j^δ , while ℓ_2 augmenting shrinks $\hat{\beta}_{\text{ols}}$ towards $\hat{\beta}_{\text{reg}}^\lambda$ with the same regularization path.

As an illustration, the right panel of Figure 1 shows $\hat{\beta}_{\ell_2}$ (on the y-axis) for ten covariates, with δ increasing from 0 (on the x-axis). The dots on the left pick out $\hat{\beta}_{\text{ols}}$; when $\delta = 0$, then $a_j^0 = 1$ and $\hat{\beta}_{\ell_2} = \hat{\beta}_{\text{ols}}$. The limit on the right shows $\hat{\beta}_{\text{reg}}^\lambda$. The smooth regularization path is characteristic of ridge regression shrinkage.

We can also view $\hat{\beta}_{\ell_2}$ as the output of a single iteration of a ridge boosting procedure, fit using Y_p and Φ_p alone. See Bühlmann and Yu (2003) and Park et al. (2009) for detailed discussion; Newey et al. (2004) makes a similar connection in the context of twicing kernels.

Proposition 4.2. *Let $\check{Y}_p = Y_p - \Phi_p \hat{\beta}_{\text{reg}}^\lambda$ be the residuals from the base learner. Let $\hat{\beta}_{\text{boost}}^\delta$ be the coefficients from the ridge regression of \check{Y}_p on Φ_p with hyperparameter δ . Then, $\hat{\beta}_{\ell_2} = \hat{\beta}_{\text{reg}}^\lambda + \hat{\beta}_{\text{boost}}^\delta$, and $\|Y_p - \Phi_p \hat{\beta}_{\ell_2}\|_2^2 \leq \|Y_p - \Phi_p \hat{\beta}_{\text{reg}}^\lambda\|_2^2$.*

So for a fixed δ , the augmented ℓ_2 balancing estimator is equivalent to estimating a new outcome model coefficient estimator $\hat{\beta}_{\ell_2}$ that *overfits* relative to $\hat{\beta}_{\text{reg}}^\lambda$ (in the sense of having smaller in-sample training error), and then applying that model to Φ_q .

Surprisingly — and in contrast to the general result in Proposition 3.2 — the augmented coefficients $\hat{\beta}_{\ell_2}$ are the same for *every* target covariate profile Φ_q . To see this, note that Proposition 4.1 shows that ℓ_2 balancing weights are always linear in $\bar{\Phi}_q$. Therefore, the corresponding regularization path a_j^δ does not depend on the target profile Φ_q ; it depends only on δ and the source distribution variances σ_j^2 . This property is closely related to *universal adaptability* in the computer science literature on multi-group fairness (Kim et al., 2022b). The particular Φ_q may nonetheless impact the choice of δ in hyperparameter selection, e.g., via cross-validating imbalance, which in turn influences the degree of overfitting; we do find this to be the case theoretically in Section 6.2.

4.2 Ridge regression outcome model

Proposition 4.1 holds for arbitrary linear outcome model coefficient estimators $\hat{\beta}_{\text{reg}}^\lambda \in \mathbb{R}^d$; we now state the corresponding result for a “double ridge” estimator, where the base learner outcome model is itself fit via ridge regression. The key takeaway is that the implied augmented coefficients are *undersmoothed* relative to the base learner ridge coefficients.

For this section, we will consider the following generalized ridge regression, sometimes known as “adaptive” ridge regression (Grandvalet, 1998). Let $\Lambda \in \mathbb{R}^{d \times d}$ be a diagonal matrix with j th diagonal entry $\lambda_j \geq 0$. Then the generalized ridge coefficients are:

$$\begin{aligned}\hat{\beta}_{\text{ridge}}^\Lambda &:= \underset{\beta \in \mathbb{R}^d}{\text{argmin}} \|\Phi_p \beta - Y_p\|_2^2 + \beta^\top \Lambda \beta \\ &= (\Phi_p^\top \Phi_p + \Lambda)^{-1} \Phi_p^\top Y_p.\end{aligned}$$

Standard ridge regression is the special case where the λ_j all take the same value and so $\Lambda = \lambda I$. As above, the generalized ridge coefficients can be rewritten as shrinking the OLS coefficients:

$$\hat{\beta}_{\text{ridge},j}^\Lambda = \left(\frac{\sigma_j^2}{\sigma_j^2 + \lambda_j} \right) \hat{\beta}_{\text{ols},j}. \quad (10)$$

We now demonstrate that the augmented ℓ_2 balancing weights estimator with base learner $\hat{\beta}_{\text{ridge}}^\Lambda$ is equivalent to a plug-in estimator using generalized ridge with *smaller* hyperparameters, $\hat{\beta}_{\text{ridge}}^\Gamma$, where Γ is a diagonal matrix with j th diagonal entry $\gamma_j \in [0, \lambda_j]$.

Proposition 4.3. *Let $\hat{\beta}_{\text{ridge}}^\Lambda$ denote the coefficients of a generalized ridge regression of Y_p on Φ_p with hyperparameters Λ , and let $\hat{w}_{\ell_2}^\delta$ denote ℓ_2 balancing weights with hyperparameter δ defined in Section 2.3. Define the diagonal matrix Γ with j th diagonal entry:*

$$\gamma_j := \frac{\delta \lambda_j}{\sigma_j^2 + \lambda_j + \delta} \leq \lambda_j.$$

Then:

$$\hat{\mathbb{E}}[\Phi_q \hat{\beta}_{\text{ridge}}^\Lambda] + \hat{\mathbb{E}}[\hat{w}_{\ell_2}^\delta (Y_p - \Phi_p \hat{\beta}_{\text{ridge}}^\Lambda)] = \hat{\mathbb{E}}[\Phi_q \hat{\beta}_{\text{ridge}}^\Gamma].$$

Furthermore, $\hat{\beta}_{\text{ridge}}^\Gamma$ are standard ridge regression coefficients (i.e., γ_j is a constant for all j) when $\lambda_j = \lambda$ and $\sigma_j = \sigma$ for all j .

The same result holds for kernel ridge regression; see Appendix B.4.

In this setting, augmenting with balancing weights is equivalent to undersmoothing the original outcome model fit. In particular, we can use the expansion in Equation (10) to see the undersmoothing in $\hat{\beta}_{\text{ridge}}^\Gamma$ explicitly:

$$\frac{\sigma_j^2}{\sigma_j^2 + \gamma_j} = \underbrace{\left(\frac{\sigma_j^2}{\sigma_j^2 + \lambda_j} \right)}_{\text{outcome model}} \underbrace{\left(\frac{\sigma_j^2 + \lambda_j + \delta}{\sigma_j^2 + \delta} \right)}_{\text{augmentation}},$$

where the first term is the shrinkage from the original generalized ridge model alone, and the second term is due to augmenting with ℓ_2 balancing weights. Importantly, the second term is in $[1, \frac{\sigma_j^2 + \lambda_j}{\sigma_j^2}]$ and therefore partially reverses the shrinkage of the original estimate. In Section 6.1, we connect this to undersmoothing in the statistical sense.

5 Augmented ℓ_∞ balancing weights

In this section, we study ℓ_∞ balancing weights estimators, which are widely used in the balancing weights literature (Zubizarreta, 2015; Athey et al., 2018) and in the AutoDML literature (Chernozhukov et al., 2022d). In the main text, we consider the special case where the covariance matrix $\Phi_p^\top \Phi_p$ is diagonal; that is, $(\Phi_p^\top \Phi_p) = \text{diag}(\sigma_1^2, \sigma_2^2, \dots, \sigma_d^2)$, with $\sigma_j^2 > 0$. Unlike with ℓ_2 balancing, this is no longer without loss of generality. We discuss this general case in Appendix E.3.

For diagonal covariance, we first show that ℓ_∞ balancing has a closed form: it is equivalent to applying a soft-thresholding operator to the feature shift from $\bar{\Phi}_p$ to $\bar{\Phi}_q$. We then write the resulting augmented estimator as applying coefficients $\hat{\beta}_{\ell_\infty}$ to Φ_q and show that $\hat{\beta}_{\ell_\infty}$ is a sparse, element-wise convex combination of the base learner coefficients and OLS coefficients. When the outcome model is also fit via the lasso, we use the resulting representation to demonstrate a familiar “double selection” phenomenon (Belloni et al., 2014), where $\hat{\beta}_{\ell_\infty}$ inherits the non-zero coefficients of both the base learner and the weighting model. This is a form of undersmoothing in the ℓ_0 “norm,” in the sense that $\hat{\beta}_{\ell_\infty}$ always has at least as many non-zero coefficients as the base learner, $\hat{\beta}_{\text{reg}}$.

5.1 Weighting alone

We first define the soft-thresholding operator and show that the ℓ_∞ balancing problem has a closed form solution.

Definition (Soft-thresholding operator). *For $t > 0$, define the soft-thresholding operator,*

$$\mathcal{T}_t(z) := \begin{cases} 0 & \text{if } |z| < t \\ z - t & \text{if } z > t \\ z + t & \text{if } z < -t \end{cases}.$$

Proposition 5.1 (ℓ_∞ Balancing). *If $\Phi_p^\top \Phi_p$ is diagonal, the solution $w_{\ell_\infty}^\delta$ to the ℓ_∞ optimization problem (13) is:*

$$\begin{aligned} \frac{1}{n} w_{\ell_\infty}^\delta &= \Phi_p (\Phi_p^\top \Phi_p)^{-1} [\bar{\Phi}_p + \mathcal{T}_\delta(\bar{\Phi}_q - \bar{\Phi}_p)] \\ &= \Phi_p (\Phi_p^\top \Phi_p)^{-1} [\bar{\Phi}_p + \mathcal{T}_\delta(\Delta)] \end{aligned}$$

where $\Delta = \bar{\Phi}_q - \bar{\Phi}_p$, where we include $\bar{\Phi}_p$ (equal to 0 by assumption) to emphasize the dependence on feature shift, and with corresponding reweighted features, $\hat{\Phi}_q^\delta = \bar{\Phi}_p + \mathcal{T}_\delta(\bar{\Phi}_q - \bar{\Phi}_p)$.

For intuition, compare the (un-augmented) ℓ_∞ balancing weights estimator to the lasso-based coefficient estimates (Hastie et al., 2009):

$$\begin{aligned} \hat{\mathbb{E}}[w_{\ell_\infty}^\delta \circ Y_p] &= \mathcal{T}_\delta(\bar{\Phi}_q)^\top \hat{\beta}_{\text{ols}} \\ \hat{\mathbb{E}}[\Phi_q \hat{\beta}_{\text{lasso}}^\lambda] &= \bar{\Phi}_q^\top \mathcal{T}_\lambda(\hat{\beta}_{\text{ols}}), \end{aligned}$$

where we simplify $\hat{\Phi}_q^\delta$ here to emphasize the connections between the methods. Whereas lasso performs soft-thresholding on the OLS coefficients (regularizing the outcome regression), ℓ_∞ balancing performs soft-thresholding on the implied feature shift to the target features.

5.2 General linear outcome model

We can then plug the closed-form solution for the weights into Proposition 3.2.

Proposition 5.2. Let $\hat{w}_{\ell_\infty}^\delta$ be defined as above. Then the augmented ℓ_∞ balancing weights estimator with outcome model fit $\hat{\beta}_{reg}^\lambda \in \mathbb{R}^d$ has the form,

$$\hat{\mathbb{E}}[\Phi_q \hat{\beta}_{reg}^\lambda] + \hat{\mathbb{E}}[\hat{w}_{\ell_\infty}^\delta (Y_p - \Phi_p \hat{\beta}_{reg}^\lambda)] = \hat{\mathbb{E}}[\Phi_q \hat{\beta}_{\ell_\infty}],$$

where the j th coefficient of $\hat{\beta}_{\ell_\infty}$ equals:

$$\hat{\beta}_{\ell_\infty, j} = \begin{cases} \hat{\beta}_{reg, j}^\lambda & \text{if } |\Delta_j| < \delta \\ \left| \frac{\delta}{\Delta_j} \right| \hat{\beta}_{reg, j}^\lambda + \left(1 - \left| \frac{\delta}{\Delta_j} \right| \right) \hat{\beta}_{ols, j} & \text{otherwise} \end{cases},$$

where $\Delta_j = \bar{\Phi}_{q, j} - \bar{\Phi}_{p, j}$.

The augmented coefficients $\hat{\beta}_{\ell_\infty}$ are an element-wise convex combination of $\hat{\beta}_{reg}^\lambda$ and $\hat{\beta}_{ols}$. For features where the mean feature shift Δ_j is small (relative to δ), $\hat{\beta}_{\ell_\infty}$ is equivalent to the base learner coefficient $\hat{\beta}_{reg}^\lambda$. The remaining coefficients are interpolated linearly toward the $\hat{\beta}_{ols}$ coefficients.

Figure 2 summarizes these results and their implications for the augmented estimator. As with Figure 1, we generate simple simulated data with $d = 10$. In the left panel, we plot the coefficients from lasso regression of Y_p on Φ_p as a function of the lasso regularization parameter. The regularization path begins with the black dots, which represent the OLS coefficients. Each lasso coefficient (represented by a colored line) then shrinks linearly to exactly zero, due to the soft-thresholding operator. The middle panel plots the reweighted covariates using ℓ_∞ balancing weights between Φ_p and Φ_q solved in the constrained form. The black dots represent $\bar{\Phi}_q$, corresponding to exact balance. Then as the weight regularization parameter increases, the reweighted covariates shrink linearly to exactly zero, just as in lasso. The right panel plots coefficients for the augmented estimator that combines a baseline outcome model fit $\hat{\beta}_{reg}^\lambda$ with ℓ_∞ balancing weights. The lines correspond to $\hat{\beta}_{\ell_\infty}$ as defined in Proposition 5.2. The regularization path begins at the black dots, where $\hat{\beta}_{\ell_\infty} = \hat{\beta}_{ols}$, and eventually converges to $\hat{\beta}_{reg}^\lambda$, showing the usual soft-thresholding behavior. The order at which the coefficients go to zero reflects the size of $\bar{\Phi}_q$, because the regularization path depends on the weight coefficients from the middle panel. Thus, the augmented estimator shrinks $\hat{\beta}_{ols}$ toward $\hat{\beta}_{reg}^\lambda$ but via a soft-thresholding operator applied to the feature shift, Δ_j .

5.3 Lasso outcome model

In the case where $\hat{\beta}_{reg}^\lambda$ is itself fit via lasso, as studied in Chernozhukov et al. (2022d), then we recover a familiar double selection phenomenon (Belloni et al., 2014).

Proposition 5.3 (Double Selection). Let $\hat{\beta}_{lasso}^\lambda$ denote the coefficients of lasso regression of Y_p on Φ_p with regularization parameter λ . Denote the indices of the non-zero coefficients as I_λ . Let $\hat{w}_{\ell_\infty}^\delta$ be ℓ_∞ balancing weights with parameter δ as in Proposition 5.1. Let I_δ denote the non-zero entries of the reweighted covariates $\hat{\Phi}_q$. Assume that $\hat{\beta}_{ols}$ is dense. Then the indices of the non-zero entries of the augmented coefficients $\hat{\beta}_{\ell_\infty}$ are $I_{aug} = I_\lambda \cup I_\delta$.

The lasso coefficients have a sparsity pattern generated by soft-thresholding the OLS coefficients. The augmented estimator then shrinks from OLS toward $\hat{\beta}_{reg}^\lambda$ by soft-thresholding the implied feature shift to the target features. As a result, wherever the lasso coefficients are non-zero *or* the weight coefficients are non-zero, the final augmented coefficients are also non-zero. The “included coefficients” for the final estimator are then the union of the coefficients included in either individual model. Therefore, augmenting a lasso outcome model with ℓ_∞ balancing also exhibits a form of undersmoothing in the ℓ_0 “norm”, $\|\hat{\beta}_{\ell_\infty}\|_0$, in the sense that there are always at least as many non-zero coefficients as for the unaugmented lasso outcome model. However, this will not correspond to undersmoothing the base learner in the traditional sense, because in general there will not exist a lasso hyperparameter λ that will produce sparsity pattern I_{aug} .

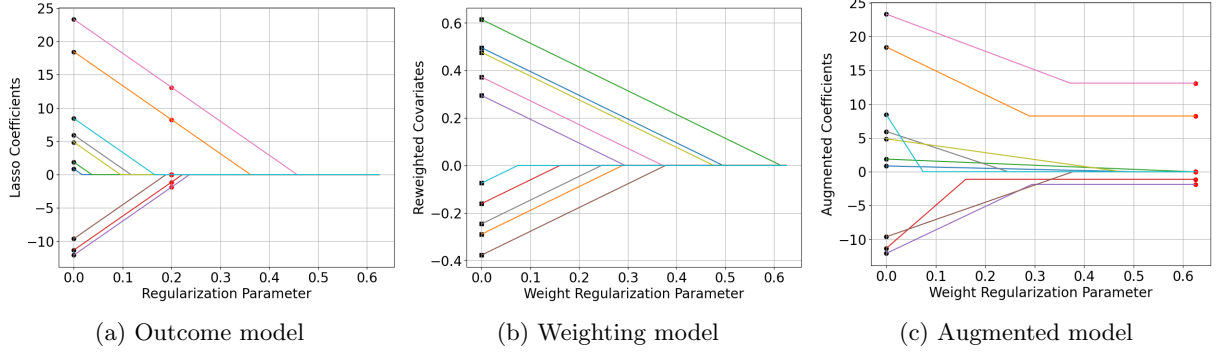


Figure 2: Regularization paths for “double lasso” augmented ℓ_∞ balancing weights. Panel (a) shows the coefficients $\hat{\beta}_{\text{reg}}^\lambda$ of a lasso regression of Y_p on Φ_p with hyperparameter λ . The black dots on the left are the OLS coefficients, with $\lambda = 0$. The red dots at $\lambda = 0.2$ illustrate the coefficients at a plausible hyperparameter value, $\hat{\beta}_{\text{reg}}^{0.2}$. Panel (b) shows re-weighted covariates, $\hat{\Phi}_q^\delta$, for the ℓ_∞ balancing weights problem with hyperparameter δ ; the black dots show exact balance, which corresponds to OLS. As δ increases, the weights converge to uniform weights and $\hat{\Phi}_q^\delta$ converges to $\bar{\Phi}_p$, which we have centered at zero. Panel (c) shows the augmented coefficients, $\hat{\beta}_{\ell_\infty}$ as a function of the weight regularization parameter δ . The black dots on the left are the OLS coefficients. As $\delta \rightarrow \infty$, the coefficients converge to $\hat{\beta}_{\text{reg}}^{0.2}$. All three regularization paths show the typical lasso “soft thresholding” behavior. The regularization path for the augmented estimator also shows “double selection” behavior.

As noted by, for example, [Tang et al. \(2023\)](#), the double selection estimator may suffer from imprecision due to adjustment for covariates that are associated with treatment but not outcome. One could in principle remove covariates that are only predictive of the treatment, but this can jeopardize statistical inference. We refer to [Moosavi et al. \(2023\)](#) for a discussion on navigating this trade-off.

6 Kernel Ridge Regression: Asymptotic and Finite Sample Analysis

The results above are *numerical*: they hold without any statistical or causal assumptions. However, the connection between augmented estimators and outcome models also presents *statistical* insights that we discuss here. In particular, we leverage the numerical result that double (kernel) ridge regression — which uses ridge regression for fitting both the outcome and weighting models — is equivalent to a single, undersmoothed outcome ridge regression plug-in estimator.

First, we consider an asymptotic analysis in Section 6.1: we use this equivalence to make explicit the connection between asymptotic results for augmented balancing weights with kernel ridge regression and prior results on optimal undersmoothing of a kernel ridge plug-in estimator. As a result, optimally undersmoothed kernel ridge regression inherits whatever guarantees can be proven for augmented ridge regression. An implication is that we can generalize the insight from [Robins et al. \(2007\)](#) that OLS is doubly robust to a wider class of non-parametric estimators. This equivalence also suggests an appropriate hyperparameter scheme when the outcome regression is an element of an RKHS.

Second, we consider a finite sample analysis in Section 6.2: we use this equivalence to derive the finite-sample design-conditional mean squared error of augmented kernel ridge regression. We then use this expression to characterize finite-sample-optimal hyperparameter tuning. We turn to hyperparameter tuning in practice in the next section.

6.1 Asymptotic Results

We now use our results in Proposition 4.3 to make explicit the connection between two otherwise distinct sets of asymptotic results. First, Wong and Chan (2018) and Singh (2021) argue that double kernel ridge regression can deliver \sqrt{n} -consistent estimation of functionals in certain scenarios. Wong and Chan (2018) also proposes an optimally undersmoothed ℓ_2 balancing weights estimator. Separately, Hirshberg et al. (2019) and Mou et al. (2023) propose optimally undersmoothed (single) kernel ridge outcome regression. Since, as we have shown in Proposition 4.3 (see also Remark 2), these three procedures are equivalent, we can connect these results and show that plug-in estimators based on optimally undersmoothed kernel ridge regression or ℓ_2 balancing weights can be \sqrt{n} -consistent. Moreover, results on RKHSs suggest a simple heuristic for hyperparameter choice. We give the high-level argument here and defer additional technical details to Appendix L.

To move from numerical results to statistical results, we must place some constraints on the data generating process. Assume that we observe n iid samples of (x_i, y_i, z_i) from p . Define $K \in \mathbb{R}^{n \times n}$ to be the kernel matrix with i, j -th entry $K_{ij} = k((x_i, z_i), (x_j, z_j))$. Let σ_j^2 denote the eigenvalues of K . We assume that $\sigma_j^2 = \sigma^2 > 0$ is constant for all j ; we can relax this at the cost of additional complexity. The “single” kernel ridge regression outcome regression estimator with parameter λ has coefficient estimates:

$$\hat{\beta}_{\text{ridge}}^\lambda = (K + \lambda I)^{-1}y.$$

Applying Proposition 4.3, the augmented “double kernel ridge” estimator with hyperparameter δ is equivalent to a plug-in estimate for a new kernel ridge model:

$$\hat{\beta}_{\text{aug}} = (K + \gamma I)^{-1}y, \quad \text{with } \gamma = \frac{\lambda\delta}{\sigma^2 + \lambda + \delta}.$$

For statistical guarantees, we must typically allow the hyperparameters to change with n ; let γ_n, λ_n and δ_n then denote sequences of hyperparameters. In the doubly robust framework, one can choose λ_n and δ_n in a way that is MSE-optimal for prediction purposes whilst ensuring that the bias of the augmented estimator is small. For two functions of n , f_n and g_n , let $f_n \asymp g_n$ denote that $f_n = O(g_n)$ and $g_n = O(f_n)$. Then due to special properties of RKHS geometry, it follows that δ_n can be of the same order as λ_n , that is $\delta_n \asymp \lambda_n$ (Singh et al., 2020, Theorem 5.2). In the next section, we consider setting $\delta = \lambda$ for hyperparameter tuning in practice; our Proposition 4.3 then implies that $\gamma_n \asymp \lambda_n^2$. We note more generally that Proposition 4.3 implies that $\gamma_n \asymp \lambda_n \delta_n$.

There are two important cases to consider. When the RKHS is finite dimensional, the choice $\lambda_n = \delta_n = n^{-1/2}$ is optimal for controlling the prediction error for both the outcome and weighting models (Caponnetto and De Vito, 2007; Singh et al., 2020). The augmented estimator is then equivalent to a single ridge regression with hyperparameter $\gamma_n \asymp n^{-1}$, which matches the rate of Hirshberg et al. (2019); Mou et al. (2023). Hence, this approach will always undersmooth relative to the MSE-optimal hyperparameter for a single ridge regression.

When the RKHS is infinite-dimensional, we find that the undersmoothed hyperparameter implied by the augmented procedure can take on a range of asymptotic rates, both faster and slower than n^{-1} , depending on effective dimension and smoothness; we give concrete examples in the Appendix. This somewhat contrasts with the results in Hirshberg et al. (2019); Mou et al. (2023). In this sense, Proposition 4.3 generalizes the standard undersmoothing arguments, which typically change the regularization schedule from $n^{-1/2}$ to n^{-1} .

Remark 8 (Single-model double robustness). *Another interesting implication of the equivalence of these two procedures is that the single kernel ridge procedure is doubly robust, much the same way OLS is. Because estimating the coefficients from an OLS regression of Y onto features of (Z, X) is equivalent to a balancing weights or an IPW estimator based on a model for the inverse weights that is linear in the same features, this procedure is consistent whenever either the weights or the outcome model is truly linear—that is, whenever either of these two linear models is correctly specified (Robins et al., 2007). Similarly, the single kernel*

ridge procedure is doubly robust in that it is consistent if either the true outcome regression or the inverse propensity score is consistently estimated. However, valid inference in the case where the inverse weight model but not the outcome model is truly linear will typically require different tuning parameter selection.

6.2 Finite Sample Mean-Squared Error

We now use our numerical equivalences to write out the exact finite-sample mean squared error of the augmented kernel ridge estimator: by re-writing the augmented balancing weights estimator as a single outcome model, we can immediately leverage existing results from [Dobriban and Wager \(2018\)](#).

Following their setup, we define the diagonal matrix $\hat{\Sigma} := \frac{1}{n}\Phi_p^T\Phi_p$; if $\hat{\Sigma}$ is not diagonal, we can apply the rotation in [Appendix E.2](#). We consider ridge regression with rescaled hyperparameter λ and solution $(\hat{\Sigma} + \lambda I)^{-1}\Phi_p Y_p/n$; this is equivalent to standard ridge regression above with hyperparameter $n\lambda$, and also accommodates kernel ridge regression with appropriate choice of Φ_p . Assume that $Y_p = \Phi_p\beta_0 + \epsilon$ with $\beta_0 \in \mathbb{R}^d$, and where $\epsilon \in \mathbb{R}^n$ are iid with mean zero and variance σ^2 . Then the exact, design-conditional, squared bias and variance of the ridge regression prediction applied to a new iid sample $(\Phi_{\text{new}}, Y_{\text{new}}) \sim p$ are:

$$B_p^2(\lambda) = \lambda^2 \beta_0^T (\hat{\Sigma} + \lambda I)^{-1} \mathbb{E}[\Phi_p^T \Phi_p] (\hat{\Sigma} + \lambda I)^{-1} \beta_0$$

$$V_p(\lambda) = \frac{\sigma^2}{n} \text{tr} \left[\hat{\Sigma} (\hat{\Sigma} + \lambda I)^{-1} \mathbb{E}[\Phi_p^T \Phi_p] (\hat{\Sigma} + \lambda I)^{-1} \right].$$

Applying [Proposition 4.3](#), we can similarly derive the squared bias and variance of an augmented ridge estimator for our linear functional estimand; we denote these quantities B_q^2 and V_q respectively. We express the bias and variance in terms of the two hyperparameters, λ and δ :

Proposition 6.1. *Let σ_j^2 denote the eigenvalues of $\hat{\Sigma}$ and define $\Gamma_{\lambda,\delta}$ to be the diagonal matrix with non-zero entries $\gamma_j := \frac{\delta\lambda}{\sigma_j^2 + \delta + \lambda}$. Then,*

$$B_q^2(\lambda, \delta) = \beta_0^T (\hat{\Sigma} + \Gamma_{\lambda,\delta})^{-1} \Gamma_{\lambda,\delta} \mathbb{E}[\Phi_q]^T \mathbb{E}[\Phi_q] \Gamma_{\lambda,\delta} (\hat{\Sigma} + \Gamma_{\lambda,\delta})^{-1} \beta_0$$

$$V_q(\lambda, \delta) = \frac{\sigma^2}{n} \text{tr} \left[\hat{\Sigma} (\hat{\Sigma} + \Gamma_{\lambda,\delta})^{-1} \mathbb{E}[\Phi_q]^T \mathbb{E}[\Phi_q] (\hat{\Sigma} + \Gamma_{\lambda,\delta})^{-1} \right].$$

In the next section, we compare — numerically and via simulation — existing hyperparameter selection schemes to the optimal trade-off between B_q^2 and V_q . However, first we note that the analysis above opens up exciting new avenues for both theoretical and methodological work. One could theoretically analyze the mean squared error to understand how the optimal δ scales with the problem parameters; for example, by using proportionate asymptotics from random matrix theory as in the high-dimensional ridge regression literature ([Hastie et al., 2022](#)). Second, our analysis here suggests a novel, more complex hyperparameter selection scheme based directly on the finite sample analysis. We leave this to future work.

7 Numerical illustrations and hyperparameter tuning

This section illustrates our results in practice. We first explore hyperparameter tuning for double ridge regression, comparing practical methods to the optimal hyperparameter computed using our results from [Proposition 6.1](#). Following our asymptotic results in [6.1](#), we recommend equating the weighting and outcome model hyperparameters in practice. We then apply both double ridge and lasso-augmented ℓ_∞ -balancing to two versions of the canonical [LaLonde \(1986\)](#) application. An important theme throughout is that some approaches for hyperparameter selection frequently lead to $\delta = 0$, which collapses the augmented estimate to OLS alone — even in settings where this is far from optimal. Overall, we take this as a warning that existing hyperparameter tuning schemes can be potentially misleading when applied naively.

7.1 Hyperparameter tuning for ridge-augmented ℓ_2 balancing

We begin with practical hyperparameter tuning for the special case of double ridge, building on the MSE expression in Section 6.2. There is an active literature on selecting hyperparameters for augmented balancing weights estimators and double machine learning estimators more broadly (Kallus, 2020; Wang and Zubizarreta, 2020; Ben-Michael et al., 2021b; Bach et al., 2024). We contribute to this literature by comparing practical hyperparameter tuning schemes with an oracle hyperparameter tuning scheme based on Proposition 6.1.

Reflecting empirical practice, we focus here on choosing hyperparameters sequentially: we first select the outcome model hyperparameter λ (e.g. by cross-validation) and then select the weighting model hyperparameter δ . Ultimately, we find strong performance for both *CV imbalance* and *CV outcome* hyperparameters, as defined below. We especially recommend the latter as a reasonable starting point in practice. In addition to theoretical support from our asymptotic analysis, the outcome model hyperparameter scheme does not require any additional algorithm or code after having fit the initial outcome model.

7.1.1 Oracle and practical hyperparameter tuning

Oracle hyperparameter. To compute oracle hyperparameters, we first compute the prediction-MSE-optimal λ using the standard ridge regression MSE expression, and then we use Proposition 6.1 to compute the corresponding optimal δ for the linear functional estimand:

$$\begin{aligned}\lambda^* &:= \operatorname{argmax}_{\lambda} \{B_p^2(\lambda) + V_p(\lambda)\} \\ \delta^* &:= \operatorname{argmax}_{\delta} \{B_q^2(\lambda^*, \delta) + V_q(\lambda^*, \delta)\}.\end{aligned}$$

While there is not a closed form for δ^* , we can nonetheless directly compute this optimal hyperparameter and characterize its behavior under a range of scenarios. We draw several conclusions about optimal δ^* for a wide range of DGPs of the form $Y_p = \Phi_p \beta_0 + \epsilon$. First, δ^* is generally increasing in the noise, σ^2 : larger σ^2 typically implies larger δ^* . Second, δ^* generally depends on the target mean, $\mathbb{E}[\Phi_q]$; that is, two DGPs that are identical except for $\mathbb{E}[\Phi_q]$ can have different values of δ^* . The optimal hyperparameter, however, does *not* depend on the magnitude of the shift in the target mean: replacing $\mathbb{E}[\Phi_q]$ with $c\mathbb{E}[\Phi_q]$ for $c \neq 0$, scales both the bias and variance by c^2 , leaving δ^* unchanged.

Practical hyperparameter. We compare the oracle hyperparameter with three implementable practical proposals. In all cases, we first pick λ by cross-validating the mean squared error of a ridge outcome model.

- *CV imbalance.* Choose δ by cross-validating the estimated imbalance, $\|\frac{1}{n}\hat{w}\Phi_p - \bar{\Phi}_q\|_2^2$, adapting a proposal from Wang and Zubizarreta (2020).
- *CV Riesz loss.* Choose δ by cross-validating the Riesz loss in Equation (6), adapting a proposal from Chernozhukov et al. (2022d); this is the dual form of cross-validating the estimated imbalance.
- *CV outcome.* Choose δ to be equal to the cross-validated ridge outcome λ , as inspired by the asymptotic theory in Singh et al. (2020).

Before presenting simulation results, we provide a preliminary analytic discussion, comparing these practical schemes to the behavior of the oracle δ^* . For the first two proposals: just like the oracle, both depend on the target mean $\mathbb{E}[\Phi_q]$ and are invariant to re-scaling. However, these two approaches are mechanically independent of the outcomes Y_p , unlike the oracle δ^* which, in general, depends on the variance of the outcomes. On the other hand, the last proposal depends on the outcomes Y_p but is mechanically independent of $\mathbb{E}[\Phi_q]$.

This suggests that any one of these tuning parameter approaches cannot perform well across all DGPs. In future work, if we pursue a theoretical analysis of the oracle hyperparameter, e.g. in a proportionate asymptotics framework, we may be able predict when either the outcomes or the covariate shift is more

Method	# of DGPs		Relative MSE			Prop. ($\delta = 0$)
	Best	Worst	Median	Best	Worst	
CV Outcome	10	3	0.58	0.097	2×10^5	0
CV Imbalance	25	2	0.39	0.001	2×10^5	0
CV Riesz Loss	1	31	3,454	0.23	3×10^7	0.56

Table 1: Mean-squared error (relative to the oracle) for four hyperparameter selection methods for *double ridge regression* from a numerical investigation of 36 data generating processes (30 synthetic and 6 semi-synthetic). The final column is the proportion of draws where the hyperparameter $\delta = 0$.

important. In this work we begin by demonstrating that no one tuning scheme does uniformly best in simulations.

7.1.2 Simulation study

To assess the behavior of these hyperparameter tuning schemes, we conduct an extensive simulation study using 36 distinct data-generating processes, 30 synthetic and 6 semi-synthetic; see Appendix H for a detailed discussion. For each DGP, we directly compute the oracle hyperparameter using the results in Section 6.2. We then compute values from the three practical hyperparameter tuning methods discussed above. The mean squared error that we consider is design-conditional, and so we draw samples of the covariates for each DGP only once.

Table 1 presents a summary of the MSE for the three methods across the 36 DGPs. Overall, we find that the *CV outcome* approach of choosing $\delta = \lambda$ and the *CV imbalance* approach both perform well in practice: these two achieve the lowest MSE in 35 of the 36 DGPs, with CV imbalance performing slightly better on average. By contrast, selecting δ via CV for the Riesz loss has numerical stability problems that compromises performance. The performance for the *outcome* and *balance* approaches, on the other hand, seem to degrade gracefully and rarely perform catastrophically. Taken together, these preliminary findings suggest researchers should begin with these two tuning methods as defaults.

Recovering the OLS point estimate. As we discuss above (see, e.g., Figure 1), when $\delta = 0$ the point estimate for the augmented balancing weights estimator is numerically identical to the OLS point estimate. Thus, when a hyperparameter tuning procedure chooses $\delta = 0$ in practice, researchers are simply estimating the equivalent of OLS — even if they are unaware they are doing so. This is especially problematic in settings where OLS is far from optimal (though see Kobak et al., 2020; Hastie et al., 2022, for counterexamples). In our synthetic and semi-synthetic DGPs, $\delta = 0$ is never optimal, and is usually associated with a very large error driven by extreme variance — see for example, Figure I.11 in the Appendix. Thus the fact that hyperparameter tuning procedures can return $\delta = 0$ in these DGPs represents a pathological case.

In our simulation study, we find that, when cross validating the Riesz loss, over half of all draws returned $\delta = 0$. By contrast, none of the other methods returned $\delta = 0$ in the synthetic DGPs, though, as we discuss below, we do observe exact zeros for δ occasionally when cross-validating imbalance in the standard LaLonde dataset. This further highlights the numeric instability of hyperparameter tuning via CV for the Riesz loss, at least in the settings we consider here. We further suggest that in these cases, practitioners assess the sensitivity of the $\delta = 0$ results to the particular tuning procedure used or to the random choice of cross-validation splits.

7.2 Application to LaLonde (1986)

We now illustrate our equivalence and hyperparameter tuning results on real-world datasets. Following Chernozhukov et al. (2022d), we focus on the canonical LaLonde (1986) data set evaluating a job training

program in the National Supported Work (NSW) Demonstration. The primary outcome of interest is annual earnings in 1978 dollars.

For these illustrations, we estimate the Average Treatment Effect on the Treated (ATT), $\mathbb{E}[Y(1) - Y(0) \mid Z = 1]$. We recover the missing conditional mean $\mathbb{E}[Y(0) \mid Z = 1]$ using the setup from Example 3 in Appendix A, where the source and target populations are the control and treated units respectively. Thus Φ_p and Φ_q correspond to the feature expansion $\phi(X)$ applied to the covariates in the control group and treated group respectively. We consider two different features expansions of the original covariates: (1) a “short” set of 11 covariates used in Dehejia and Wahba (1999);¹ and (2) an expanded, “long” set of 171 interacted features used in Farrell (2015).

Our goal is to explicate how augmented estimators under different hyperparameter tuning schemes under-smooth in practice in both low and high-dimensional settings. In some cases, the augmented estimator collapses to exactly OLS as we document above. Appendix I contains extensive additional analyses, including dataset summaries, additional results from the Infant Health Development Program (IHDP), and sensitivity of these numerical results to cross-fitting.

7.2.1 High-dimensional setting

Following Chernozhukov et al. (2022d), we first consider the expanded set of 171 features for LaLonde (1986) used in Farrell (2015). Figure 3 shows estimates for ridge-augmented ℓ_2 balancing (top row) and lasso-augmented ℓ_∞ balancing (bottom row). We explicitly characterize these results in terms of undersmoothing in Appendix I.4. The left two panels of each row show the cross-validation curves for the outcome regression and balancing weights, respectively. The right panels show the point estimate as a function of the weighting hyperparameter δ , holding the outcome model hyperparameter λ fixed; the black triangle represents the OLS plug-in point estimate. For context, the corresponding experimental estimate is \$1,794 (see Dehejia and Wahba, 1999). The green and red dotted lines correspond to hyperparameters chosen by cross-validating balance and the Riesz loss, respectively. For the double ridge estimate, the purple line corresponds to $\delta = \hat{\lambda}$, the outcome hyperparameter selected via cross validation.

Figure 3 highlights that both the imbalance and the point estimate are highly nonlinear close to zero. Thus, even small departures from OLS (at $\delta = 0$) lead to large changes in the point estimate — in Appendix I.5 we give some suggestive evidence that the variance blows up relative to the bias in this range. We can also assess the sensitivity of the point estimate to the hyperparameter selection scheme. In this case, choosing δ via CV balance leads to meaningfully larger choices than via other methods.

Finally, the selected δ is always strictly greater than zero for this high-dimensional dataset. However, we find this is sensitive to small perturbations in the problem parameters. For example, when we perturb $\mathbb{E}[\Phi_q]$ by adding a small value to all the even elements, then the cross-validated ℓ_2 Riesz loss chooses $\delta = 0$ in 38% of draws of the cross-validation splits. As suggested by Appendix I.5 and our simulation results, this is likely to result in extremely large mean squared error.

7.2.2 Low-dimensional setting: Recovering OLS

Finally, we apply double ridge to the “short” version of the LaLonde (1986) data set with 11 features. Figure 4 shows the cross-validation curves for the outcome and weighting models, as well as the point estimate as a function of the balance hyperparameter, with the OLS estimate given by the black triangle. As above, the green, red, and purple dotted lines correspond to hyperparameters chosen by cross-validating balance, cross-validating the Riesz loss, and choosing $\delta = \lambda$ respectively.

Unlike for the “long” dataset in Figure 3, Figure 4 does not display quite as stark nonlinearity around zero. Importantly, however, setting δ by cross-validating imbalance or the Riesz loss yields $\delta = 0$ (up to numerical

¹These are: age, years of education, Black indicator, Hispanic indicator, married indicator, 1974 earnings, 1975 earnings, age squared, years of education squared, 1974 earnings squared, and 1975 earnings squared.

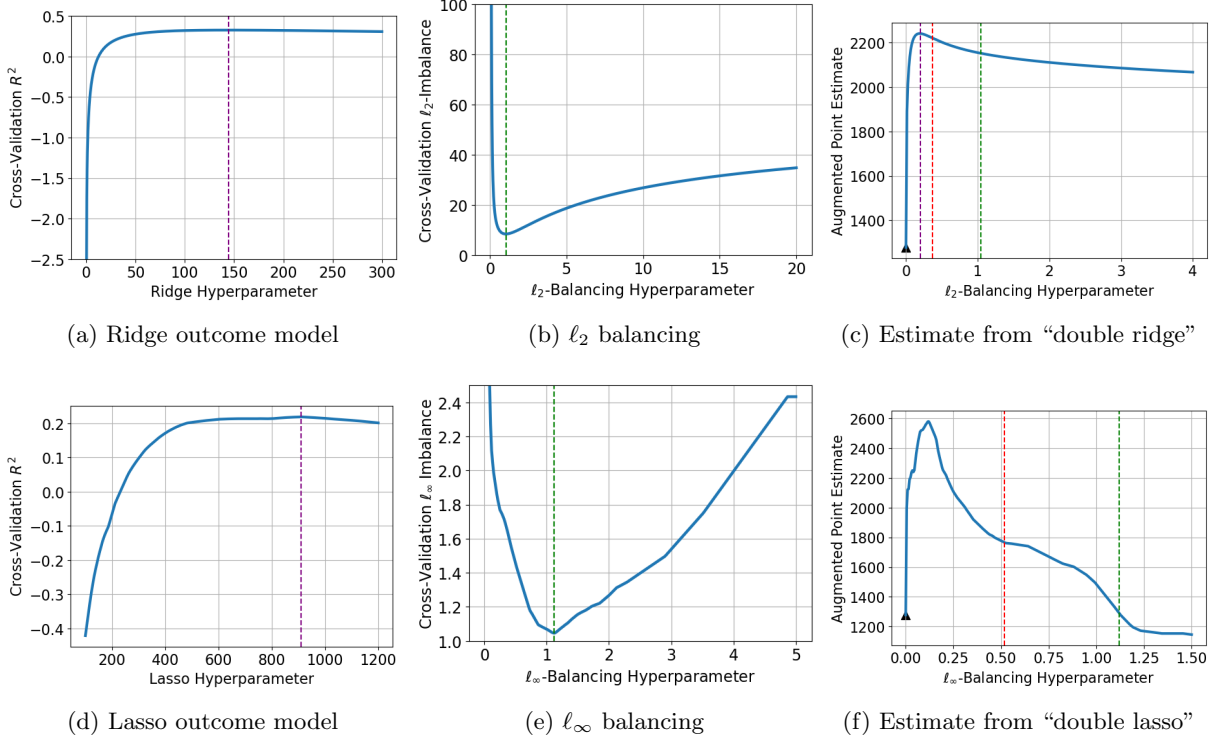


Figure 3: Augmented balancing weights estimates for the LaLonde (1986) data set with the expanded set of 171 features used in Farrell (2015); the top row shows ridge-augmented ℓ_2 balancing, and the bottom row shows lasso-augmented ℓ_∞ balancing. Panels (a) and (d) show the 3-fold cross-validated R^2 for the ridge- and lasso-penalized regression of Y_p on Φ_p among control units across the hyperparameter λ ; the purple dotted lines show the CV-optimal value for each. Panel (b) and (e) show the 3-fold cross-validated imbalance for ℓ_2 and ℓ_∞ balancing weights across the hyperparameter δ ; the green dotted lines show the CV-optimal value for each. Panels (c) and (f) show the point estimates for the augmented estimators across the weighting hyperparameter δ ; the black triangles correspond to the OLS point estimate; the green and red dotted lines correspond to the cross-validated balance and Riesz loss respectively; the purple line corresponds to the cross-validated ridge hyperparameter (for $\delta = \hat{\lambda}$). The variance-based hyperparameter for ridge is $\hat{\sigma}^2/n^2 = 104.8$ and for lasso is 137.5. The corresponding point estimates are 1923.6 and 725.8 respectively, essentially equal to the plug-in outcome model estimates.

imprecision), which reduces the augmented estimator to exactly the estimate from a simple OLS regression — even though the base learner ridge outcome model is heavily regularized. By contrast, our preferred hyperparameter tuning scheme of choosing $\delta = \lambda$ results in an estimate that is roughly \$400 dollars smaller than the OLS estimate.

8 Discussion

We have shown that augmenting a plug-in regression estimator with linear balancing weights results in a new plug-in estimator with coefficients that are shrunk towards — in some cases all the way to — the estimates from OLS fit on the same observations. We generalize this equivalence for different choices of outcome and weighting regressions. In the asymptotic setting, we draw the explicit connection between augmented estimators and undersmoothing for the special case of kernel ridge regression. Then we derive the design-conditional finite sample MSE for the double ridge estimator, and use it to solve numerically for

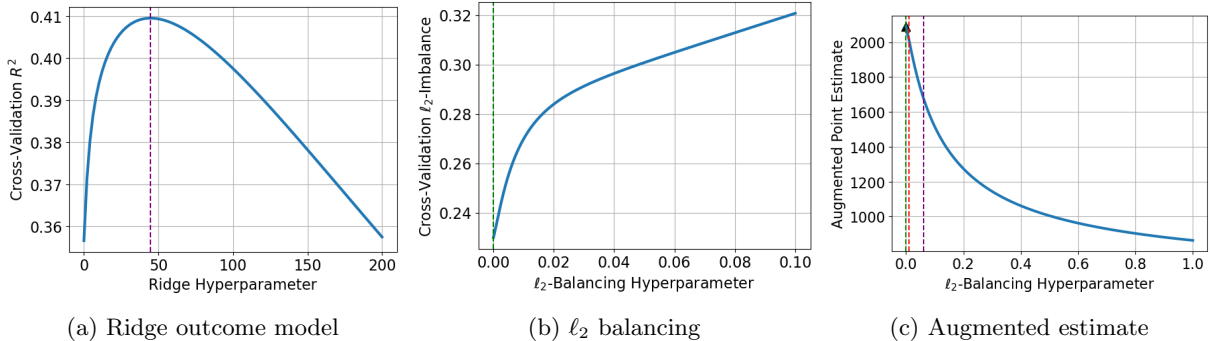


Figure 4: Ridge-augmented ℓ_2 balancing weights (“double ridge”) for LaLonde (1986) with the original 11 covariates. Panel (a) shows the 3-fold cross-validated R^2 for the Ridge-penalized regression of Y_p on $\hat{\Phi}_p$ among control units across the hyperparameter λ ; the purple dotted line shows the CV-optimal value, $\hat{\lambda}$. Panel (b) shows the 3-fold cross-validated imbalance for ℓ_2 balancing weights across the hyperparameter δ ; the green dotted line shows the CV-optimal value, which is $\delta = 0$ or exact balance. Panel (c) shows the point estimate for the augmented estimator across the weighting hyperparameter δ ; the black triangle corresponds to the OLS point estimate, the green dotted line corresponds to cross-validated balance, the red dotted line corresponds to cross-validated Riesz loss, and the purple dotted line corresponds to the ridge outcome hyperparameter.

oracle hyperparameters. We compare the oracle hyperparameters with three practical tuning schemes and then illustrate our results on the canonical LaLonde data set. In the Appendix also explore many extensions, including to nonlinear weights and to high-dimensional features.

There are many promising avenues for future research. The fundamental connection between doubly robust estimation and undersmoothing opens up several theory directions. While we focus on the special case of kernel ridge regression in Section 6.1, we anticipate that these connections will hold more broadly. Similarly, while our focus in this paper has been on interpreting balancing weights as a form of linear regression, the converse is also valid: we could instead focus on how many outcome regression-based plug-in estimators are, in fact, a form of balancing weights; see Lin and Han (2022) for connections between outcome modeling and density ratio estimation.

We also anticipate that the MSE we derive in Section 6.2 is a starting place for future theoretical analysis that can inform practice. We demonstrate in our simulation study that existing hyperparameter selection methods cannot perform uniformly well over all DGPs. We expect that analyzing the optimal hyperparameters, for example in a proportionate asymptotics regime, can either help devise new tuning schemes or inform which tuning method will work best on the dataset at hand.

We conjecture that these results may provide new insights into the estimation of causal effects in the proximal causal inference framework (Tchetgen Tchetgen et al., 2020). This framework uses proxy variables to identify causal effects in the presence of unmeasured confounding. Estimation has been complicated by the fact that, in the absence of strong parametric assumptions, estimators of proximal causal effects are solutions to ill-posed Fredholm integral equations. Ghassami et al. (2022) and Kallus et al. (2021) recently proposed tractable nonparametric estimators in this setting. They use an “adversarial” version of double kernel ridge regression — allowing the weighting and outcome models to have different bases — to estimate the solution to the required Fredholm integral equations. Our results apply immediately to standard augmented estimators with different bases for the outcome and weighting models, either via a union basis (Chernozhukov et al., 2022d) or by applying an appropriate projection as in Hirshberg and Wager (2021), and extending these results to proximal causal effect estimators might help in constructing new proximal balancing weights, matching, or regression estimators with attractive asymptotic properties.

Finally, many common panel data estimators are forms of augmented balancing weight estimation ([Abadie et al., 2010](#); [Ben-Michael et al., 2021c](#); [Arkhangelsky et al., 2021](#)). We plan to use the numeric results here, especially the results for simplex-constrained weights in [Appendix D.2](#), to better understand connections between methods and to inform inference.

References

- A. Abadie, A. Diamond, and J. Hainmueller. Synthetic control methods for comparative case studies: Estimating the effect of california’s tobacco control program. *Journal of the American statistical Association*, 105(490):493–505, 2010.
- A. Agarwal and R. Singh. Causal inference with corrupted data: Measurement error, missing values, discretization, and differential privacy. *arXiv preprint arXiv:2107.02780*, 2021.
- A. Agarwal, Y. S. Tan, O. Ronen, C. Singh, and B. Yu. Hierarchical shrinkage: Improving the accuracy and interpretability of tree-based models. In K. Chaudhuri, S. Jegelka, L. Song, C. Szepesvari, G. Niu, and S. Sabato, editors, *Proceedings of the 39th International Conference on Machine Learning*, volume 162 of *Proceedings of Machine Learning Research*, pages 111–135. PMLR, 17–23 Jul 2022. URL <https://proceedings.mlr.press/v162/agarwal22b.html>.
- D. Arbour and A. Feller. The role of simplex constraints in regularizing treatment effect estimates. 2024.
- D. Arkhangelsky, S. Athey, D. A. Hirshberg, G. W. Imbens, and S. Wager. Synthetic difference-in-differences. *American Economic Review*, 111(12):4088–4118, 2021.
- A. Armagan, M. Clyde, and D. Dunson. Generalized beta mixtures of gaussians. *Advances in neural information processing systems*, 24, 2011.
- S. Athey, G. W. Imbens, and S. Wager. Approximate residual balancing: debiased inference of average treatment effects in high dimensions. *Journal of the Royal Statistical Society: Series B (Statistical Methodology)*, 80(4):597–623, 2018.
- P. Bach, O. Schacht, V. Chernozhukov, S. Klaassen, and M. Spindler. Hyperparameter tuning for causal inference with double machine learning: A simulation study. *arXiv preprint arXiv:2402.04674*, 2024.
- R. Bai and M. Ghosh. The inverse gamma-gamma prior for optimal posterior contraction and multiple hypothesis testing. *arXiv preprint arXiv:1710.04369*, 2017.
- P. L. Bartlett, P. M. Long, G. Lugosi, and A. Tsigler. Benign overfitting in linear regression. *Proceedings of the National Academy of Sciences*, 117(48):30063–30070, 2020.
- F. Bauer, S. Pereverzev, and L. Rosasco. On regularization algorithms in learning theory. *Journal of complexity*, 23(1):52–72, 2007.
- A. Belloni, V. Chernozhukov, and C. Hansen. Inference on treatment effects after selection among high-dimensional controls. *The Review of Economic Studies*, 81(2):608–650, 2014.
- E. Ben-Michael, A. Feller, and E. Hartman. Multilevel calibration weighting for survey data. *arXiv preprint arXiv:2102.09052*, 2021a.
- E. Ben-Michael, A. Feller, D. A. Hirshberg, and J. R. Zubizarreta. The balancing act in causal inference. *arXiv preprint arXiv:2110.14831*, 2021b.
- E. Ben-Michael, A. Feller, and J. Rothstein. The augmented synthetic control method. *Journal of the American Statistical Association*, 116(536):1789–1803, 2021c.
- D. Benkeser and M. Van Der Laan. The highly adaptive lasso estimator. In *2016 IEEE international conference on data science and advanced analytics (DSAA)*, pages 689–696. IEEE, 2016.
- D. A. Bruns-Smith and A. Feller. Outcome assumptions and duality theory for balancing weights. In *International Conference on Artificial Intelligence and Statistics*, pages 11037–11055. PMLR, 2022.

- P. Bühlmann and B. Yu. Boosting with the l_2 loss: regression and classification. *Journal of the American Statistical Association*, 98(462):324–339, 2003.
- A. Caponnetto and E. De Vito. Optimal rates for the regularized least-squares algorithm. *Foundations of Computational Mathematics*, 7:331–368, 2007.
- C. M. Carvalho, N. G. Polson, and J. G. Scott. The horseshoe estimator for sparse signals. *Biometrika*, 97(2):465–480, 2010.
- A. Chattopadhyay and J. R. Zubizarreta. On the implied weights of linear regression for causal inference. *arXiv preprint arXiv:2104.06581*, 2021.
- A. Chattopadhyay, C. H. Hase, and J. R. Zubizarreta. Balancing vs modeling approaches to weighting in practice. *Statistics in Medicine*, 39(24):3227–3254, 2020.
- V. Chernozhukov, D. Chetverikov, M. Demirer, E. Duflo, C. Hansen, W. Newey, and J. Robins. Double/debiased machine learning for treatment and structural parameters. *The Econometrics Journal*, 21(1):C1–C68, 01 2018a.
- V. Chernozhukov, W. K. Newey, and R. Singh. Learning l_2 -continuous regression functionals via regularized riesz representers. *arXiv preprint arXiv:1809.05224*, 8, 2018b.
- V. Chernozhukov, J. C. Escanciano, H. Ichimura, W. K. Newey, and J. M. Robins. Locally robust semiparametric estimation. *Econometrica*, 90(4):1501–1535, 2022a.
- V. Chernozhukov, W. Newey, V. M. Quintas-Martinez, and V. Syrgkanis. Riesznet and forestriesz: Automatic debiased machine learning with neural nets and random forests. In *International Conference on Machine Learning*, pages 3901–3914. PMLR, 2022b.
- V. Chernozhukov, W. Newey, R. Singh, and V. Syrgkanis. Automatic debiased machine learning for dynamic treatment effects and general nested functionals. *arXiv preprint arXiv:2203.13887*, 2022c.
- V. Chernozhukov, W. K. Newey, and R. Singh. Automatic debiased machine learning of causal and structural effects. *Econometrica*, 90(3):967–1027, 2022d.
- V. Chernozhukov, W. K. Newey, and R. Singh. Debiased machine learning of global and local parameters using regularized riesz representers. *The Econometrics Journal*, 2022e.
- V. Chernozhukov, W. K. Newey, V. Quintas-Martinez, and V. Syrgkanis. Automatic debiased machine learning via riesz regression, 2024.
- R. H. Dehejia and S. Wahba. Causal effects in nonexperimental studies: Reevaluating the evaluation of training programs. *Journal of the American statistical Association*, 94(448):1053–1062, 1999.
- J.-C. Deville and C.-E. Särndal. Calibration estimators in survey sampling. *Journal of the American statistical Association*, 87(418):376–382, 1992.
- E. Dobriban and S. Wager. High-dimensional asymptotics of prediction: Ridge regression and classification. *The Annals of Statistics*, 46(1):247–279, 2018.
- J. C. Duchi, P. W. Glynn, and H. Namkoong. Statistics of robust optimization: A generalized empirical likelihood approach. *Mathematics of Operations Research*, 46(3):946–969, 2021.
- M. H. Farrell. Robust inference on average treatment effects with possibly more covariates than observations. *Journal of Econometrics*, 189(1):1–23, 2015.
- S. Fischer and I. Steinwart. Sobolev norm learning rates for regularized least-squares algorithms. *The Journal of Machine Learning Research*, 21(1):8464–8501, 2020.

- W. A. Fuller. Regression estimation for survey samples. *Survey Methodology*, 28(1):5–24, 2002.
- C. Gao, S. Yang, and J. K. Kim. Soft calibration for selection bias problems under mixed-effects models. *arXiv preprint arXiv:2206.01084*, 2022.
- A. Ghassami, A. Ying, I. Shpitser, and E. T. Tchetgen. Minimax kernel machine learning for a class of doubly robust functionals with application to proximal causal inference. In *International Conference on Artificial Intelligence and Statistics*, pages 7210–7239. PMLR, 2022.
- L. Goldstein and K. Messer. Optimal plug-in estimators for nonparametric functional estimation. *The annals of statistics*, pages 1306–1328, 1992.
- B. S. Graham, C. C. de Xavier Pinto, and D. Egel. Inverse probability tilting for moment condition models with missing data. *The Review of Economic Studies*, 79(3):1053–1079, 2012.
- Y. Grandvalet. Least absolute shrinkage is equivalent to quadratic penalization. In *International Conference on Artificial Neural Networks*, pages 201–206. Springer, 1998.
- A. Gretton, K. M. Borgwardt, M. J. Rasch, B. Schölkopf, and A. Smola. A kernel two-sample test. *The Journal of Machine Learning Research*, 13(1):723–773, 2012.
- J. Hainmueller. Entropy balancing for causal effects: A multivariate reweighting method to produce balanced samples in observational studies. *Political analysis*, 20(1):25–46, 2012.
- C. Harshaw, F. Sävje, D. Spielman, and P. Zhang. Balancing covariates in randomized experiments with the gram–schmidt walk design. *arXiv preprint arXiv:1911.03071*, 2019.
- T. Hastie, R. Tibshirani, J. H. Friedman, and J. H. Friedman. *The elements of statistical learning: data mining, inference, and prediction*, volume 2. Springer, 2009.
- T. Hastie, A. Montanari, S. Rosset, and R. J. Tibshirani. Surprises in high-dimensional ridgeless least squares interpolation. *Annals of statistics*, 50(2):949, 2022.
- C. Hazlett. Kernel balancing. *Statistica Sinica*, 30(3):1155–1189, 2020.
- J. K. Hellerstein and G. W. Imbens. Imposing moment restrictions from auxiliary data by weighting. *Review of Economics and Statistics*, 81(1):1–14, 1999.
- J. L. Hill. Bayesian nonparametric modeling for causal inference. *Journal of Computational and Graphical Statistics*, 20(1):217–240, 2011.
- K. Hirano, G. W. Imbens, and G. Ridder. Efficient estimation of average treatment effects using the estimated propensity score. *Econometrica*, 71(4):1161–1189, 2003.
- D. A. Hirshberg and S. Wager. Augmented minimax linear estimation. *The Annals of Statistics*, 49(6):3206–3227, 2021.
- D. A. Hirshberg, A. Maleki, and J. R. Zubizarreta. Minimax linear estimation of the retargeted mean. *arXiv preprint arXiv:1901.10296*, 2019.
- K. Imai and M. Ratkovic. Covariate balancing propensity score. *Journal of the Royal Statistical Society: Series B: Statistical Methodology*, pages 243–263, 2014.
- A. Jacot, F. Gabriel, and C. Hongler. Neural tangent kernel: Convergence and generalization in neural networks. *Advances in neural information processing systems*, 31, 2018.
- N. Kallus. Generalized optimal matching methods for causal inference. *J. Mach. Learn. Res.*, 21:62–1, 2020.

- N. Kallus, X. Mao, and M. Uehara. Causal inference under unmeasured confounding with negative controls: A minimax learning approach. *arXiv preprint arXiv:2103.14029*, 2021.
- E. H. Kennedy. Semiparametric doubly robust targeted double machine learning: a review. *arXiv preprint arXiv:2203.06469*, 2022.
- K. Kim, B. A. Niknam, and J. R. Zubizarreta. Scalable kernel balancing weights in a nationwide observational study of hospital profit status and heart attack outcomes. 2022a.
- M. P. Kim, C. Kern, S. Goldwasser, F. Kreuter, and O. Reingold. Universal adaptability: Target-independent inference that competes with propensity scoring. *Proceedings of the National Academy of Sciences*, 119(4):e2108097119, 2022b.
- P. Kline. Oaxaca-blinder as a reweighting estimator. *American Economic Review*, 101(3):532–37, 2011.
- D. Kobak, J. Lomond, and B. Sanchez. The optimal ridge penalty for real-world high-dimensional data can be zero or negative due to the implicit ridge regularization. *The Journal of Machine Learning Research*, 21(1):6863–6878, 2020.
- A. Krishna, H. D. Bondell, and S. K. Ghosh. Bayesian variable selection using an adaptive powered correlation prior. *Journal of statistical planning and inference*, 139(8):2665–2674, 2009.
- R. J. LaLonde. Evaluating the econometric evaluations of training programs with experimental data. *The American economic review*, pages 604–620, 1986.
- R. R. Lin, H. Z. Zhang, and J. Zhang. On reproducing kernel banach spaces: Generic definitions and unified framework of constructions. *Acta Mathematica Sinica, English Series*, 38(8):1459–1483, 2022.
- Z. Lin and F. Han. On regression-adjusted imputation estimators of the average treatment effect. *arXiv preprint arXiv:2212.05424*, 2022.
- T. Lumley, P. A. Shaw, and J. Y. Dai. Connections between survey calibration estimators and semiparametric models for incomplete data. *International Statistical Review*, 79(2):200–220, 2011.
- A. Menon and C. S. Ong. Linking losses for density ratio and class-probability estimation. In *International Conference on Machine Learning*, pages 304–313. PMLR, 2016.
- N. Moosavi, J. Häggström, and X. de Luna. The costs and benefits of uniformly valid causal inference with high-dimensional nuisance parameters. *Statistical Science*, 38(1):1–12, 2023.
- W. Mou, P. Ding, M. J. Wainwright, and P. L. Bartlett. Kernel-based off-policy estimation without overlap: Instance optimality beyond semiparametric efficiency, 2023. URL <https://arxiv.org/abs/2301.06240>.
- J. Murray and A. Feller. Bayesian causal models from a weighting perspective: Balance, bias, and double robustness. 2024.
- W. K. Newey. The asymptotic variance of semiparametric estimators. *Econometrica: Journal of the Econometric Society*, pages 1349–1382, 1994.
- W. K. Newey and J. R. Robins. Cross-fitting and fast remainder rates for semiparametric estimation. *arXiv preprint arXiv:1801.09138*, 2018.
- W. K. Newey and R. J. Smith. Higher order properties of gmm and generalized empirical likelihood estimators. *Econometrica*, 72(1):219–255, 2004.
- W. K. Newey, F. Hsieh, and J. Robins. Undersmoothing and bias corrected functional estimation. 1998.
- W. K. Newey, F. Hsieh, and J. M. Robins. Twicing kernels and a small bias property of semiparametric estimators. *Econometrica*, 72(3):947–962, 2004.

- B. Park, Y. Lee, and S. Ha. l_2 boosting in kernel regression. *Bernoulli*, 15(3):599–613, 2009.
- J. Piironen and A. Vehtari. Sparsity information and regularization in the horseshoe and other shrinkage priors. *Electronic Journal of Statistics*, 11(2):5018 – 5051, 2017. doi: 10.1214/17-EJS1337SI. URL <https://doi.org/10.1214/17-EJS1337SI>.
- N. G. Polson and J. G. Scott. Shrink globally, act locally: Sparse bayesian regularization and prediction. *Bayesian statistics*, 9(501-538):105, 2010.
- J. Qin and B. Zhang. Empirical-likelihood-based inference in missing response problems and its application in observational studies. *Journal of the Royal Statistical Society: Series B (Statistical Methodology)*, 69(1):101–122, 2007.
- J. Robins, M. Sued, Q. Lei-Gomez, and A. Rotnitzky. Comment: Performance of double-robust estimators when “inverse probability” weights are highly variable. *Statistical Science*, 22(4):544–559, 2007.
- J. Robins, L. Li, E. Tchetgen, A. van der Vaart, et al. Higher order influence functions and minimax estimation of nonlinear functionals. In *Probability and statistics: essays in honor of David A. Freedman*, volume 2, pages 335–422. Institute of Mathematical Statistics, 2008.
- J. M. Robins, A. Rotnitzky, and L. P. Zhao. Estimation of regression coefficients when some regressors are not always observed. *Journal of the American statistical Association*, 89(427):846–866, 1994.
- A. Rotnitzky, E. Smucler, and J. M. Robins. Characterization of parameters with a mixed bias property. *Biometrika*, 108(1):231–238, 2021.
- D. B. Rubin. Randomization analysis of experimental data: The fisher randomization test comment. *Journal of the American statistical association*, 75(371):591–593, 1980.
- M. Rubinstein, A. Haviland, and D. Choi. Balancing weights for region-level analysis: the effect of medicaid expansion on the uninsurance rate among states that did not expand medicaid. *arXiv preprint arXiv:2105.02381*, 2021.
- D. Shen, P. Ding, J. Sekhon, and B. Yu. A tale of two panel data regressions. *arXiv preprint arXiv:2207.14481*, 2022.
- X. Shen. On methods of sieves and penalization. *The Annals of Statistics*, 25(6):2555–2591, 1997.
- R. Singh. Debiased kernel methods. *arXiv preprint arXiv:2102.11076*, 2021.
- R. Singh, L. Xu, and A. Gretton. Kernel methods for causal functions: Dose, heterogeneous, and incremental response curves. *arXiv preprint arXiv:2010.04855*, 2020.
- R. Singh, L. Sun, et al. Double robustness for complier parameters and a semiparametric test for complier characteristics. Technical report, 2022.
- P. Speckman. Minimax estimates of linear functionals in a hilbert space. *Unpublished Manuscript*, 1979.
- Z. Tan. Regularized calibrated estimation of propensity scores with model misspecification and high-dimensional data. *Biometrika*, 107(1):137–158, 2020.
- D. Tang, D. Kong, W. Pan, and L. Wang. Ultra-high dimensional variable selection for doubly robust causal inference. *Biometrics*, 79(2):903–914, 2023.
- E. J. T. Tchetgen Tchetgen, A. Ying, Y. Cui, X. Shi, and W. Miao. An introduction to proximal causal learning. *arXiv preprint arXiv:2009.10982*, 2020.
- M. J. Van Der Laan and D. Rubin. Targeted maximum likelihood learning. *The international journal of biostatistics*, 2(1), 2006.

- M. J. Van der Laan, S. Rose, et al. *Targeted learning: causal inference for observational and experimental data*, volume 4. Springer, 2011.
- K. Vermeulen and S. Vansteelandt. Bias-reduced doubly robust estimation. *Journal of the American Statistical Association*, 110(511):1024–1036, 2015.
- Y. Wang and J. R. Zubizarreta. Minimal dispersion approximately balancing weights: asymptotic properties and practical considerations. *Biometrika*, 107(1):93–105, 2020.
- R. K. Wong and K. C. G. Chan. Kernel-based covariate functional balancing for observational studies. *Biometrika*, 105(1):199–213, 2018.
- Q. Zhao. Covariate balancing propensity score by tailored loss functions. *The Annals of Statistics*, 47(2): 965–993, 2019.
- Q. Zhao and D. Percival. Entropy balancing is doubly robust. *Journal of Causal Inference*, 5(1), 2017.
- J. R. Zubizarreta. Stable weights that balance covariates for estimation with incomplete outcome data. *Journal of the American Statistical Association*, 110(511):910–922, 2015.

Contents

1	Introduction	1
1.1	Related work	2
2	Problem setup and background	3
2.1	Setup and motivation	3
2.1.1	Example: Estimating counterfactual means	3
2.1.2	General class of functionals via the Riesz representer	3
2.2	Balancing weights: Background and general form	4
2.3	Linear balancing weights	4
3	Novel equivalence results for (augmented) balancing weights and outcome regression models	6
3.1	Weighting alone	6
3.2	Augmented balancing weights	7
4	Augmented ℓ_2 Balancing Weights	9
4.1	General linear outcome model	9
4.2	Ridge regression outcome model	11
5	Augmented ℓ_∞ balancing weights	12
5.1	Weighting alone	12
5.2	General linear outcome model	12
5.3	Lasso outcome model	13
6	Kernel Ridge Regression: Asymptotic and Finite Sample Analysis	14
6.1	Asymptotic Results	15
6.2	Finite Sample Mean-Squared Error	16
7	Numerical illustrations and hyperparameter tuning	16
7.1	Hyperparameter tuning for ridge-augmented ℓ_2 balancing	17
7.1.1	Oracle and practical hyperparameter tuning	17
7.1.2	Simulation study	18
7.2	Application to LaLonde (1986)	18
7.2.1	High-dimensional setting	19
7.2.2	Low-dimensional setting: Recovering OLS	19
8	Discussion	20
A	Additional background and examples	31
A.1	Examples of general linear functionals via the Riesz representer	31
A.2	Examples of balancing weights	31
A.3	Causal inference	32
A.4	Equivalences of outcome regression and balancing weighting methods	33
B	Details for when $d > n$	34
B.1	Balancing weights when $d > n$	34
B.2	Equivalences from Appendix A.4 when $d > n$	35
B.3	Propositions 3.1 and 3.2 when $d > n$	36
B.4	The RKHS Setting	36
C	Sample Splitting and Cross-Fitting	37

C.1	Proposition 3.2 with Sample Splitting	38
C.2	Unregularized Outcome Model	38
C.3	Unregularized Weight Model	39
C.4	“Double Ridge”	39
D	Nonlinear weights	39
D.1	General nonlinear weights	40
D.1.1	Illustration: LaLonde	41
D.2	Constraining weights to be non-negative	41
D.3	Non-Linear Differentiable Outcome Models	42
E	Results with Correlated Features	43
E.1	Overview	43
E.2	Augmented ℓ_2 Balancing Weights with Correlated Features	43
E.3	Augmented ℓ_∞ balancing weights	46
F	Undersmoothing with general weights as viewed by the normal equations	47
G	Comparison to TMLE with Balancing Weights	48
H	Simulation Study Details	49
H.1	Setup	49
H.2	Synthetic DGPs	49
H.3	Semi-Synthetic DGPs	50
I	Additional Numerical Experiments	50
I.1	Dataset Summaries	50
I.2	Numerical Example with cross-fitting	51
I.3	Additional Experiments	51
I.3.1	Low Dimensional	51
I.3.2	High Dimensional	52
I.4	Undersmoothing in LaLonde	52
I.4.1	Undersmoothing for double ridge	52
I.4.2	Undersmoothing in norm	53
I.5	Semi-Synthetic Bias vs Variance	53
J	Empirical Bayes Interpretation of Augmented ℓ_2 Balancing Weights	53
J.1	Fixed outcome coefficients	54
J.2	Accounting for uncertainty in outcome model coefficients via global-local shrinkage priors	55
J.2.1	Scale mixture of Normals	55
J.2.2	Inverse-Gamma Gamma Prior	57
J.2.3	Application to double ridge	57
J.3	Connection to Zellner’s g prior	60
K	Additional Proofs	62
L	Additional Details for Asymptotic Results	65

A Additional background and examples

A.1 Examples of general linear functionals via the Riesz representer

Example 1 (Counterfactual mean). Let $Z = \{0, 1\}$ and $\psi(m) = \mathbb{E}[m(X, 1)]$. Under SUTVA and conditional ignorability, this estimand is equal to $E[Y(1)]$. The Riesz representer is the IPW, $\alpha(X, Z) = Z/e(X)$.

Example 2 (Average derivative). Let $Z \in \mathbb{R}$ and $\psi(m) = \mathbb{E}[\frac{\partial}{\partial z} m(X, Z)]$. Under an appropriate generalization of SUTVA and conditional ignorability, this estimand corresponds to the average derivative effect of a continuous treatment. Under regularity conditions the Riesz representer is given by $\alpha(X, Z) = -\frac{\frac{d}{dz} p(Z|X)}{p(Z|X)}$ where $p(z|x)$ is the conditional density of Z given X .

Example 3 (Distribution shift). Consider an example without Z , following the machine learning literature on covariate shift. Let p denote the source distribution of the observed data, and let p^* over \mathcal{X} denote the target distribution. The estimand is then $\psi(m) = \int_{\mathcal{X}} m(x) dp^*(x)$. In a causal inference setting, this can recover the Average Treatment Effect on the Treated (ATT) under SUTVA and conditional ignorability; i.e., let p be the distribution of covariates and outcomes for units assigned to control and p^* be the distribution of the covariates for units assigned to treatment. The Riesz representer is the density ratio, $\alpha(X) = \frac{dp^*}{dp}(X)$.

Example 4 (Exact balancing weights). The most common balancing weights estimation problem finds the minimum weights that exactly balance each element of Φ . In the constrained form, exact balancing solves

$$\begin{aligned} \min_{w \in \mathbb{R}^n} \|w\|_2^2 \\ \text{such that } \frac{1}{n} w \phi_{pj} = \bar{\phi}_{qj} \quad \text{for all } j \end{aligned} \tag{11}$$

A.2 Examples of balancing weights

Example 5 (ℓ_2 balancing). The ℓ_2 balancing weights problem is usually expressed via its penalized form:

$$\min_{w \in \mathbb{R}^n} \left\{ \left\| \frac{1}{n} w \Phi_p - \bar{\Phi}_q \right\|_2^2 + \delta \|w\|_2^2 \right\}. \tag{12}$$

The automatic form is a ridge-penalized regression for the Riesz representer.

Example 6 (ℓ_∞ balancing). The constrained form of the ℓ_∞ balancing weights problem is

$$\begin{aligned} \min_{w \in \mathbb{R}^n} \|w\|_2^2 \\ \text{such that } \left\| \frac{1}{n} w \Phi_p - \bar{\Phi}_q \right\|_\infty \leq \delta \end{aligned} \tag{13}$$

The automatic form is a lasso-penalized regression for the Riesz representer, sometimes known as the Minimum Distance Lasso (Chernozhukov et al., 2022d).

Example 7 (Kernel balancing). As a brief preview of the balancing problem in the infinite-dimensional setting, we provide an example where $\mathcal{F} = \mathcal{H}$ is a reproducing kernel Hilbert space on $\mathcal{X} \times \mathcal{Z}$ with norm $\|\cdot\|_{\mathcal{H}}$ and kernel $\mathcal{K} : (\mathcal{X} \times \mathcal{Z}) \times (\mathcal{X} \times \mathcal{Z}) \rightarrow \mathbb{R}$. Then for any $x_i \in \mathcal{X}, z_i \in \mathcal{Z}$, the representer $\phi(x_i, z_i) := \mathcal{K}(x_i, z_i, \cdot, \cdot) \in \mathcal{H}$. Using infinite-dimensional matrix notation, we denote $\Phi_p \in \mathcal{H}^n$ and $\bar{\Phi}_q \in \mathcal{H}$ as above. The penalized balancing weights problem for $\mathcal{F} = \mathcal{H}$ is:

$$\min_{w \in \mathbb{R}^n} \left\{ \left\| \frac{1}{n} w \Phi_p - \bar{\Phi}_q \right\|_{\mathcal{H}}^2 + \delta \|w\|_2^2 \right\}. \tag{14}$$

See Appendix B for details and references.

A.3 Causal inference

We now return to Example 1 above. Here the goal is estimating the unobserved potential outcomes in an observational study. Let Y be the potential outcome under control (with appropriate restrictions, such as SUTVA; Rubin, 1980), let p be the population of individuals in the control condition, and let q be the population of individuals in the treatment condition. Then Y is observed for population p but not for population q , and the missing mean, $\mathbb{E}_q[Y]$, is the average potential outcome under control for the individuals who in fact were treated. Letting Y be the potential outcome under treatment, p the population of individuals in the treatment condition, and q the population of individuals in the control condition, $\mathbb{E}_q[Y]$ is the average potential outcome under treatment for the individuals who in fact received control.

For both examples, the crucial assumption for identification is *conditional ignorability*: the conditional distribution of Y given X is the same in the source and target populations. This is also known as “conditional exchangeability,” “selection on observables,” or “no unmeasured confounding.” For our purposes, we will require the mean, but not distributional, version of this assumption: $\mathbb{E}_p[Y|X] = \mathbb{E}_q[Y|X]$.

Since we assume the conditional expectations are the same in the two populations, we occasionally denote the common conditional mean functional without subscripts, $\mathbb{E}[Y|X]$. Under this assumption, we can identify $\mathbb{E}_q[Y]$ with the *regression functional*, also known as the *adjustment formula* or *g-formula*:

$$\mathbb{E}_q [\mathbb{E}_p[Y|X]] = \mathbb{E}_q [\mathbb{E}_q[Y|X]] = \mathbb{E}_q[Y]. \quad (15)$$

A complementary approach instead relies on the density ratio between the marginal covariate distributions in the source and target populations, $\frac{dq}{dp}(X)$, also known as the Radon-Nikodym derivative, importance sampling weights, or inverse propensity score weights (IPW).² This is also a special case of a Riesz representer (Chernozhukov et al., 2022d). Under an additional *population overlap assumption* that $q(x)$ is absolutely continuous with respect to $p(x)$, we can identify $\mathbb{E}_q[Y]$ via the *weighting functional*, also known as the *IPW functional*:

$$\mathbb{E}_p \left[\frac{dq}{dp}(X) Y \right] = \mathbb{E}_p \left[\frac{dq}{dp}(X) \mathbb{E}_p[Y|X] \right] = \mathbb{E}_q[\mathbb{E}_p[Y|X]] = \mathbb{E}_q[Y]. \quad (16)$$

Finally, we can combine the regression and weighting functionals to create a third identifying functional, known as the *doubly robust functional* (Robins et al., 1994):

$$\mathbb{E}_q [\mathbb{E}_p[Y|X]] + \mathbb{E}_p \left[\frac{dq}{dp}(X) \{Y - \mathbb{E}_p[Y|X]\} \right]. \quad (17)$$

This functional has the attractive property of being equal to $\mathbb{E}_q[Y]$ even if either one of $\frac{dq}{dp}(X)$ or $\mathbb{E}_p[Y|X]$ is replaced with an arbitrary function of X , hence the term “doubly robust.”³ See Chernozhukov et al. (2018a); Kennedy (2022) for recent overviews of the active literature in causal inference and machine learning focused on estimating versions of Equation (3).

The *augmented* estimators that we analyze in this paper are based on estimating this doubly robust functional. These estimators *augment* an estimator of the regression functional based on an outcome regression (or *base learner*) with appropriately weighted residuals. Alternatively, they *augment* an estimator of the weighting functional with an outcome regression-based estimator of the regression functional (subtracting off the implied estimator of $\frac{dq}{dp}(X)\mathbb{E}_p[Y|X]$).

²Using Bayes Rule, we can equivalently express $\frac{dq}{dp}(X)$ via the *propensity score* $P(1_p|X)$, where 1_p is the indicator that an observation from the size-proportional mixture distribution of p and q is from population p : $\frac{dq}{dp}(X) = \frac{1-P(1_p|X)}{P(1_p|X)} \frac{P(1_p)}{1-P(1_p)}$

³This functional is equal to $\mathbb{E}_q[Y]$ if $\mathbb{E}_p[Y|X]$ is replaced with an arbitrary well-behaved functional of X_p , because the first and last terms cancel and we are left with the weighting functional $\mathbb{E}_p[\frac{dq}{dp}(X)Y]$. It is also equal to $\mathbb{E}_q[Y]$ if $\frac{dq}{dp}(X)$ is replaced with an arbitrary well-behaved functional of X_p , because the $\mathbb{E}_p[h(X)(Y - \mathbb{E}_p[Y|X])]$ is equal to 0 for any h and therefore we are left with the regression functional $\mathbb{E}_q[\mathbb{E}_p[Y|X]]$.

Recall that under linearity the imbalance over all $f \in \mathcal{F}$ has a simple closed form. For any $f(x, z) = \theta^\top \phi(x, z) \in \mathcal{F}$, $\mathbb{E}[h(X, Z, f)] = \theta^\top \mathbb{E}[h(X, Z, \phi)]$, where $h(X, Z, \phi)$ is short-hand for the vector with j th entry $h(X, Z, \phi_j)$. We can then write the imbalance in terms of a transformed feature space $h(X, Z, \phi)$, giving a closed form that we can readily calculate by applying the linear functional ψ from (1) to the features ϕ :

$$\begin{aligned} \text{Imbalance}_{\mathcal{F}}(w) &:= \sup_{f \in \mathcal{F}} \left\{ \mathbb{E}[w(X, Z)f(X, Z)] - \mathbb{E}[h(X, Z, f)] \right\} \\ &= \sup_{\|\theta\| \leq 1} \left\{ \theta^\top \mathbb{E}[w(X, Z)\phi(X, Z)] - \theta^\top \mathbb{E}[h(X, Z, \phi)] \right\} \\ &= \left\| \mathbb{E}[w(X, Z)\phi(X, Z)] - \mathbb{E}[h(X, Z, \phi)] \right\|_*. \end{aligned}$$

Consider the counterfactual mean estimand $\psi(m) = \mathbb{E}[m(X, 0)|Z = 1]$. We have

$$\text{Imbalance}_{\mathcal{F}}(w) = \left\| \mathbb{E}[w(X, Z)\phi(X, Z)] - \mathbb{E}[\phi(X, 0)|Z = 1] \right\|_*.$$

For simplicity let $\phi(x, z) = x$. Now we get $\text{Imbalance}_{\mathcal{F}}(w) = |\mathbb{E}[w(X, Z)X] - \mathbb{E}[X|Z = 1]|$ and therefore, the balancing optimization problem finds weights w that reweight the total mean $\mathbb{E}[X]$ to approximate the conditional mean $\mathbb{E}[X|Z = 1]$.

A.4 Equivalences of outcome regression and balancing weighting methods

For the special case of ℓ_2 kernel balancing, the balancing weights problem is numerically equivalent to directly estimating the conditional expectation $\mathbb{E}[Y_p|\Phi_p]$ via kernel ridge regression and applying the estimated coefficients to $\bar{\Phi}_q$. We begin with the special case of unregularized linear regression and then present the more general setting. We initially present the results assuming $d < n$ and that Φ_p has rank d , turning to the high-dimensional case with $d > n$ in Appendix B.

Linear regression. Ordinary least squares regression is equivalent to a weighting estimator that exactly balances the feature means. See Fuller (2002) for discussion in the survey sampling literature; see Robins et al. (2007), Abadie et al. (2010), Kline (2011), and Chattopadhyay et al. (2020) for relevant discussions in the causal inference literature.

In particular, let \hat{w}_{exact} be the solution to the exact balancing weights problem in Example 4 in the main text. Let $\hat{\beta}_{\text{ols}} = (\Phi_p^\top \Phi_p)^{-1} \Phi_p^\top Y_p$ be the OLS coefficients from the regression of Y_p on Φ_p . We then have the following numerical equivalence:

$$\begin{aligned} \hat{\mathbb{E}}[\bar{\Phi}_q \hat{\beta}_{\text{ols}}] &= \hat{\mathbb{E}}[\hat{w}_{\text{exact}} \circ Y_p] \\ \underbrace{\bar{\Phi}_q (\Phi_p^\top \Phi_p)^{-1} \Phi_p^\top Y_p}_{\hat{\beta}_{\text{ols}}} &= \underbrace{\bar{\Phi}_q (\Phi_p^\top \Phi_p)^{-1} \Phi_p^\top}_{\frac{1}{n} \hat{w}_{\text{exact}}} Y_p, \end{aligned} \tag{18}$$

where the weights have the closed form $\frac{1}{n} \hat{w}_{\text{exact}} = \bar{\Phi}_q (\Phi_p^\top \Phi_p)^{-1} \Phi_p^\top$.

Ridge regression. This equivalence immediately extends to ridge regression (Speckman, 1979; Hirshberg et al., 2019; Kallus, 2020).⁴ Let $\hat{w}_{\ell_2}^\delta$ be the minimizer of the ℓ_2 balancing weights problem in Example 5 in the main text, with hyperparameter δ . Let

$$\hat{\beta}_{\text{ridge}}^\delta := \underset{\beta \in \mathbb{R}^d}{\text{argmin}} \left\{ \|Y_p - \Phi_p \beta\|_2^2 + \delta \|\beta\|_2^2 \right\} \tag{19}$$

⁴See Harshaw et al. (2019) for an interesting connection of this equivalence to experimental design. See Ben-Michael et al. (2021c) and Shen et al. (2022) for related applications in the panel data setting.

be the ridge regression coefficients from least squares regression of Y_p on Φ_p . We then have the following numerical equivalence:

$$\begin{aligned} \hat{\mathbb{E}}[\Phi_q \hat{\beta}_{\text{ridge}}^\delta] &= \hat{\mathbb{E}}[\hat{w}_{\ell_2}^\delta \circ Y_p] \\ \underbrace{\bar{\Phi}_q (\Phi_p^\top \Phi_p + \delta I)^{-1} \Phi_p^\top Y_p}_{\hat{\beta}_{\text{ridge}}^\delta} &= \underbrace{\bar{\Phi}_q (\Phi_p^\top \Phi_p + \delta I)^{-1} \Phi_p^\top Y_p}_{\frac{1}{n} \hat{w}_{\ell_2}^\delta}, \end{aligned} \tag{20}$$

where the weights have the closed form $\frac{1}{n} \hat{w}_{\ell_2}^\delta = \bar{\Phi}_q (\Phi_p^\top \Phi_p + \delta I)^{-1} \Phi_p^\top$. Thus, the estimate from ridge regression is identical to the estimate using the ℓ_2 balancing weights. We leverage this equivalence in Section 3 below.

Kernel ridge regression. In general, the same equivalence holds in the non-parametric setting where ϕ is the feature map induced by an RKHS. In particular, let $\mathcal{F} = \{f \in \mathcal{H} : \|f\|_{\mathcal{H}} \leq r\}$, where \mathcal{H} is a reproducing kernel Hilbert space (RKHS) on $\mathcal{X} \times \mathcal{Z}$ with kernel \mathcal{K} , $\|\cdot\|_{\mathcal{H}}$ denotes the norm of the RKHS, and $r > 0$. Then the equivalence above holds for $\phi(x, z) := \mathcal{K}(x, z, \cdot, \cdot)$. Although ϕ is typically infinite-dimensional, the Riesz Representer Theorem shows that the least squares regression and, equivalently, the balancing optimization problem have closed-form solutions. The least squares regression approach is *kernel ridge regression* and the weighting estimator is *kernel balancing weights* (see Hazlett, 2020; Kim et al., 2022a). Hirshberg et al. (2019) leverage this equivalence to analyze the asymptotic bias of kernel balancing weights. For further discussion of this equivalence see Gretton et al. (2012); Kallus (2020).

Finally, we briefly mention some additional papers that discuss relevant equivalences. In the context of panel data, Shen et al. (2022) establish connections between different forms of regression, which is especially relevant for our discussion of high-dimensional features in Appendix B. In addition, Lin and Han (2022) provide an interesting alternative perspective by demonstrating that a large class of outcome regression estimators can be viewed as implicitly estimating the density ratio of the covariate distributions in the two treatment groups. Our results generalize and unify many of these existing numeric equivalences.

B Details for when $d > n$

In this section, we extend our results to the high-dimensional setting. In all that follows we will assume that $d > n$ and we will assume Φ_p^\top has rank n .⁵ For $d = \infty$, we replace \mathbb{R}^d with any infinite-dimensional Hilbert space \mathcal{H} and we require the norm defining \mathcal{F} to be the norm of the Hilbert space. In this case, it should be understood that $\Phi_p \in \mathcal{H}^n$.

B.1 Balancing weights when $d > n$

In the main text, recall that there are three equivalent versions of the balancing weights problem: the penalized, constrained, and automatic form with hyperparameters $\delta_1, \delta_2, \delta_3 \geq 0$ respectively. When $\Phi_p^\top \Phi_p$ is no longer invertible, a unique solution may fail to exist for certain values of these hyperparameters. We provide the relevant technical caveats here.

We begin by mentioning that for $\delta_1 > 0$, the penalized form of the balancing weights optimization problem is strictly convex, and therefore a unique solution exists, regardless of whether $d > n$. However, when $\delta_1 = 0$, there could potentially be infinite many solutions. In this setting, we choose the one with the minimum

⁵Alternatively, we could follow Bartlett et al. (2020) and assume that, almost surely, the projection of Φ_p on the space orthogonal to any eigenvector of $\mathbb{E}[\Phi_p \Phi_p^\top]$ spans a space of dimension n . But as our results are numerical this has no real advantage.

norm:

$$\begin{aligned} & \min_{w \in \mathbb{R}^n} \|w\|_2^2 \\ \text{such that } & \|w\Phi_p - \bar{\Phi}_q\|_*^2 = \min_v \|v\Phi_p - \bar{\Phi}_q\|_*^2. \end{aligned} \tag{21}$$

If we define $\delta_{\min} := \min_v \|v\Phi_p - \bar{\Phi}_q\|_*^2$, we see that the minimum norm solution in Equation (21) corresponds to a solution to the constrained form of balancing weights with $\delta_2 = \delta_{\min}$. Importantly, no solution exists for $\delta_2 < \delta_{\min}$, and we must make the additional restriction that $\delta_2 \geq \delta_{\min}$. In particular, no solution exists for $\delta_2 = 0$ and we cannot achieve exact balance; that is, for all w , $w\Phi_p \neq \bar{\Phi}_q$.

As in the penalized form, the automatic form is strictly convex and a unique solution exists for $\delta_3 > 0$. When $\delta_3 = 0$ we choose the minimum norm solution: by duality this will be equivalent to the minimum norm solution to the penalized problem (see [Bruns-Smith and Feller, 2022](#)).

Note that for $d = \infty$, each ‘‘row’’ of Φ_p is a vector in a Hilbert space \mathcal{H} . To solve the balancing weights problem computationally, we need a closed-form solution to the Hilbert space norm $\|\cdot\|_{\mathcal{H}}$. For example, this is a tractable computation when \mathcal{H} is an RKHS.

[Singh \(2021\)](#) gives the automatic form of this problem. See also [Wong and Chan \(2018\)](#), [Hazlett \(2020\)](#), and [Kallus \(2020\)](#).

B.2 Equivalences from Appendix A.4 when $d > n$

We now extend the equivalences from Appendix A.4 to the high-dimensional case. Let $\delta \geq 0$ be the hyperparameter for the penalized form of balancing weights — as we note above, this is important to state explicitly, since the constrained form will not have a solution for all values of its hyperparameter. For hyperparameter $\delta > 0$, the solutions to ℓ_2 balancing weights and ridge regression are identical as in Equation (19) with no alterations; ridge regression works by default when $d > n$. On the other hand, when $\delta = 0$, there exist infinitely many solutions to the normal equations that define the solution to the OLS optimization problem. Since $(\Phi_p^\top \Phi_p)$ is not invertible, Equation (19) does not apply directly. Instead, we introduce the minimum norm solution to OLS:

$$\begin{aligned} & \min_{\beta \in \mathbb{R}^d} \|\beta\|_2^2 \\ \text{such that } & \|\Phi_p \beta - Y_p\|_2^2 = \min_{\beta'} \|\Phi_p \beta' - Y_p\|_2^2. \end{aligned}$$

See [Bartlett et al. \(2020\)](#) for an extensive discussion of this optimization problem and its statistical properties as an OLS estimator. For $d > n$, the minimum norm solution is:

$$\hat{\beta}_{\text{ols}} := (\Phi_p^\top \Phi_p)^\dagger \Phi_p^\top Y_p = \Phi_p^\top (\Phi_p \Phi_p^\top)^{-1} Y_p,$$

where A^\dagger denotes the pseudoinverse of a matrix A . Note that the definition holds in general.⁶ In the low-dimensional setting in the main text, $(\Phi_p^\top \Phi_p)$ is invertible, and so $(\Phi_p^\top \Phi_p)^\dagger = (\Phi_p^\top \Phi_p)^{-1}$. The second equality holds only when $d > n$.

A version of Equation (18) holds between the minimum norm ℓ_2 balancing weights and minimum norm OLS estimators. Because the minimum norm ℓ_2 balancing weights do not achieve exact balance, we change the notation from \hat{w}_{exact} to $\hat{w}_{\ell_2}^0$. In this setting, $\|\cdot\|_* = \|\cdot\|_2$ and the minimum-norm balancing weights problem in Equation (21) is also a minimum norm linear regression, but of $\bar{\Phi}_q \in \mathbb{R}^d$ on $\Phi_p^\top \in \mathbb{R}^{d \times n}$:

$$\hat{w}_{\ell_2}^0 = \Phi_p^\top (\Phi_p^\top \Phi_p)^\dagger \bar{\Phi}_q = (\Phi_p \Phi_p^\top)^{-1} \Phi_p \bar{\Phi}_q.$$

⁶For example, when $\Phi_p \in \mathcal{H}^n$ for an infinite-dimensional Hilbert space \mathcal{H} , $(\Phi_p^\top \Phi_p)^\dagger$ is guaranteed to exist, since it is bounded and has closed range.

Therefore, Equation (18) holds by replacing the inverse with the pseudo-inverse:

$$\begin{aligned}\hat{\mathbb{E}}[\Phi_q \hat{\beta}_{\text{ols}}] &= \hat{\mathbb{E}}[\hat{w}_{\ell_2}^0 \circ Y_p] \\ \hat{\mathbb{E}}[\underbrace{\Phi_q (\Phi_p^\top \Phi_p)^\dagger \Phi_p^\top Y_p}_{\hat{\beta}_{\text{ols}}}] &= \hat{\mathbb{E}}[\underbrace{\bar{\Phi}_q (\Phi_p^\top \Phi_p)^\dagger \Phi_p^\top \circ Y_p}_{\hat{w}_{\ell_2}^0}], \\ \hat{\mathbb{E}}[\underbrace{\Phi_q \Phi_p^\top (\Phi_p \Phi_p^\top)^{-1} Y_p}_{\hat{\beta}_{\text{ols}}}] &= \hat{\mathbb{E}}[\underbrace{\bar{\Phi}_q \Phi_p^\top (\Phi_p \Phi_p^\top)^{-1} \circ Y_p}_{\hat{w}_{\ell_2}^0}].\end{aligned}$$

B.3 Propositions 3.1 and 3.2 when $d > n$

The results in Propositions 3.1 and 3.2 apply to the setting where $d > n$ without any further alteration using the pseudo-inverse.

Proof of Proposition 3.1.

$$Y_p^\top \Phi_p \hat{\theta}^\delta = Y_p^\top \Phi_p \Phi_p^\dagger \Phi_p \hat{\theta}^\delta = Y_p^\top \Phi_p (\Phi_p^\top \Phi_p)^\dagger \Phi_p^\top \Phi_p \hat{\theta}^\delta = \hat{\beta}_{\text{ols}} \hat{\Phi}_q,$$

where the first two equalities follow from the pseudoinverse identities $A = AA^\dagger A$ and $A^\dagger = (A^\top A)^\dagger A^\top$ for any matrix A . \square

Likewise Proposition 3.2 holds exactly for $\hat{\beta}_{\text{ols}}$ defined with the pseudoinverse.

B.4 The RKHS Setting

The results for $d = \infty$ can be computed efficiently for reproducing kernel Hilbert spaces. For notational simplicity, we will consider the distribution shift setting from Example 3. Let \mathcal{H} be a possibly-infinite-dimensional RKHS on \mathcal{X} with kernel \mathcal{K} and induced feature map via the representer theorem, $\phi : \mathcal{X} \rightarrow \mathcal{H}$ with $\phi(x) = \mathcal{K}(x, \cdot)$. Let $\|\cdot\|_{\mathcal{H}}$ denote the norm of \mathcal{H} . Let K_p be the matrix with entries $\mathcal{K}(x_i, x_j)$, where $x_i, x_j \in \mathcal{X}$ are the i th and j th entries of X_p . Then $\Phi_p \Phi_p^\top = K_p$ is invertible.

We will write out the versions of the main results for $\mathcal{F} = \mathcal{H}$ to demonstrate how to compute the corresponding results for RKHSs even though $d = \infty$. Denote the solution to the regularized least squares problem in \mathcal{H} with $\lambda \geq 0$:

$$\hat{f}^\delta := \operatorname{argmin}_{f \in \mathcal{H}} \|f(X_p) - Y_p\|_2^2 + \lambda \|f\|_{\mathcal{H}}^2.$$

This is equivalent to the following problem by the representer theorem:

$$\begin{aligned}\hat{\beta}_{\mathcal{H}}^\delta &:= \operatorname{argmin}_{\beta \in \mathbb{R}^n} \|K\beta - Y_p\|_2^2 + \lambda \beta^\top K \beta \\ &= (K_p + \lambda I)^{-1} Y_p.\end{aligned}$$

Let $K_{x,p} \in \mathbb{R}^n$ be the row vector with entries $\mathcal{K}(x, x_i)$ where x is an arbitrary element of \mathcal{X} and x_i is the i th entry of X_p . Then for any element $x \in \mathcal{X}$, $\hat{f}^\delta(x) = K_{x,p} \hat{\beta}_{\mathcal{H}}^\delta$. In particular, let define $K_{q,p}$ as the matrix with (i, j) th entry $\mathcal{K}(x_{qi}, x_{pj})$ where x_{qi} is the i th sample from the target population and x_{qj} is the j th entry of X_p . Furthermore, define $\bar{K}_{q,p} := \hat{\mathbb{E}}[K_{p,q}] \in \mathbb{R}^n$. Then, for any solution $\hat{w}_{\mathcal{H}}^\delta$ to the penalized form of balancing weights with function class \mathcal{F} and hyperparameter $\delta \geq 0$:

$$\hat{w}_{\mathcal{H}}^\delta = (K_p + \lambda I)^{-1} \bar{K}_{q,p}. \quad (22)$$

The proof follows from the closed-form of $\operatorname{Imbalance}_{\mathcal{H}}(w)$, known as the Maximum Mean Discrepancy (MMD) (Gretton et al., 2012); see, e.g., Hirshberg et al. (2019); Kallus (2020); Bruns-Smith and Feller (2022).

With these preliminaries, we immediately have the following equivalence from [Hirshberg et al. \(2019\)](#), which generalizes [Appendix A.4](#) to the RKHS case:

$$\begin{aligned}\hat{\mathbb{E}}[K_{q,p}\hat{\beta}_{\mathcal{H}}^\delta] &= \hat{\mathbb{E}}[\hat{w}_{\mathcal{H}}^\delta \circ Y_p] \\ \hat{\mathbb{E}}[K_{q,p}\underbrace{(K_p + \delta I)Y_p}_{\hat{\beta}_{\mathcal{H}}^\delta}] &= \hat{\mathbb{E}}[\underbrace{\bar{K}_{q,p}(K_p + \delta I)^{-1} \circ Y_p}_{\hat{w}_{\mathcal{H}}^\delta}].\end{aligned}\tag{23}$$

Likewise, we have the following form for [Proposition 3.1](#). Define $\hat{K}_{q,p} := \hat{w}_{\mathcal{H}}^{\delta T} K_p$. Then, for any $\delta \geq 0$:

$$\hat{\mathbb{E}}[\hat{w}_{\mathcal{H}}^\delta \circ Y_p] = \hat{\mathbb{E}}[\hat{K}_{q,p}\hat{\beta}_{\mathcal{H}}^0].$$

The resulting expression for [Proposition 3.2](#) is:

$$\hat{\mathbb{E}}[\hat{w}_{\mathcal{H}}^\delta \circ Y_p] + \hat{\mathbb{E}}\left[\left(K_{q,p} - \hat{K}_{q,p}^\delta\right)\hat{\beta}_{\mathcal{H}}^\lambda\right] = \hat{\mathbb{E}}[K_{q,p}\hat{\beta}_{\text{aug}}],$$

where the j th element of $\hat{\beta}_{\text{aug}}$ is:

$$\begin{aligned}\hat{\beta}_{\text{aug},j} &:= (1 - a_j^\delta)\hat{\beta}_{\mathcal{H},j}^\lambda + a_j^\delta\hat{\beta}_{\mathcal{H},j}^0 \\ a_j^\delta &:= \frac{\hat{\Delta}_j^\delta}{\Delta_j},\end{aligned}$$

where $\Delta_j = \bar{K}_{q,p,j} - \bar{K}_{p,j}$ and $\hat{\Delta}_j^\delta = \hat{K}_{q,p,j}^\delta - \bar{K}_{p,j}$ with $\bar{K}_{p,j} := \hat{\mathbb{E}}[K_p]$.

Identical versions for the RKHS setting apply to [Section 4](#). These follow directly from the expressions above so we will omit repeating them explicitly. Importantly, equivalent versions for ℓ_∞ balancing in [Section 5](#) do *not* follow immediately because an infinite dimensional vector space equipped with the ℓ_1 norm does not form a Hilbert space. We conjecture that such extensions could be constructed using the Reproducing Kernel Banach Space literature ([Lin et al., 2022](#)).

C Sample Splitting and Cross-Fitting

We briefly discuss the application of our numerical results in the setting with sample splitting. In standard balancing weights, we fit the weighting model θ^δ using data Φ_p from population p — and then also apply the weighting model at Φ_p . Cross-fitting breaks possible dependencies by only applying parameters on samples that were not used for estimation; this is a core technique in AutoDML ([Chernozhukov et al., 2022d](#)) and has been widely studied in the recent literature on doubly robust estimation (see, for example [Newey and Robins, 2018](#); [Kennedy, 2022](#)). With cross-fitting, our numerical results only hold approximately, though we argue that the overall behavior of the estimators is qualitatively similar.

To illustrate this, let the n samples from population p be split into S partitions or “splits” and assume for simplicity that each split has size $n' := n/S$. Denote the split s covariates $\Phi_{p,s}$ and outcomes $Y_{p,s}$. Let $\Phi_{p,-s}$ and $Y_{p,-s}$ denote covariates and outcomes that are not in split s . As a simple example, consider cross-fit, unaugmented ℓ_2 balancing weights with parameter $\delta = 0$ (i.e., OLS). For each split, we first solve the balancing problem *out-of-sample* by solving for the coefficients as in the example in [Equation \(18\)](#):

$$\begin{aligned}\hat{\theta}_{-s}^0 &:= \operatorname{argmin}_{\theta \in \mathbb{R}^d} \left\{ \left\| \frac{1}{n-n'} \theta \Phi_{p,-s}^\top \Phi_{p,-s} - \bar{\Phi}_q \right\|_2^2 \right\} \\ &= (n - n') \bar{\Phi}_q (\Phi_{p,-s}^\top \Phi_{p,-s})^\dagger.\end{aligned}$$

Note that we have re-written the balancing problem to be in terms of the coefficients θ instead of the weights $w = \theta \Phi_{p,-s}$, in order to emphasize that the goal is to apply this weighting model to the split s samples to

obtain weights $\hat{\theta}_{-s}^0 \Phi_{p,s}^\top$. The split s balancing weights estimate is then $\frac{1}{n'} \hat{\theta}_{-s}^0 \Phi_{p,s}^\top Y_{p,s}$ and the final cross-fit estimator averages over these splits:

$$\frac{1}{S} \sum_{s=1}^S \hat{\theta}_{-s}^0 \Phi_{p,s}^\top Y_{p,s}.$$

Note that the coefficients $\hat{\theta}_{-s}^0$ enforce exact balance — but only for data outside split s . In general, these weights will not achieve exact balance for split s . That is:

$$\begin{aligned} \left\| \frac{1}{n-n'} \hat{\theta}_{-s}^0 \Phi_{p,-s}^\top \Phi_{p,-s} - \bar{\Phi}_q \right\|_2 &= 0, \\ \left\| \frac{1}{n'} \hat{\theta}_{-s}^0 \Phi_{p,-s}^\top \Phi_{p,s} - \bar{\Phi}_q \right\|_2 &\neq 0. \end{aligned}$$

For an augmented estimator, we would also fit an outcome model using data from outside split s . For example, we could fit OLS:

$$\hat{\beta}_{\text{ols},-s} := (\Phi_{p,-s}^\top \Phi_{p,-s})^\dagger \Phi_{p,-s}^\top Y_{p,-s}.$$

The augmented estimator combining $\hat{\theta}_{-s}^0$ with $\hat{\beta}_{\text{ols},-s}$ would give:

$$\frac{1}{S} \sum_{s=1}^S \left(\bar{\Phi}_q \hat{\beta}_{\text{ols},-s} + \frac{1}{n'} \hat{\theta}_{-s}^0 \Phi_{p,s}^\top (Y_{p,s} - \Phi_{p,s} \hat{\beta}_{\text{ols},-s}) \right).$$

C.1 Proposition 3.2 with Sample Splitting

For Proposition 3.2 with sample splitting, within a single split the numerical result is identical, but the substantive point of interest is that we always shift coefficients toward the *in-sample* OLS coefficients.

Let the coefficients $\hat{\beta}_{-s}^\lambda$ and $\hat{\theta}_{-s}^\delta$ be fixed vectors; in practice they will be models fit using samples not in s . Define $\hat{\Phi}_{q,s}^\delta := \frac{1}{n'} \hat{\theta}_{-s}^\delta \Phi_{p,s}^\top \Phi_{p,s}$, and $\hat{\beta}_{\text{ols},s} := (\Phi_{p,s}^\top \Phi_{p,s})^\dagger \Phi_{p,s}^\top Y_{p,s}$. Then the augmented estimator in the s th partition follows immediately from Proposition 3.2 in the main text:

$$\hat{\mathbb{E}}[\Phi_q \hat{\beta}_{\text{aug},s}],$$

where the j th element of $\hat{\beta}_{\text{aug},s}$ is:

$$\begin{aligned} \hat{\beta}_{\text{aug},s,j} &:= (1 - a_{j,s}^\delta) \hat{\beta}_{-s,j}^\lambda + a_{j,s}^\delta \hat{\beta}_{\text{ols},s,j} \\ a_{j,s}^\delta &:= \frac{\hat{\Delta}_{j,s}^\delta}{\Delta_{j,s}}, \end{aligned}$$

where $\Delta_{j,s} = \bar{\Phi}_{q,j} - \bar{\Phi}_{p,s,j}$ and $\hat{\Delta}_{j,s}^\delta = \hat{\Phi}_{q,s,j}^\delta - \bar{\Phi}_{p,j}$.

C.2 Unregularized Outcome Model

Whereas Proposition 3.2 is unchanged by sample splitting, some of the equivalence results are affected by sample splitting. For example, we know from [Robins et al. \(2007\)](#) that when the base learner is unregularized, i.e., $\hat{\beta}_{\text{reg}}^\lambda = \hat{\beta}_{\text{ols}}$, then the entire estimator collapses to OLS alone. With sample splitting, this is only true if $\hat{\beta}_{\text{reg}}^\lambda = \hat{\beta}_{\text{ols},s}$. With cross-fitting, however, the outcome model would typically be estimated using only data from outside split s .

For example, consider $\hat{\beta}_{\text{ols},-s}$ introduced above. Plugging this into the result in Appendix C.1 yields:

$$\hat{\beta}_{\text{aug},s,j} := (1 - a_{j,s}^\delta) \hat{\beta}_{\text{ols},-s,j}^\lambda + a_{j,s}^\delta \hat{\beta}_{\text{ols},s,j}.$$

When the OLS coefficients are fit out of sample, this prevents overfitting to the l th split. Augmentation shifts the out-of-split OLS coefficients back toward the in-split OLS coefficients. As the sample size in each split goes to infinity, then both $\hat{\beta}_{\text{ols},s}$ and $\hat{\beta}_{\text{ols},-s}$ converge to the same population OLS coefficients and the augmented coefficients converge to standard OLS for any weighting model $\theta^\delta \in \mathbb{R}^d$.

C.3 Unregularized Weight Model

Consider the opposite case where $\hat{\beta}_{\text{reg}}^\lambda$ is arbitrary and the weight model θ_{-s}^0 achieves exact balance between $\Phi_{p,-s}$ and Φ_q , as defined above. Then, as suggested in Appendix C.1, $\hat{\Phi}_{q,s}^0 := \hat{\theta}_{-s}^0 \Phi_{p,s}^\top \Phi_{p,s} \neq \bar{\Phi}_q$ in general. Instead, we only have an approximation:

$$a_{j,s}^\delta := \frac{\hat{\Phi}_{q,s,j}^0 - \bar{\Phi}_{p,s,j}}{\bar{\Phi}_{q,j} - \bar{\Phi}_{p,s,j}} \approx 1,$$

where the approximation becomes equality as the sample size in each split goes to infinity. As a result, $\hat{\beta}_{\text{aug},s} \approx \hat{\beta}_{\text{ols},s}$, the in-split OLS coefficients, where again these coefficients are equal as the sample size in each split goes to infinity.

C.4 “Double Ridge”

Similarly, whereas Proposition 4.3 reduced to a single ridge outcome model, with sampling splitting we instead obtain an affine combination of in-split and out-of-split ridge regressions. Let $\hat{\beta}_{-s}^\lambda$ and $\hat{\theta}_{-s}^\delta$ denote ridge and ℓ_2 balancing coefficients respectively fit outside of the l th split. For notational simplicity, assume that $(\Phi_{p,s}^\top \Phi_{p,s}) = \text{diag}(\sigma_{1,s}^2, \dots, \sigma_{d,s}^2)$ and similarly for $-s$. Then the augmented estimator in the s th split equals $\hat{\mathbb{E}}[\Phi_q \hat{\beta}_{\text{aug},s}]$, where

$$\hat{\beta}_{\text{aug},s,j} := \left(\frac{\sigma_{j,-s}^2 - \sigma_{j,s}^2 + \delta}{\sigma_{j,-s}^2 + \delta} \right) \hat{\beta}_{-s,j}^\lambda + \left(\frac{\sigma_{j,s}^2 + \delta}{\sigma_{j,-s}^2 + \delta} \right) \hat{\beta}_{s,j}^\delta.$$

D Nonlinear weights

Our main results focus on *linear* balancing weights, where $\hat{w} = \hat{\theta} \Phi_p^\top$. A rich tradition in survey statistics (e.g., [Deville and Särndal, 1992](#)), machine learning (e.g., [Menon and Ong, 2016](#)), and causal inference (e.g., [Zhao, 2019](#)) focuses instead on *non-linear* balancing weights, such as when the weights correspond to a specific *link function* $g(\cdot)$ applied to the linear predictor, $\hat{w} = g(\hat{\theta} \Phi_p^\top)$, or, equivalently, when the balancing weights problem penalizes an alternative dispersion penalty. Other balancing weights estimators are inherently nonlinear, for instance with weights estimated via a neural network ([Chernozhukov et al., 2022b](#)).

In this section, we extend our results to nonlinear weights. We first consider general, arbitrary weights. We then consider the special case of minimum-variance weights that are constrained to be non-negative, which includes many important examples ([Zubizarreta, 2015](#); [Athey et al., 2018](#); [Abadie et al., 2010](#)). For this special case, we show that the non-negativity constraint corresponds to sample trimming.

Before turning to these results, we briefly review several important examples of nonlinear weights.

- **Entropy balancing and alternative dispersion measures.** There is a large literature exploring alternative dispersion penalties for balancing weights and other calibrated estimators; see [Deville and Särndal \(1992\)](#) for a discussion in survey sampling and [Zhao \(2019\)](#) for a discussion in causal inference. The most common alternative to the variance penalty is *entropy balancing* ([Hainmueller, 2012](#)), which has a dual representation as linear weights passed through an exponential link function, $\hat{w} = \exp(\hat{\theta} \Phi_p^\top)$. For estimands like the Average Treatment Effect on the Treated, this implies a (calibrated) logistic regression model for the propensity score:

$$\hat{w} = \exp(\hat{\theta} \Phi_p^\top) = \text{logit}^{-1}(\hat{\theta} \Phi_p^\top) / \left(1 - \text{logit}^{-1}(\hat{\theta} \Phi_p^\top) \right).$$

See [Tan \(2020\)](#) for further discussion.

- **Traditional IPW via maximum likelihood estimation.** Importantly, the form above is purely numeric and does not depend on the particular estimation procedure for the dual parameters, θ . Thus, our results below also apply to the common practice of IPW with a maximum likelihood (or other) estimate of a logistic regression propensity score model, as well as to AIPW and *Double Machine Learning* estimators (Chernozhukov et al., 2018a).
- **Generalized Empirical Likelihood.** The balancing weights literature is closely related to the empirical likelihood approach, which also finds weights over units to estimate an outcome model. Examples of (generalized) empirical likelihood in similar settings include Hellerstein and Imbens (1999), Qin and Zhang (2007), Newey and Smith (2004), Graham et al. (2012), and Duchi et al. (2021). See Hirano et al. (2003, Sec 3) for a didactic example connecting inverse propensity score weighting, outcome modeling, and the empirical likelihood approach. Standard Empirical Likelihood estimators penalize the log of the weights, $\log(w)$. Many other dispersion choices are common; see, for example, Newey and Smith (2004).

Our results also apply to weighting methods that do not have this same structure, such as Covariate Balancing Propensity Scores (Imai and Ratkovic, 2014). Finally, the implied weights could also arise from an outcome model that can be represented as a linear smoother, such as a random forest; see, for example, Lin et al. (2022).

D.1 General nonlinear weights

We now show that Proposition 3.1 holds approximately for arbitrary, non-linear weights.

Proposition D.1. *Let $\hat{w} \in \mathbb{R}^n$, be any arbitrary weights. Denote the corresponding weighted features $\hat{\Phi}_q := \frac{1}{n} \hat{w} \Phi_p$. Let $\hat{\beta}_{ols} = (\Phi_p^\top \Phi_p)^\dagger \Phi_p^\top Y_p$ be the OLS coefficients of the regression of Y_p on Φ_p . Then for any $\eta \in \mathbb{R}^d$, $c \in \mathbb{R}$:*

$$\hat{\mathbb{E}}[\hat{w} \circ Y_p] = \hat{\Phi}_q \hat{\beta}_{ols} + \underbrace{(\hat{w} - \Phi_p \eta - c)^\top (Y_p - \Phi_p \hat{\beta}_{ols})}_{\text{approximation error}}.$$

Importantly, Proposition D.1 holds for arbitrary weights and, as we discuss above, does not require estimating the weights via a balancing weights optimization problem.

Because Proposition D.1 holds for any η and c , we have the following bound on the approximation error:

$$|\hat{\mathbb{E}}[\hat{w} \circ Y_p] - \hat{\Phi}_q \hat{\beta}_{ols}| \leq \min_{c, \eta} \|\hat{w} - \Phi_p \eta - c\|_2 \|Y_p - \Phi_p \hat{\beta}_{ols}\|_2, \quad (24)$$

where we could replace the 2-norms with any valid Hölder inequality pair.

The approximation error will necessarily depend on the specific data and target functional. We can nonetheless offer some remarks. First, when $d > n$, we have $\|Y_p - \Phi_p \hat{\beta}_{ols}\|_2 = 0$, and we recover Proposition 3.1 exactly. Thus, in the high dimensional setting, Proposition 3.2 holds exactly for arbitrary non-linear weights. For $n > d$, our bound on the approximation error will generally be non-zero and depends on the size of the deviations of \hat{w} from its linear projection — a natural measure of the “non-linearity” of the weights. For a given weight vector, we can compute this measure by first fitting an unpenalized linear regression of the weights on Φ_p and then taking the norm of the residuals. By a simple Taylor approximation argument, this value will be small when Φ_p is tightly concentrated around its mean.

Finally, following the argument in Section 3, we can extend this proposition to augmented estimators with nonlinear weights: the augmented estimator equals $\hat{\mathbb{E}}[\Phi_q \hat{\beta}_{aug}]$ (just as before) plus the approximation error in Proposition D.1. Therefore if *nonlinear* weights \hat{w} give exact balance, i.e., if $\hat{\Phi}_q = \bar{\Phi}_q$, then $\hat{\beta}_{aug} = \hat{\beta}_{ols}$, and the final point estimate differs from OLS by the approximation error in Proposition D.1.

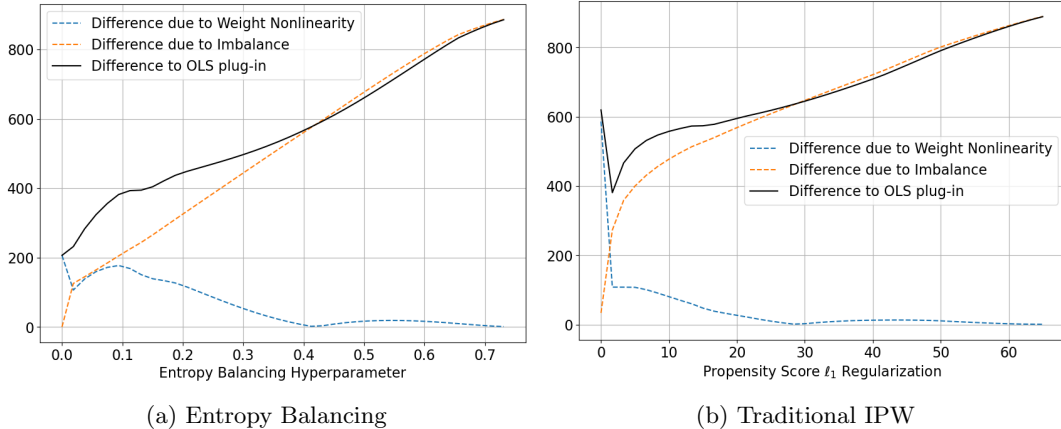


Figure D.1: Decomposing the estimate from nonlinear augmented balancing weights for the “short” LaLonde (1986) example.

D.1.1 Illustration: LaLonde

As an illustration, we compute both entropy balancing weights and logistic regression IPW weights for the “short” LaLonde dataset with $d = 11$ features. When targeting the Average Treatment Effect on the Treated, both weights have the same exponential link form.

We use a (cross-validated) lasso-penalized regression for the outcome model, and compute the corresponding augmented estimators, $\hat{\psi} := \bar{\Phi}_q^\top \hat{\beta}_{\text{reg}} + \hat{w}^\top (Y_p - \Phi_p \hat{\beta}_{\text{reg}})$, and augmented coefficients $\hat{\beta}_{\text{aug}}$ as defined in Proposition 3.2. We compare the augmented estimators to the plug-in OLS estimate via a triangle-inequality-type decomposition:

$$\begin{aligned} \text{Difference to OLS plug-in: } & |\bar{\Phi}_q^\top \hat{\beta}_{\text{ols}} - \hat{\psi}| \\ \text{Difference due to weight non-linearity: } & |\bar{\Phi}_q^\top \hat{\beta}_{\text{aug}} - \hat{\psi}| \\ \text{Difference due to imbalance: } & |\bar{\Phi}_q^\top \hat{\beta}_{\text{ols}} - \bar{\Phi}_q^\top \hat{\beta}_{\text{aug}}| \end{aligned}$$

We plot these metrics as a function on the entropy balancing hyperparameter and an ℓ_1 penalty for the propensity score model in Figure D.1.

Figure D.1 shows that there are two countervailing features at play here. First, as the weights become linear, $\hat{\psi} \rightarrow \bar{\Phi}_q^\top \hat{\beta}_{\text{aug}}$ with the difference quantified by Proposition D.1. This occurs as the regularization strength increases because regularization pushes the weights to be uniform. Second, as the imbalance goes to zero, $\hat{\beta}_{\text{aug}} \rightarrow \hat{\beta}_{\text{ols}}$. For entropy balancing, this happens exactly as the hyperparameter goes to zero. The IPW weights typically yield substantially larger imbalance, and this imbalance does not vanish as the regularization parameter goes to zero.

D.2 Constraining weights to be non-negative

A common modification of the (minimum variance) balancing weights problem is to constrain the estimated weights to be non-negative.⁷ Such weights have a number of attractive practical properties: they limit extrapolation; they ensure that the final weighting estimator is sample bounded; and they are typically sparse, which can sometimes aid interpretability (Robins et al., 2007; Abadie et al., 2010). Examples of constrained ℓ_∞ weights include Stable Balancing Weights and extensions (Zubizarreta, 2015; Athey et al.,

⁷Recall that we already impose the constraint that the weights sum to 1. So imposing non-negativity is equivalent to constraining the weights to be on the simplex.

2018; Wang and Zubizarreta, 2020); examples of constrained ℓ_2 weights include popular variants of the synthetic control method (Abadie et al., 2010; Ben-Michael et al., 2021c).

Using the dual form of the problem, Ben-Michael et al. (2021b) show that (minimum variance) linear balancing weights with a non-negativity constraint have the form $\hat{w} = \{\Phi_p \hat{\theta}^\delta\}_+$, where $\{x\}_+ = \max(x, 0)$ and where the coefficients $\hat{\theta}^\delta$ are generally different from the corresponding coefficients in the unconstrained model.⁸ We can apply this insight to extend Proposition 3.1 to non-negative weights.

Proposition D.2. *Let $\hat{w}_+^\delta := \{\Phi_p \hat{\theta}^\delta\}_+$, with $\hat{\theta}^\delta \in \mathbb{R}^d$ and where $\{x\}_+ = \max(x, 0)$, be any linear balancing weights with a non-negativity constraint, with corresponding weighted covariates $\hat{\Phi}_q^\delta := \hat{w}_+ \Phi_p$. Let Φ_{p+} , and Y_{p+} denote the respective quantities restricted to those data points where $\hat{w}_+^\delta > 0$. Let $\hat{\beta}_{ols}^+ := (\Phi_{p+}^\top \Phi_{p+})^{-1} \Phi_{p+}^\top Y_{p+}$ be the OLS coefficients of the regression of Y_{p+} on Φ_{p+} . Then:*

$$\hat{\mathbb{E}}[\hat{w}_+^\delta \circ Y_p] = \hat{\Phi}_q^\delta \hat{\beta}_{ols}^+.$$

So with the non-negativity constraint, we recover Proposition 3.1 almost exactly, except that the usual OLS coefficients from the entire population p , $\hat{\beta}_{ols}$, are replaced with the OLS coefficients from only those units with positive weight, $\hat{w}_+^\delta > 0$, $\hat{\beta}_{ols}^+$. We can therefore view the non-negativity constraint as a form of sample trimming. In particular, we can think of the data points where $\hat{w}_+^\delta = 0$ as a set of outliers — too dissimilar from the target population Φ_q — that we trim before applying OLS. But the key is that the definition of “outlier” depends the choice of δ and \mathcal{F} , and even the target covariates Φ_q : in general, changing δ , \mathcal{F} , or Φ_q will change the set where $\hat{w}_+^\delta > 0$. Defining and characterizing how this set changes is a promising avenue for future research. Finally, note that it is not generally the case that re-estimating the balancing weights problem after sample trimming will lead to non-negative weights (though this does hold for OLS).

Proposition D.2 simplifies further when the balancing weights achieve exact balance; see Rubinstein et al. (2021, Proposition 10) for a discussion of this special case. When $\hat{\Phi}_q = \Phi_q$, the balancing weight estimator with the non-negativity constraint is equivalent to $\hat{\mathbb{E}}[\Phi_q \hat{\beta}_{ols}^+]$. Thus, linear balancing weights with a simplex constraint is equivalent to trimming the control group and applying standard OLS (note that the trimming does not affect the target covariate profile, Φ_q).

Finally, we can extend the results in Proposition 3.2 for augmented balancing weights to incorporate a non-negativity constraint. Many popular augmented balancing weights estimators have the form of Proposition 3.2, including Athey et al. (2018) and Ben-Michael et al. (2021c). Understanding the implications of this connection is an interesting direction for future work.

D.3 Non-Linear Differentiable Outcome Models

In this section, we provide a very preliminary sketch of how the results might be extended to the case where \mathcal{F} is non-linear but still differentiable in its parameters.

Let $\mathcal{F} = \{f(X, \theta) : \theta \in \mathbb{R}^d, \nabla_\theta f(X, \theta) \text{ exists}\}$. Then just like Proposition 3.1 relates any w that are linear in X to the OLS coefficients, we can relate any $w \in \mathcal{F}$ to the least squares regressor in the function class \mathcal{F} .

First, let θ_{LS} be the unregularized least squares regressor (where we choose the least norm θ to break ties):

$$\theta_{LS} := \min_{\theta} \|Y_p - f(\theta, X_p)\|_2^2$$

We have the first-order condition:

$$\nabla_\theta f(\theta_{LS}, X_p)^\top (Y_p - f(\theta_{LS}, X_p)) = 0$$

⁸This “positive part link” representation is unique to the minimum variance weights. Other dispersion penalties, such as the entropy of the weights, imply a different link function. See Zhao (2019) and Ben-Michael et al. (2021b).

Now we can get a version of Proposition 2.1 for $w \in \mathcal{F}$ by considering the following Taylor expansion:

$$w(X_p) := f(\theta_w, X_p) \approx f(\theta_{LS}, X_p) + \nabla_{\theta} f(\theta_{LS}, X_p)(\theta_w - \theta_{LS})$$

In which case, applying the first-order condition above, we get:

$$w(X_p)^\top y \approx \underbrace{w(X_p)^\top f(\theta_{LS}, X_p)}_{\text{identical to 3.1}} + \underbrace{f(\theta_{LS}, X_p)^\top (Y_p - f(\theta_{LS}, X_p))}_{\text{this term is zero in linear case}}.$$

E Results with Correlated Features

E.1 Overview

Throughout the main text, we have made the assumption that $\Phi_p^\top \Phi_p$ is a diagonal matrix. This is a useful simplifying assumption for illustrating the intuition behind our results. Our central result, Proposition 3.2, holds for arbitrary $\Phi_p^\top \Phi_p$. However, when $\Phi_p^\top \Phi_p$ is not diagonal, i.e. the covariates are correlated, there are some important additional subtleties for interpreting the results.

In Appendix E.2, we show that the results in the main text for ℓ_2 balancing weights still hold for non-diagonal $\Phi_p^\top \Phi_p$ by applying an additional rotation step. By contrast, in Appendix E.3, we demonstrate that diagonal $\Phi_p^\top \Phi_p$ is *not* without loss of generality for ℓ_∞ balancing. Not only do the weights not have a closed form, but the resulting augmented coefficients will not be sparse.

E.2 Augmented ℓ_2 Balancing Weights with Correlated Features

To begin, we provide the following characterization of ℓ_2 augmenting with correlated features *directly*, that is, without using Proposition 3.2:

Proposition E.1. *Let $\hat{w}_{\ell_2}^\delta$ denote the solution to the penalized linear form of balancing weights with parameter δ and $\mathcal{F} = \{f(x) = \theta^\top \phi(x) : \|\theta\|_2 \leq r\}$. Then,*

$$\hat{w}_{\ell_2}^\delta = \Phi_p (\Phi_p^\top \Phi_p + \delta I)^{-1} \bar{\Phi}_q.$$

Therefore, the augmented ℓ_2 balancing weights estimator with outcome model $\hat{\beta}_{reg} \in \mathbb{R}^d$ has the form,

$$\begin{aligned} \hat{\mathbb{E}}[\Phi_q \hat{\beta}_{reg}] + \hat{\mathbb{E}}[\hat{w}_{\ell_2}^\delta (Y_p - \Phi_p \hat{\beta}_{reg})] &= \hat{\mathbb{E}}[\Phi_q \hat{\beta}_{\ell_2}], \\ \hat{\beta}_{\ell_2} &:= (I - A_\delta) \hat{\beta}_{reg} + A_\delta \hat{\beta}_{ols} \\ A_\delta &:= (\Phi_p^\top \Phi_p + \delta I)^{-1} (\Phi_p^\top \Phi_p). \end{aligned} \tag{25}$$

For comparison, ridge regression with parameter δ has closed-form coefficients:

$$\hat{\beta}_{ridge}^\delta = (\Phi_p^\top \Phi_p + \delta I)^{-1} \Phi_p^\top Y_p = A_\delta \beta_{ols}.$$

This is a generalization of Proposition 4.1 to the correlated setting. The result follows by simply plugging in the closed-form of $\hat{w}_{\ell_2}^\delta$ into the augmented estimator. We will now show that the resulting $\hat{\beta}_{\ell_2}$ is equivalent to applying Proposition 3.2 to rotated versions of the outcome and weighting coefficients.

First, we define the rotated version of Proposition 3.2:

Proposition E.2. Let $\Phi_p^\top \Phi_p$ be arbitrary, with eigendecomposition $\Phi_p^\top \Phi_p = VD^2V^\top$ where D^2 is a diagonal matrix with j th entry σ_j^2 . For any $\hat{\beta}_{reg}^\lambda \in \mathbb{R}^d$, and any linear balancing weights estimator with estimated coefficients $\hat{\theta}^\delta \in \mathbb{R}^d$, and with $\hat{w}^\delta := \hat{\theta}^\delta \Phi_p^\top$ and $\hat{\Phi}_q^\delta := \hat{w}^\delta \Phi_p$, the resulting augmented estimator

$$\begin{aligned} & \hat{\mathbb{E}}[\hat{w}^\delta \circ Y_p] + \hat{\mathbb{E}} \left[\left(\Phi_q - \hat{\Phi}_q^\delta \right) \hat{\beta}_{reg}^\lambda \right] \\ &= \hat{\mathbb{E}}[\Phi_q V \hat{\beta}_{aug}^{rot}], \end{aligned}$$

where the j th element of $\hat{\beta}_{aug}^{rot}$ is:

$$\begin{aligned} \hat{\beta}_{aug,j}^{rot} &:= (1 - a_j^{rot}) \hat{\beta}_{reg,j}^{rot} + a_j^{rot} \hat{\beta}_{ols,j}^{rot} \\ a_j^{rot} &:= \frac{\hat{\Delta}_j^{rot}}{\Delta_j^{rot}}, \end{aligned}$$

defined in terms of the rotated quantities:

$$\begin{aligned} \hat{\beta}_{reg}^{rot} &:= V^\top \hat{\beta}_{reg}^\lambda, \\ \hat{\beta}_{ols}^{rot} &:= V^\top \hat{\beta}_{ols}^\lambda, \\ \hat{\Delta}^{rot} &:= (\hat{\Phi}_q - \bar{\Phi}_p)V, \\ \Delta^{rot} &:= (\bar{\Phi}_q - \bar{\Phi}_p)V. \end{aligned}$$

Proof. First notice that:

$$\begin{aligned} & \hat{\mathbb{E}}[\hat{w}^\delta \circ Y_p] + \hat{\mathbb{E}} \left[\left(\Phi_q - \hat{\Phi}_q^\delta \right) \hat{\beta}_{reg}^\lambda \right] \\ &= \hat{\mathbb{E}} \left[\hat{\Phi}_q^\delta \hat{\beta}_{ols}^\lambda + \left(\Phi_q - \hat{\Phi}_q^\delta \right) \hat{\beta}_{reg}^\lambda \right] \\ &= \hat{\mathbb{E}} \left[\hat{\Phi}_q^\delta V V^\top \hat{\beta}_{ols}^\lambda + \left(\Phi_q - \hat{\Phi}_q^\delta \right) V V^\top \hat{\beta}_{reg}^\lambda \right] \end{aligned}$$

Then the result follows immediately from Proposition 3.2 applied to the covariates $\Phi_p V$ and $\Phi_q V$ with weights \hat{w} and outcome model $V^\top \hat{\beta}_{reg}^\lambda$. \square

Note that we could also compute $\hat{\beta}_{aug}$ directly as in Proposition 3.2 because the original derivation does not depend on $\Phi_p^\top \Phi_p$ being diagonal. Combining the two propositions we have that:

$$\hat{\mathbb{E}}[\Phi_q \hat{\beta}_{aug}] = \hat{\mathbb{E}}[\Phi_q V \hat{\beta}_{aug}^{rot}].$$

However, *it is not the case* that $\hat{\beta}_{aug} = V \hat{\beta}_{aug}^{rot}$ in general. For ℓ_2 balancing weights, $V \hat{\beta}_{aug}^{rot}$ is the correct generalization of Proposition 3.2 to the correlated setting as we demonstrate in the next few propositions.

Proposition E.3. Let $\hat{\beta}_{\ell_2}$ be defined as in Equation (25). For the same weights $\hat{w}_{\ell_2}^\delta$, let $\hat{\beta}_{aug}$ and $\hat{\beta}_{aug}^{rot}$ be defined as in Propositions 3.2 and E.2 respectively. Then for any $\Phi_p^\top \Phi_p$ (diagonal or not):

$$\hat{\mathbb{E}}[\Phi_q \hat{\beta}_{\ell_2}] = \hat{\mathbb{E}}[\Phi_q V \hat{\beta}_{aug}^{rot}] = \hat{\mathbb{E}}[\Phi_q \hat{\beta}_{aug}].$$

Additionally, when $\Phi_p^\top \Phi_p$ is diagonal, then

$$\hat{\beta}_{\ell_2} = V \hat{\beta}_{aug}^{rot} = \hat{\beta}_{aug}.$$

However, when $\Phi_p^\top \Phi_p$ is not diagonal, then in general

$$\hat{\beta}_{\ell_2} = V \hat{\beta}_{aug}^{rot} \neq \hat{\beta}_{aug}.$$

Proof. The first claim follows from Propositions 3.2, E.2, and E.1. For the second claim, if $\Phi_p^\top \Phi_p$ is diagonal, then $V = I$ and $\hat{\beta}_{\text{aug}} = \hat{\beta}_{\text{aug}}^{\text{rot}}$. Next we will show for general $\Phi_p^\top \Phi_p$ that $\hat{\beta}_{\ell_2} = V\hat{\beta}_{\text{aug}}^{\text{rot}}$. Note that

$$A_\delta = V(D^2 + \delta I)^{-1}D^2V^\top,$$

and that

$$\begin{aligned}\hat{\Delta}^{\text{rot}} &= \bar{\Phi}_q(\Phi_p^\top \Phi_p + \delta I)^{-1}(\Phi_p^\top \Phi_p)V \\ &= \bar{\Phi}_qV(D^2 + \delta I)^{-1}D^2\end{aligned}$$

and so $\text{diag}(a^{\text{rot}}) = (D^2 + \delta I)^{-1}D^2$. Therefore,

$$\begin{aligned}V\hat{\beta}_{\text{aug}}^{\text{rot}} &= V(I - \text{diag}(a^{\text{rot}}))V^\top \hat{\beta}_{\text{reg}} + V\text{diag}(a^{\text{rot}})V^\top \hat{\beta}_{\text{ols}} \\ &= (VV^\top - A_\delta)\hat{\beta}_{\text{reg}} + A_\delta\hat{\beta}_{\text{ols}} \\ &= (I - A_\delta)\hat{\beta}_{\text{reg}} + A_\delta\hat{\beta}_{\text{ols}}.\end{aligned}$$

Finally, for a counter-example where $V\hat{\beta}_{\text{aug}}^{\text{rot}} \neq \hat{\beta}_{\text{aug}}$, see Appendix E.2. \square

Proposition E.4. *Consider the setting in Proposition E.3, but now assume that the outcome model $\hat{\beta}_{\text{reg}} = \hat{\beta}_{\text{ridge}}^\lambda$, the ridge regression coefficients of Y_p on Φ_p with hyperparameter λ . Then:*

$$\hat{\beta}_{\ell_2} = V(D^2 + \text{diag}(\gamma))^{-1}V^\top \Phi_p^\top Y_p,$$

where $\text{diag}(\gamma)$ is the diagonal matrix with j th entry

$$\gamma_j := \frac{\delta\lambda}{\sigma_j^2 + \lambda + \delta}.$$

Furthermore,

$$\|\hat{\beta}_{\text{ridge}}^\lambda\|_2 \leq \|\hat{\beta}_{\ell_2}\|_2 = \|V\hat{\beta}_{\text{aug}}^{\text{rot}}\|_2 \leq \|\hat{\beta}_{\text{ols}}\|_2,$$

but in general it is possible that:

$$\|\hat{\beta}_{\text{ols}}\|_2 < \|\hat{\beta}_{\text{aug}}\|_2.$$

Proof.

$$\begin{aligned}\hat{\beta}_{\ell_2} &= (I - A_\delta)(\Phi_p^\top \Phi_p + \lambda I)^{-1}\Phi_p^\top Y_p + A_\delta(\Phi_p^\top \Phi_p)^{-1}\Phi_p^\top Y_p \\ &= V\left[(I - (D^2 + \delta I)^{-1}D^2)(D^2 + \lambda I)^{-1} + (D^2 + \delta I)^{-1}D^2(D^2)^{-1}\right]V^\top \Phi_p^\top Y_p \\ &= V(D^2 + (\delta + \lambda)I)(D^2 + \delta I)^{-1}(D^2 + \lambda I)^{-1}V^\top \Phi_p^\top Y_p \\ &= V(D^2 + \text{diag}(\gamma))^{-1}V^\top \Phi_p^\top Y_p.\end{aligned}$$

We now demonstrate the two norm inequalities. First,

$$\begin{aligned}\|\hat{\beta}_{\text{ridge}}^\lambda\|_2^2 &\leq \|\hat{\beta}_{\ell_2}\|_2^2 \\ \iff \|V(D^2 + \lambda I)^{-1}V^\top \Phi_p^\top Y_p\|_2^2 &\leq \|V(D^2 + \text{diag}(\gamma))^{-1}V^\top \Phi_p^\top Y_p\|_2^2 \\ \iff Y_p^\top \Phi_p(V[(D^2 + \lambda I)^{-1}(D^2 + \lambda I)^{-1} - (D^2 + \text{diag}(\gamma))^{-1}(D^2 + \text{diag}(\gamma))^{-1}]V^\top)\Phi_p^\top Y_p &\geq 0 \\ \iff (D^2 + \lambda I)^{-1}(D^2 + \lambda I)^{-1} \preceq (D^2 + \text{diag}(\gamma))^{-1}(D^2 + \text{diag}(\gamma))^{-1} & \\ \iff (D^2 + \lambda I)^{-1} \preceq (D^2 + \text{diag}(\gamma))^{-1}. &\end{aligned}$$

Note that

$$\frac{1}{\sigma_j^2 + \gamma_j} = \left(\frac{1}{\sigma_j^2 + \lambda} \right) \left(\frac{\sigma_j^2 + \lambda + \delta}{\sigma_j^2 + \delta} \right), \quad (26)$$

and that

$$\frac{\sigma_j^2 + \lambda + \delta}{\sigma_j^2 + \delta} \geq 1. \quad (27)$$

Combining facts (26) and (27), we have $1/(\sigma_j^2 + \gamma_j) > 1/(\sigma_j^2 + \lambda)$, and we're done.

Similarly, for the second inequality:

$$\begin{aligned} \|\hat{\beta}_{\ell_2}\|_2^2 &\leq \|\hat{\beta}_{\text{ols}}\|_2^2 \\ \iff \|V(D^2 + \text{diag}(\gamma))^{-1}V^\top\Phi_p^\top Y_p\|_2^2 &\leq \|V(D^2)^{-1}V^\top\Phi_p^\top Y_p\|_2^2 \\ \iff (D^2 + \text{diag}(\gamma))^{-1} &\preceq (D^2)^{-1} \end{aligned}$$

which follows because $\gamma \geq 0$.

Finally, for a counter-example where $\|\hat{\beta}_{\text{ols}}\|_2 < \|\hat{\beta}_{\text{aug}}\|_2$, see Table E.1. \square

Even when $\Phi_p^\top\Phi_p$ is diagonal, if $\hat{\beta}_{\text{reg}}$ can be arbitrary — and in particular, adversarially chosen — then we are not guaranteed to see undersmoothing. Consider an arbitrary $\hat{\beta}_{\text{reg}}$ that ℓ_2 -smoothed with respect to OLS. That is, $\|\hat{\beta}_{\text{reg}}\|_2 \leq \|\hat{\beta}_{\text{ols}}\|_2$. If there are no other constraints on $\hat{\beta}_{\text{reg}}$, then there exist problem instances where $\hat{\beta}_{\ell_2}$ has ℓ_2 -norm larger than $\hat{\beta}_{\text{ols}}$ or smaller than $\hat{\beta}_{\text{reg}}$. For a simple example, consider $a^\delta = [0, 1/(1 + \delta)]$, and $\hat{\beta}_{\text{ols}} = [0, 1]$ — note that these are jointly realizable by some Φ_p, Y_p . Then $\hat{\beta}_{\text{reg}} = [1, 0]$ will have ℓ_2 -norm bigger than 1 for sufficiently large δ .

Empirical Results for augmented ℓ_2 -balancing weights. To see in practice that the rotated procedure obtains the properly undersmoothed augmented coefficients, we report norm values for ℓ_2 augmented estimators using both a ridge and a lasso base learner in the high-dimensional LaLonde and IHDP settings. The key takeaway is that $\hat{\beta}_{\ell_2} = V\hat{\beta}_{\text{aug}}^{\text{rot}}$ has the correct undersmoothing properties.

$\hat{\beta}_{\text{reg}}$	$\ \hat{\beta}_{\text{reg}}\ _2$	$\ \hat{\beta}_{\ell_2}\ _2$	$\ \hat{\beta}_{\text{ols}}\ _2$	$\ \hat{\beta}_{\text{aug}}\ _2$
LaLonde Ridge	6.495e3	1.160e4	4.469e7	4.633e7
LaLonde Lasso	7.273e3	1.154e4	4.469e7	4.633e7
IHDP Ridge	1.038	8.569	9.299	9.722
IHDP Lasso	1.262	8.666	9.299	9.626

Table E.1: The ℓ_2 norm of base learner coefficients, unrotated augmented coefficients, OLS coefficients, and properly rotated augmented coefficients. Results are reported for the LaLonde and IHDP datasets using their respective high-dimensional feature sets and with both ridge and lasso base learners.

E.3 Augmented ℓ_∞ balancing weights

When we use ℓ_∞ balancing for the weighting model (or equivalently the minimum distance lasso estimator for the Riesz representer), the story becomes more complicated. When $\Phi_p^\top\Phi_p$ is not diagonal, both the Lasso outcome model and the ℓ_∞ balancing weights lack a closed-form solution.

For Lasso with correlated features, the regularization path is qualitatively similar to the diagonal case. The coefficients start at OLS and shrink exactly to zero at different rates. However, due to the correlation between the features, each coefficient no longer linearly (or even monotonically) moves toward zero. Likewise, for ℓ_∞ balancing weights, we see similar behavior for the coefficients of the Riesz representer model. These coefficients are sparse, with regularization paths that move toward zero (but not monotonically).

In the diagonal setting, the regularization path for the augmented estimator, a_j^δ , is proportionate (element-wise) to $\hat{\theta}$. Therefore, because $\hat{\theta}$ is sparse, the augmented estimator coefficients defined in Proposition 3.2 is also sparse. For general design, the impact of $\hat{\theta}$ on the augmented coefficients also depends on the empirical covariance matrix.

Lemma E.5. *Let \hat{w} be the solution to balancing weights with hyperparameter δ for $\mathcal{F} = \{f(x) = \theta^\top \phi(x) : \|\theta\| \leq r\}$, where $\|\cdot\|$ is any norm. Let $\hat{\theta}$ be the corresponding solution to the dual form of balancing weights, so that $\hat{w} = \Phi_p \hat{\theta}$. Then,*

$$\hat{\Phi}_q = \hat{\theta}^\top \Sigma,$$

and

$$a_j^\delta = \frac{\hat{\theta}^\top \Sigma_j}{\bar{\Phi}_{q,j}}.$$

In the case of ℓ_∞ balancing, since $\hat{\theta}$ is sparse, a_j^δ is a sparse combination of the elements of the j th column of the empirical covariance matrix Σ . But unless this combination is exactly zero (typically a measure zero event), the resulting a^δ will not inherit sparsity from $\hat{\theta}$.

F Undersmoothing with general weights as viewed by the normal equations

Our key numerical result, Proposition 3.2, allows us to write augmented weighting estimators as a plug-in estimator using coefficients $\hat{\beta}_{\text{aug}}$. Notably, this result holds for weights \hat{w} as long as $\hat{w} = \hat{\theta} \Phi_p^\top$ for *any* vector $\hat{\theta} \in \mathbb{R}^d$. The numerical result holds even if $\hat{\theta}$ doesn't result in a reasonable estimator of the Riesz representer.

It is interesting to see under what conditions on \hat{w} does $\hat{\beta}_{\text{aug}}$ still behave as an “undersmoothed” estimator. We discussed some ways to define this in Appendix E.2; for example requiring that the ℓ_2 -norm of the coefficients be between that of the base learner $\hat{\beta}$ and $\hat{\beta}_{\text{ols}}$. In this section, we develop a different notion of “undersmoothing” in terms of the size of the normal equation violations. In penalized linear regression, the smaller the penalty, the closer the LHS of the normal equation gets to zero. Therefore one way to view “undersmoothing” is to measure the size of the normal equation violations. Formally, the first order condition of (unpenalized) linear regression with coefficients β is:

$$\mathcal{N}(\hat{\beta}_{\text{ols}}) := \Phi_p^\top (Y_p - \Phi_p \hat{\beta}_{\text{ols}}) = 0.$$

Define A to be the diagonal matrix with j th entry a_j as defined in Proposition 3.2. Then the corresponding normal equation violation (the gradient of the squared loss) for $\hat{\beta}_{\text{aug}}$ is:

$$\begin{aligned} \mathcal{N}(\hat{\beta}_{\text{aug}}) &= \Phi_p^\top (Y_p - \Phi_p A \hat{\beta}_{\text{ols}} - \Phi_p (I - A) \hat{\beta}) \\ &= \Phi_p^\top (Y - \Phi_p \hat{\beta}) + (\Phi_p^\top \Phi_p) A (\hat{\beta} - \hat{\beta}_{\text{ols}}) \\ &= \Phi_p^\top (Y - \Phi_p \hat{\beta}_{\text{ols}}) + (\Phi_p^\top \Phi_p) (A - I) (\hat{\beta} - \hat{\beta}_{\text{ols}}) \\ &= (\Phi_p^\top \Phi_p) (I - A) (\hat{\beta}_{\text{ols}} - \hat{\beta}) \end{aligned}$$

Note that when $A = 0$, we recover the original outcome model, e.g. $\hat{\beta}_{\text{aug}} = \hat{\beta}$ and so the normal equation violations of $\hat{\beta}$ can be written:

$$\mathcal{N}(\hat{\beta}) = (\Phi_p^\top \Phi_p)(\hat{\beta}_{\text{ols}} - \hat{\beta}).$$

In other words, how close $\hat{\beta}$ is to optimizing the squared loss (in terms of the size of the gradient) is just equal to how close the coefficients are to the OLS coefficients, but mediated via the sample covariance matrix. E.g. large eigenvalues of $\Phi_p^\top \Phi_p$ will amplify the difference more, and small eigenvalues less. The only difference with the augmented coefficients $\hat{\beta}_{\text{aug}}$ is the introduction of the scaling diagonal matrix $(I - A)$. If A is uniformly close to zero, it will damp the eigenvalues of the covariance matrix and result in small normal equation violations. This is most clear when the sample covariance matrix is diagonal with entries σ_j^2 . In this case, the j th element of the squared loss gradient becomes:

$$\sigma_j^2(1 - a_j)(\hat{\beta}_{\text{ols},j} - \hat{\beta}_j).$$

Whenever all a_j are between 0 and 2, then the violations of the normal equations for $\hat{\beta}_{\text{aug}}$ are guaranteed to be uniformly at least as small as that of $\hat{\beta}$.

G Comparison to TMLE with Balancing Weights

As pointed out in [Chernozhukov et al. \(2022d\)](#), the balancing weights estimator of the Riesz representer can be applied to any doubly-robust meta algorithm. In the main text, we used the standard AIPW form, but we can also consider the TMLE form [Van Der Laan and Rubin \(2006\)](#); [Van der Laan et al. \(2011\)](#). In the linear setting, for an outcome model $\hat{\beta}$ and weights $\hat{w} := \Phi_p \hat{\theta}$ this takes the form:

$$\bar{\Phi}_q^T(\hat{\beta} + \hat{\epsilon}\hat{\theta}),$$

where

$$\begin{aligned} \hat{\epsilon} &:= \operatorname{argmin}_\epsilon \left\{ \|Y_p - \Phi_p \hat{\beta} - \epsilon \hat{w}\|_2^2 \right\} \\ &= \frac{\hat{w}^T (Y_p - \Phi_p \hat{\beta})}{\hat{w}^T \hat{w}}. \end{aligned}$$

In this section, we show the explicit connection between the AIPW and TMLE forms which are closely related. This connection can be stated in two ways, an ‘‘AIPW-centric’’ form and a ‘‘TMLE-centric’’ form.

AIPW-centric version of stating the connection:

$$\begin{aligned} \text{AIPW: } & \bar{\Phi}_q^T \hat{\beta} + \frac{1}{n} \hat{w}^T (Y_p - \Phi_p \hat{\beta}) \\ \text{TMLE: } & \bar{\Phi}_q^T \hat{\beta} + \underbrace{\left(\frac{\bar{\Phi}_q^T \hat{\theta}}{\hat{\theta}^T \Phi_p^T \Phi_p \hat{\theta}} \right)}_{\text{scaled ratio of terms in Riesz loss}} \hat{w}^T (Y_p - \Phi_p \hat{\beta}) \end{aligned}$$

TMLE-centric version of stating the connection:

$$\begin{aligned}
 \text{TMLE: } & \bar{\Phi}_q^T \hat{\beta} + \hat{\epsilon} \bar{\Phi}_q^T \hat{\theta} \\
 \text{AIPW: } & \bar{\Phi}_q^T \hat{\beta} + \underbrace{\hat{\epsilon} \hat{\Phi}_q^T \hat{\theta}}_{\hat{\Phi}_q \text{ instead of } \bar{\Phi}_q}
 \end{aligned}$$

From the ‘‘AIPW-centric’’ version of the connection, we see the familiar $\hat{w}^T Y_p$ term appear in the TMLE, and can apply our main results to rewrite the TMLE estimator around $\hat{\beta}_{\text{ols}}$. However, because we now weight the average by a term that is different from $\frac{1}{n}$, the results may have different variance properties. We think this is a promising direction for future research.

H Simulation Study Details

H.1 Setup

We consider 36 different data generating processes (DGPs) for our simulation study. For each of them, we compare an oracle baseline with three feasible hyperparameter tuning schemes.

For the remainder of this section, we we say ‘‘numerically optimize’’, we mean using the `scipy.optimize.minimize` solver with tolerance `1e-12`. In particular, we pre-compute the SVD of the covariance matrix before solving, so that we can compute the pseudoinverse for all involved expressions in closed form without performing traditional matrix inversion during optimization.

For the oracle hyperparameters, we compute λ^* by numerically optimizing the in-distribution mean squared error for ridge regression from Section 6.2. We then fix $\lambda = \lambda^*$ and then numerically optimize the expression in Proposition 6.1 to get the MSE-optimal δ^*

The three feasible hyperparameter tuning schemes we consider, by contrast, use a particular draw of Y_p . In all cases, we choose λ by cross-validating a ridge outcome model. Then we considering choosing δ by: (1) cross-validating balance, (2) cross-validating the Riesz loss, and (3) setting δ equal to the cross-validated ridge λ . In all cases, cross-validation is performed 5-fold via numerical optimization as described above instead of using a grid.

Note that the oracle hyperparameters are only optimal in a setting where we have to pick a single λ and δ for each draw of Y_p . Cross-validation picks a new λ for each Y_p and so can theoretically outperform the oracle. This happens very rarely, but a non-zero amount of the time. Overall, the results in Table 1 suggest that this is still a very good baseline. Finally, note that we could have picked λ by cross validation for the oracle, and then solved for the optimal δ^* separately for each Y_p , fixing the CV value of λ . However, we cannot guarantee that the resulting δ will have any optimality properties, since the mean squared error expression is derived by averaging over Y_p draws for fixed values of λ and δ . But this could be an interesting follow up experiment.

In all cases, we take 1000 draws of Y_p and then compute the squared error and take their average as a monte carlo estimate of the mean squared error.

H.2 Synthetic DGPs

To compute the oracle λ^* and δ^* from Section 6.2, we need: the true coefficients, β_0 , the population covariance matrix, $\mathbb{E}[\Phi_p^T \Phi_p]$, a sample covariance matrix $\hat{\Sigma}$, the conditional variance σ^2 , and the target covariance mean, $\mathbb{E}[\Phi_q]$. So for each DGP, we need to specify these five objects.

We consider synthetic DGPs with three basic setups. They all use $n = 2000$ and $d = 50$. For each of the three setups, we draw a random β_0 , that is the absolute value of a d -dimensional standard normal, that is then normalized to have 2-norm equal to 1. The three setups each generate a population covariance matrix in roughly the same way. In each case, we choose a maximum and minimum eigenvalue, η_{\min} and η_{\max} respectively. We then generate an equally spaced grid between $\eta_{\min}^{1/c}$ and $\eta_{\max}^{1/c}$ for some curvature constant c . We choose the eigenvalues of the covariance matrix to be the numbers in this grid raised to the c th power. We then draw a random eigenvector matrix from the special orthogonal group, U , and form the covariance matrix from the eigenvectors and eigenvalues in the standard way. Next, we draw an Φ_p with $n = 2000$ samples from a mean-zero normal distribution with this covariance matrix, and compute $\hat{\Sigma} = \Phi_p^T \Phi_p / n$.

The three basic setups differ in the choice of η_{\min}, η_{\max} , and c . For setting 1 we choose $\eta_{\min} = 1e - 4$, $\eta_{\max} = 3$ and $c = 5000$. For setting 2 we choose $\eta_{\min} = 1e - 8$, $\eta_{\max} = 3$, and $c = 5000$. For setting 3, we choose $\eta_{\min} = 1e - 10$, $\eta_{\max} = 5$, $c = 10$.

Then for each of these basic setups, we create 10 DGPs, by consider all combinations of a list of $\mathbb{E}[\Phi_q]$ and σ^2 . We use $\sigma^2 \in \{0.1, 2\}$. For $\mathbb{E}[\Phi_q]$ we use: the vector of all 0.1, the vector of all 2, and then 3 vectors chosen randomly uniformly between -1 and 1 which are then scaled to have norm 1. Thus the total of $2 \times 5 = 10$ DGPs for each setup.

H.3 Semi-Synthetic DGPs

We then also use semi-synthetic DGPs based on Lalonde Long and IHDP Long (see Appendix I for details on these datasets). For each of these datasets, we recenter Φ_p and Y_p to have mean-zero. Then we choose β_0 to be the coefficients from cross-validated ridge regression of Y_p on Φ_p . We let σ^2 be the variance of the residuals from this regression, and we choose the population covariance matrix to be $\Phi_p^T \Phi_p / n$. Next, we *redraw* a new matrix of samples from a mean-zero normal distribution with this covariance matrix, and compute the sample covariance $\hat{\Sigma}$ from these *new* samples. For targets, we use the actual $\mathbb{E}[\Phi_q]$, but also include two perturbed versions where all even elements of $\mathbb{E}[\Phi_q]$ are either increased or decreased by a proportion of the norm of $\mathbb{E}[\Phi_q]$. For IHDP, the perturbation is 1/10 times the norm, for Lalonde, the perturbation is 1/100 times the norm.

So since for each semi-synthetic setting we have three values of $\mathbb{E}[\Phi_q]$ and one value of σ^2 , that corresponds to 6 DGPs each, for a total of 36 together with the synthetic DGPs.

I Additional Numerical Experiments

I.1 Dataset Summaries

The following table summarizes the number of samples and features in the datasets used for numerical illustrations. In the main text, we presented results for “LaLonde Short” and “LaLonde Long”, the [LaLonde \(1986\)](#) data with the original 11 features and the expanded 171 features from [Farrell \(2015\)](#).

In Appendix I.3, we also provide results for the Infant Health and Development Program (IHDP) dataset, a standard observational causal inference benchmark from [Hill \(2011\)](#). IHDP is based on data from a randomized control trial of an intensive home visiting and childcare intervention for low birth weight infants born in 1985. For all children, we have a range of baseline covariates (contained in “IHDP Short”), including both categorical covariates, like the mother’s educational attainment, and continuous covariates, like the child’s birth weight. Our goal is to estimate the average outcome (a standardized test score) in the absence of the intensive intervention. We additionally create an “IHDP Long” extended feature set that includes all pair-wise interaction terms between the discrete covariates and a second-order polynomial expansion of all continuous covariates.

Dataset	Features	Train Samples	Test Samples
LaLonde Short	11	727	185
LaLonde Long	171	727	185
IHDP Short	25	608	139
IHDP Long	193	608	139

Table I.2: Summary of the four datasets used for numerical illustrations including the number of features, the number of control/train observations (used as samples from p) and the number of treated/test observations (used as samples from q).

I.2 Numerical Example with cross-fitting

In Section 7.2.2, we demonstrated that for the low-dimensional NSW setting, the cross-validated weighting hyperparameter is $\delta = 0$. As a result, for any linear base learner, the augmented estimator is numerically equivalent to a simple OLS plug-in estimate. As discussed in Appendix C.3, with cross-fitting this should only remain approximately true. In this section, we numerically assess the sensitivity of this result to cross-fitting.

We repeat the experiment with the 11-dimensional NSW covariates using a lasso base learner and ℓ_∞ balancing weights. We perform 5-fold cross-fitting with random splits. In each split, we compute the augmented estimate using models fit with data from the other 4 splits as described at the beginning of Appendix C. Each model has its hyperparameter chosen separately by cross-validation. Thus for 5-fold cross-fitting, we fit 5 lasso regressions and 5 balancing weights estimators each with 4/5ths the sample size and a separate hyperparameter. In the manner of bootstrapping, we re-run this end-to-end procedure 1000 times for different random choices of the splits.

Note that there are two main ways that cross-fitting might cause the final estimate to deviate from simple OLS. The first is the variation due to only applying the models out of sample. The second is that with smaller sample sizes, cross-validation might select larger values for the hyperparameter. We find that for 80% of the 5×1000 weighting models, $\delta = 0$. In the remaining 20% some of the hyperparameters take on a very small but non-zero value. The mean δ is 0.0037 and the CDF across the 5×1000 models is given in Figure I.2a.

Figure I.2b shows a smoothed density plot for the cross-fit augmented estimates over the 1000 draws. The black dotted line marks the augmented estimate without cross-fitting (recall that this is identical to the plug-in OLS estimate for this dataset). The red dotted line marks the mean of the cross-fit estimates over the 1000 draws. *On average*, cross-fitting has virtually no effect on the augmented estimate — at least in this setting where the weighting hyperparameter is usually close to zero. However, there is substantial variation across the 1000 draws. In particular, the density is skewed and the mode of the cross-fit estimates is slightly smaller than the OLS point estimate. There is also a meaningful tail of estimates larger than the OLS point estimate, including a second larger mode.

I.3 Additional Experiments

I.3.1 Low Dimensional

We begin by providing corroborating results for the low dimensional setting. We repeat the experiments in Section 7.2.2 in three additional settings: the LaLonde low-dimensional setting with ℓ_2 balancing weights in Figure 4, the IHDP low-dimensional setting with ℓ_∞ balancing weights in Figure I.4, and the IHDP low-dimensional setting with ℓ_2 balancing weights in Figure I.5. In all of these cases, cross-validation for the weighting hyperparameter choose $\delta = 0$, and thus the augmented estimator is equivalent to the OLS plug-in estimate. These plots can be compared to Figure I.3 in the main text.

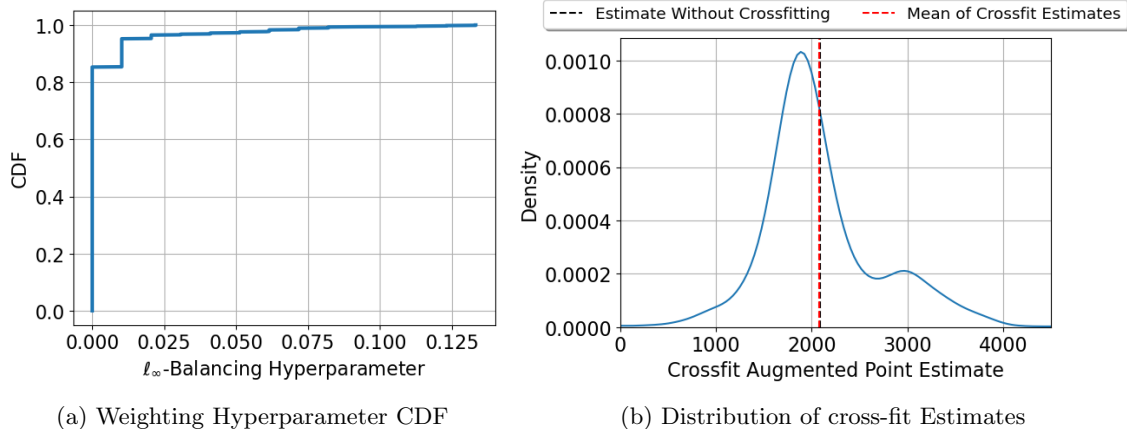


Figure I.2: Results with 5-fold cross-fitting for the LaLonde (1986) dataset with the low-dimensional set of 11 features. The cross-fitting procedure is repeated 1000 times. Panel (a) plots the empirical cumulative distribution of weighting hyperparameters over the 1000×5 weighting models; in the main text, the ℓ_∞ hyperparameter extends from 0 to 1 (here truncated at 0.12). Panel (b) shows a density plot for the cross-fit augmented point estimates over the 1000 repeats.

I.3.2 High Dimensional

We also replicate the experiments in Section 7.2.1 for high dimensional double ridge and double lasso but using the IHDP data with a high dimensional feature set. Figure I.6 replicates the reporting of point estimates and cross-validation curves for double lasso and double ridge with IHDP as in Figure 3; Figure I.7 replicates undersmoothing in double ridge as in Figure I.9; and Figure I.8 replicates undersmoothing in the ℓ_0 “norm” as in Figure I.10.

I.4 Undersmoothing in LaLonde

I.4.1 Undersmoothing for double ridge

For the special case of double ridge, we now illustrate our result from Proposition 4.3 that ℓ_2 balancing weights produce a new outcome model that is *undersmoothed* relative to the original ridge regression model. Recall that when the base learner is a generalized ridge model with parameters λ_j , then the augmented estimator is equivalent to plugging in a generalized ridge models with parameters $\gamma_j \leq \lambda_j$. In this example, the λ_j are all equal to the same value (chosen via cross-validation), indicated by the purple dotted line in Figure 3a. We compute the corresponding γ_j for δ chosen by cross-validation, indicated by the green dotted line in Figure 3b.

Figure I.9a plots the λ_j and γ_j , with j on the x -axis sorted in the order of the eigenvalues of $\Phi_p^\top \Phi_p$ from largest to smallest. Figure I.9b plots the corresponding eigenvalues. For standard ridge regression, the key idea is to push the eigenvalues of $\Phi_p^\top \Phi_p$ away from zero so that the resulting matrix $\Phi_p^\top \Phi_p + \lambda I$ is invertible and well-conditioned. Thus, the original ridge regression applies the same amount of regularization across the spectrum, as shown by the blue line in Figure I.9a. By contrast, the implied outcome model from the augmented procedure uses far less regularization and is substantially undersmoothed. Importantly, the augmented estimator undersmooths more where the eigenvalues of $\Phi_p^\top \Phi_p$ are large and undersmooths less where the eigenvalues of $\Phi_p^\top \Phi_p$ are close to zero. The augmented estimator therefore avoids bias by only regularizing the spectral directions that are the most significant sources of variation — and even these to a much smaller degree than is optimal for MSE predictions.

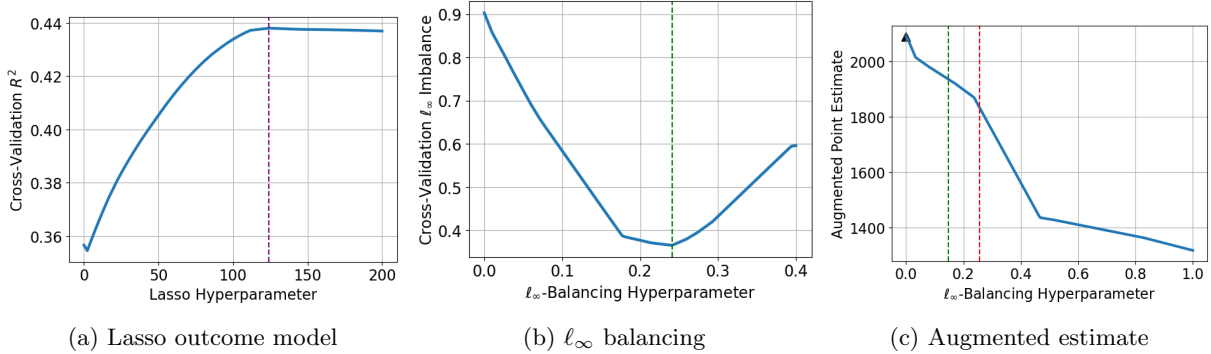


Figure I.3: Lasso-augmented ℓ_∞ balancing weights (“double lasso”) for LaLonde (1986) with the original 11 features. Panel (a) shows the 10-fold cross-validated R^2 for the Lasso-penalized regression of Y_p on Φ_p among control units across the hyperparameter λ ; the purple dotted line shows the CV-optimal value. Panel (b) shows the 10-fold cross-validated imbalance for ℓ_∞ balancing weights across the hyperparameter δ ; the green dotted line shows the CV-optimal value. Panel (c) shows the point estimate for the augmented estimator across the weighting hyperparameter δ ; the black triangle corresponds to the OLS point estimate, the green dotted line corresponds to cross-validating imbalance, the red dotted line corresponds to cross-validating the Riesz loss.

I.4.2 Undersmoothing in norm

For the special case with diagonal covariates, both double ridge and double lasso undersmooth in a particular norm of $\|\hat{\beta}_{\text{aug}}\|$, relative to the unaugmented outcome model. We demonstrate this phenomenon in Figure I.10, where we first use the eigenvectors of $\Phi_p^\top \Phi_p$ to decorrelate the features; as we discuss above, this is without loss of generality for ℓ_2 balancing but not for ℓ_∞ balancing. In particular, Figures I.10a and I.10c show the ℓ_2 norm and the number of included covariates (the ℓ_0 “norm”) for the ridge and lasso outcome regression models, respectively, as a function of the outcome hyperparameter λ . The purple dotted lines show the values of λ chosen via cross validation, and the corresponding values of the ℓ_2 and ℓ_0 norms. Figures I.10b and I.10d show the corresponding norm for the unaugmented and balancing weights estimators, “double ridge” and “double lasso,” respectively. For both, the norms for the augmented estimators are always at least as large as the norms for the outcome model alone. While the patterns are qualitatively the same, the behavior for ℓ_∞ balancing does not correspond to traditional undersmoothing, since the union of non-zero coefficients of the outcome and weighting models *cannot* generally be recovered by changing the hyperparameter of the lasso outcome model.

I.5 Semi-Synthetic Bias vs Variance

For the Lalonde long data, we use the same semi-synthetic strategy as in Appendix I, and then plot the analytical design conditional bias and variance in Figure I.11. Note that the variance dominates, and there’s an especially large non-linearity when δ is close to zero.

J Empirical Bayes Interpretation of Augmented ℓ_2 Balancing Weights

This section discusses possible Empirical Bayes interpretations of augmented ℓ_2 balancing weights. We begin with the simple case with fixed outcome model coefficients, before exploring models that incorporate the uncertainty in these coefficients. While plausible, we do not find this interpretation particularly compelling, and instead point interested readers to recent work on weighting and Bayesian double robustness, especially Murray and Feller (2024).

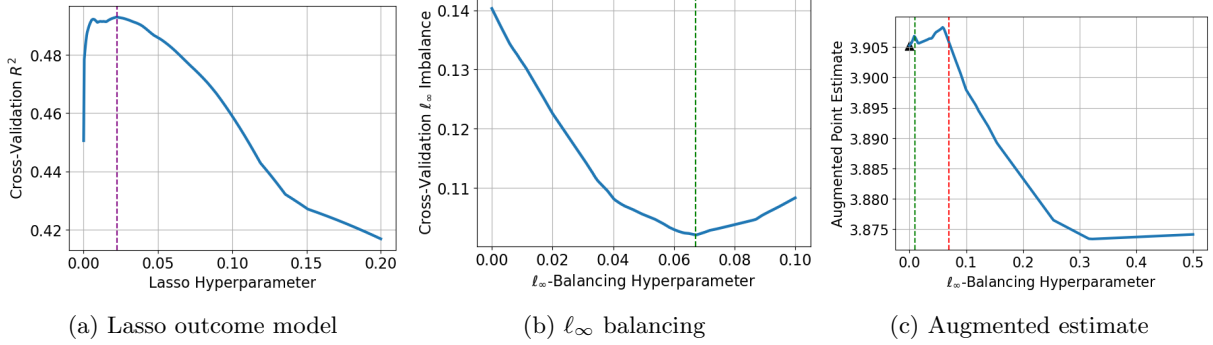


Figure I.4: Lasso-augmented ℓ_∞ balancing weights (“double lasso”) for IHDP with the original 25 covariates. Panel (a) shows the 10-fold cross-validated R^2 for the Lasso-penalized regression of Y_p on Φ_p among control units across the hyperparameter λ ; the purple dotted line shows the CV-optimal value. Panel (b) shows the 10-fold cross-validated imbalance for ℓ_∞ balancing weights across the hyperparameter δ ; the green dotted line shows the CV-optimal value. Panel (c) shows the point estimate for the augmented estimator across the weighting hyperparameter δ ; the black triangle corresponds to the OLS point estimate, the dotted green line corresponds to cross-validated imbalance, and the dotted red line corresponds to cross-validated Riesz loss.

J.1 Fixed outcome coefficients

We initially consider the straightforward special case where the outcome model coefficients $\hat{\beta}_{\text{reg}}$ are considered fixed, for example if obtained from an entirely different sample.

To fix ideas, consider a basic Bayesian linear model for a single data point i with covariates $x \in \mathbb{R}^J$ and outcome $y \in \mathbb{R}$:

$$y_i = \beta^\top x_i + \varepsilon_i, \quad \varepsilon_i \sim N(0, 1).$$

As in the main text, we assume that the covariance matrix is diagonal with entries $\sigma_1^2, \dots, \sigma_J^2$.

We briefly review the Bayesian interpretation of ridge regression as the posterior mean of β corresponding to the following prior:

$$\beta_j \mid \tau^2 \sim N(0, \tau^2),$$

with hyperparameter τ^2 . The posterior for β_j is conditionally Normal:

$$\beta_j \mid \tau^2 \sim N\left(\frac{\tau^2}{\tau^2 + \frac{1}{\sigma_j^2}} \hat{\beta}_{\text{ols},j}, \frac{1}{\frac{1}{\tau^2} + \sigma_j^2}\right)$$

where the posterior mean equals:

$$\left(\frac{\sigma_j^2}{\sigma_j^2 + \frac{1}{\tau^2}}\right) \hat{\beta}_{\text{ols},j} + \left(\frac{\frac{1}{\tau^2}}{\sigma_j^2 + \frac{1}{\tau^2}}\right) 0 = \left(\frac{\sigma_j^2}{\sigma_j^2 + \frac{1}{\tau^2}}\right) \hat{\beta}_{\text{ols},j}.$$

To recover the augmented ℓ_2 balancing weights form, we simply center the prior for β_j at the fixed $\hat{\beta}_{\text{reg},j}$:

$$\beta_j \mid \tau^2 \sim N(\hat{\beta}_{\text{reg},j}, \tau^2)$$

The posterior mean is then equal to:

$$\left(\frac{\sigma_j^2}{\sigma_j^2 + \frac{1}{\tau^2}}\right) \hat{\beta}_{\text{ols},j} + \left(\frac{\frac{1}{\tau^2}}{\sigma_j^2 + \frac{1}{\tau^2}}\right) \hat{\beta}_{\text{reg},j}$$

Setting $\tau^2 = \frac{1}{8}$ recovers the augmented ℓ_2 result from the main text.

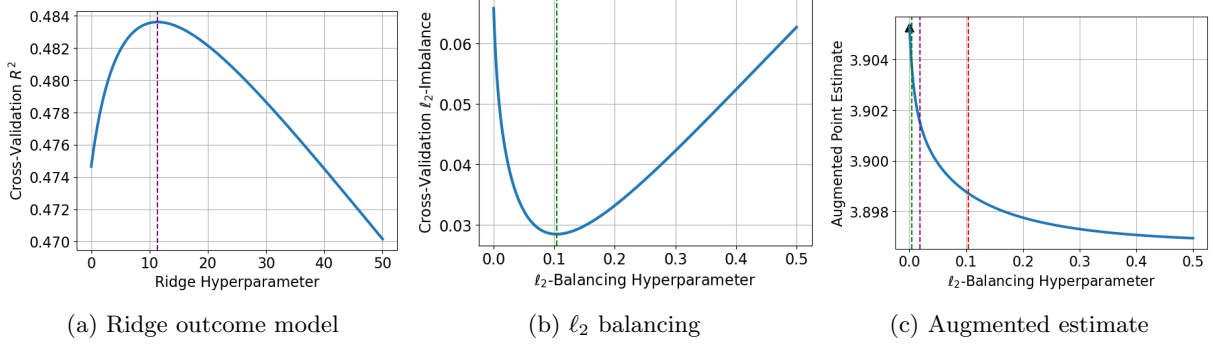


Figure I.5: Ridge-augmented ℓ_2 balancing weights (“double ridge”) for IDHP with the original 25 covariates. Panel (a) shows the 10-fold cross-validated R^2 for the Ridge-penalized regression of Y_p on Φ_p among control units across the hyperparameter λ ; the purple dotted line shows the CV-optimal value. Panel (b) shows the 10-fold cross-validated AutoDML loss (6) for ℓ_2 balancing weights across the hyperparameter δ ; the green dotted line shows the CV-optimal value, which is $\delta = 0$ or exact balance. Panel (c) shows the point estimate for the augmented estimator across the weighting hyperparameter δ ; the black triangle corresponds to the OLS point estimate, the green dotted line corresponds to cross-validated balance, the red dotted line corresponds to cross-validated Riesz loss, and the purple dotted line corresponds to the cross-validated ridge outcome hyperparameter.

J.2 Accounting for uncertainty in outcome model coefficients via global-local shrinkage priors

We now instead consider an Empirical Bayes interpretation of the “double ridge” form:

$$\left(\frac{\sigma_j^2}{\sigma_j^2 + \frac{\delta\lambda}{\sigma_j^2 + \lambda + \delta}} \right) \hat{\beta}_{ols,j}.$$

Note that we cannot simply replace $\hat{\beta}_{reg,j}$ in the derivation above with $\left(\frac{\sigma_j^2}{\sigma_j^2 + \lambda} \right) \hat{\beta}_{ols,j}$ since this ignores the uncertainty in estimating these coefficients.

J.2.1 Scale mixture of Normals

Again consider a general Bayesian linear model for a single data point i :

$$y_i = \beta^\top x_i + \varepsilon_i, \quad \varepsilon_i \sim N(0, 1)$$

with the following general class of *global-local shrinkage priors* (Polson and Scott, 2010):

$$\begin{aligned} \beta_j \mid \xi_j, \tau, \sigma_j &\sim N(0, \tau^2 \xi_j^2) \\ \xi_j &\sim p(\xi) \\ \tau &\sim p(\tau), \end{aligned}$$

where τ is called the *global* parameter, and ξ_j is called the *local* parameter. To simplify exposition, we again assume that the covariates are uncorrelated with zero mean and variances $\sigma_1^2, \dots, \sigma_j^2$ (e.g., the principal components). As above, the posterior for β_j is conditionally Normal:

$$\beta_j \mid \tau^2, \xi_j, \sigma_j \sim N \left(\frac{\tau^2 \xi_j^2}{\tau^2 \xi_j^2 + \frac{1}{\sigma_j^2}} \hat{\beta}_j, \frac{1}{\tau^2 \xi_j^2 + \sigma_j^2} \right),$$

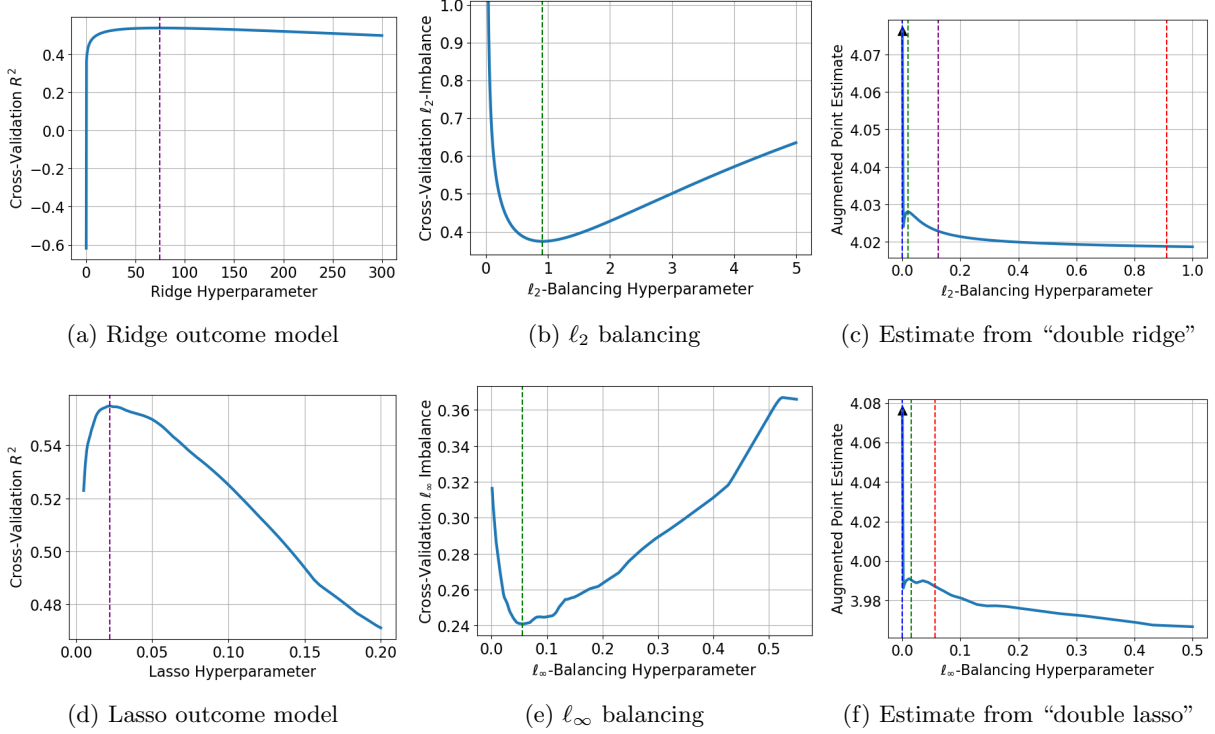


Figure I.6: Augmented balancing weights estimates for the IHDP data set with the expanded set of 193 features; the top row shows ridge-augmented ℓ_2 balancing, and the bottom row shows lasso-augmented ℓ_∞ balancing. Panels (a) and (d) show the 3-fold cross-validated R^2 for the ridge- and lasso-penalized regression of Y_p on Φ_p among control units across the hyperparameter λ ; the purple dotted lines show the CV-optimal value for each. Panel (b) and (e) show the 10-fold cross-validated AutoDML loss (6) for ℓ_2 and ℓ_∞ balancing weights across the hyperparameter δ ; the green dotted lines show the CV-optimal value for each. Panels (c) and (f) show the point estimates for the augmented estimators across the weighting hyperparameter δ ; the black triangles correspond to the OLS point estimate, and the green dotted lines show the CV-optimal value of δ for each.

where $\hat{\beta}$ is the usual OLS estimate.

Let $\tilde{\beta}_j$ be the posterior mean. We can write this in the following canonical shrinkage form:

$$\tilde{\beta}_j = (1 - \kappa_j)\hat{\beta}_j,$$

where

$$\kappa_j = \frac{1}{1 + \tau^2 \xi_j^2 \sigma_j^2}.$$

Here $\kappa_j = 0$ implies no shrinkage and $\kappa_j = 1$ implies complete shrinkage. Piironen and Vehtari (2017) show that all regression priors that are scale-mixture of Normals can be written in this form. Some prominent examples include:

- **Ridge.** Standard ridge regression sets $\xi_j^2 = 1$.
- **Horseshoe prior.** Here $\xi_j \sim C^+(0, 1)$, where C^+ denotes the half-Cauchy density (Carvalho et al., 2010).
- **Spike-and-slab priors.** When the spike is a point mass at 0, the resulting prior also has this shrinkage form.

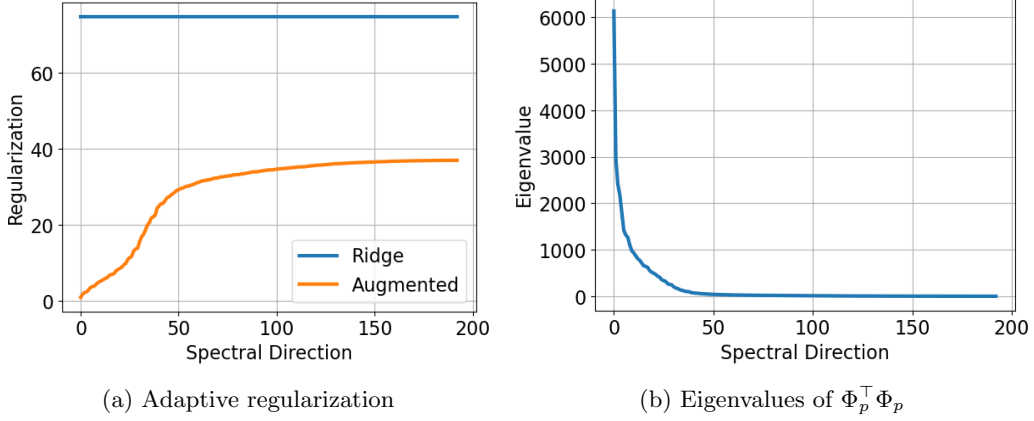


Figure I.7: Single and double ridge regression applied to the “high-dimensional” version of the IHDP data set. Panel (a) shows λ_j , the single ridge hyperparameter, and γ_j , the implied double ridge hyperparameter, as functions of the spectral direction j . Panel (b) shows the corresponding eigenvalues.

- **Zellner’s g prior.** While not a proper prior, Zellner’s g prior has the same canonical form, with $\xi_j^2 = \frac{1}{\sigma_j^2}$ in the case of a diagonal covariance matrix, with corresponding $\kappa_j = \frac{1}{1+\tau^2}$.

J.2.2 Inverse-Gamma Gamma Prior

We focus on a flexible hierarchical prior known as the *Inverse Gamma-Gamma* prior (Bai and Ghosh, 2017) or, equivalently, *Beta-prime* prior (Armagan et al., 2011):

$$\begin{aligned} \beta_j \mid \xi_j, \tau &\sim N(0, \tau^2 \xi_j^2) \\ \xi_j^2 &\sim \text{Gamma}(a, 1) \\ \frac{1}{\tau^2} &\sim \text{Gamma}(b, 1) \end{aligned}$$

This formulation guarantees that the product $\xi^2 \tau^2 \sim \text{Beta-prime}(a, b)$, also known as the inverse-Beta distribution. For $\sigma_j^2 = 1$, we then have $(1 - \kappa_j) \equiv \frac{\xi_j^2 \tau^2}{1 + \xi_j^2 \tau^2} \sim \text{Beta}(a, b)$, and by symmetry, $\kappa_j \sim \text{Beta}(b, a)$; with the expectation of $\kappa_j = \frac{b}{a+b} = \frac{1}{1+\frac{a}{b}}$. The horseshoe is a special case with $a = b = 1/2$. Incorporating σ_j^2 , the implied prior distribution for the shrinkage factor is $\kappa_j \sim \text{Beta}(b, a\sigma_j^2)$, with expectation $\frac{b}{a\sigma_j^2 + b} = \frac{1}{1 + \frac{a\sigma_j^2}{b}}$.

J.2.3 Application to double ridge

With a bit of algebra, we can write the shrinkage factor for double ridge as:

$$\kappa_j^* = \frac{1}{1 + \frac{\sigma_j^2(\sigma_j^2 + \lambda + \delta)}{\delta\lambda}}$$

This corresponds to an Inverse Gamma-Gamma prior with $a = \sigma_j^2 + \lambda + \delta$ and $b = \delta\lambda$.

$$\begin{aligned} \beta_j \mid \xi_j, \tau &\sim N(0, \tau^2 \xi_j^2) \\ \xi_j^2 \mid \delta, \lambda, \sigma_j^2 &\sim \text{Gamma}(\sigma_j^2 + \lambda + \delta, 1) \\ \frac{1}{\tau^2} \mid \delta, \lambda &\sim \text{Gamma}(\delta\lambda, 1), \end{aligned}$$

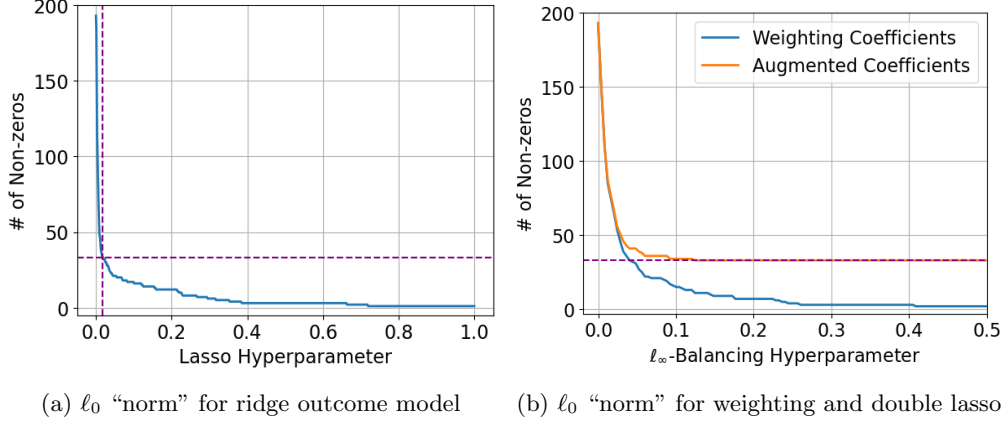


Figure I.8: Undersmoothing in ℓ_0 “norm” for augmented balancing weights applied to the “high dimensional” version of the IHDP data set. Panels (a) shows the number of non-zero covariates (the ℓ_0 “norm”) for lasso regression of Y_p on Φ_p among control units. Panels (b) shows the number of non-zero covariates for the weighting model and augmented coefficients. The dotted purple line is the outcome model hyperparameter chosen via cross validation.

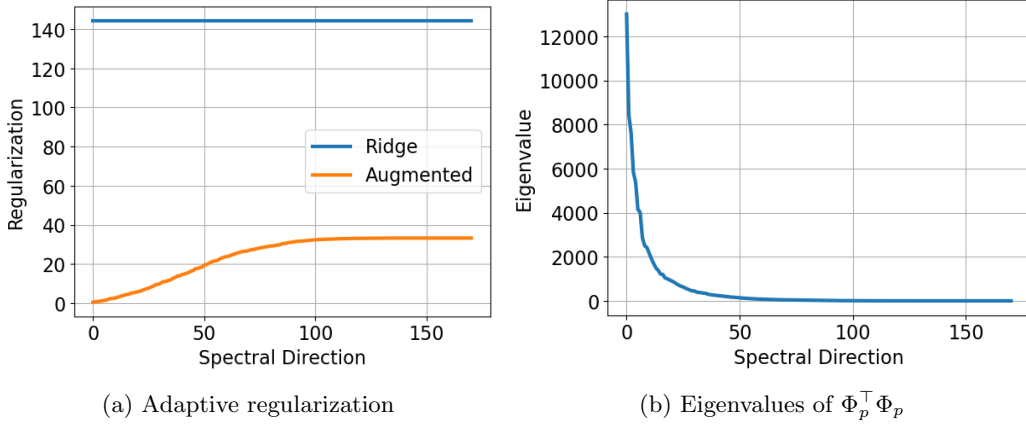


Figure I.9: Single and double ridge regression applied to the “high-dimensional” version of the [LaLonde \(1986\)](#) data set. Panel (a) shows λ_j , the single ridge hyperparameter, and γ_j , the implied double ridge hyperparameter, as functions of the spectral direction j . Panel (b) shows the corresponding eigenvalues.

where the implied prior for κ_j^* is:

$$\kappa_j^* \mid \delta, \lambda, \sigma_j^2 \sim \text{Beta}(\delta\lambda, \sigma_j^2(\sigma_j^2 + \delta + \lambda))$$

As expected, δ and λ have symmetric roles — the hyperprior distributions only depend on their product and sum. We can assess the behavior of this prior in two extreme cases. First, when $\delta \rightarrow \infty$ or $\lambda \rightarrow \infty$, the prior on κ_j^* tends to $\text{Beta}(b^*, a^*)$ with $a^* \rightarrow \infty, b^* \rightarrow \infty$. The corresponding expectation of κ_j^* tends to 1, which implies full shrinkage, $\tilde{\beta}_j = 0$. Second, when $\delta \rightarrow 0$ or $\lambda \rightarrow 0$, the prior on κ_j^* tends to $\text{Beta}(b^*, a^*)$ with $a^* \rightarrow \sigma_j^4, b^* \rightarrow 0$. The corresponding expectation of κ_j^* tends to 0, or no shrinkage, $\tilde{\beta}_j = \hat{\beta}_j$.

As Figure J.12 shows, the shrinkage depends strongly on the eigenvalue σ_j^2 and the hyperparameters δ and λ . Holding δ and λ fixed, κ_j is decreasing in σ_j^2 — i.e., there is less shrinkage for larger σ_j^2 . Holding σ_j^2 fixed,

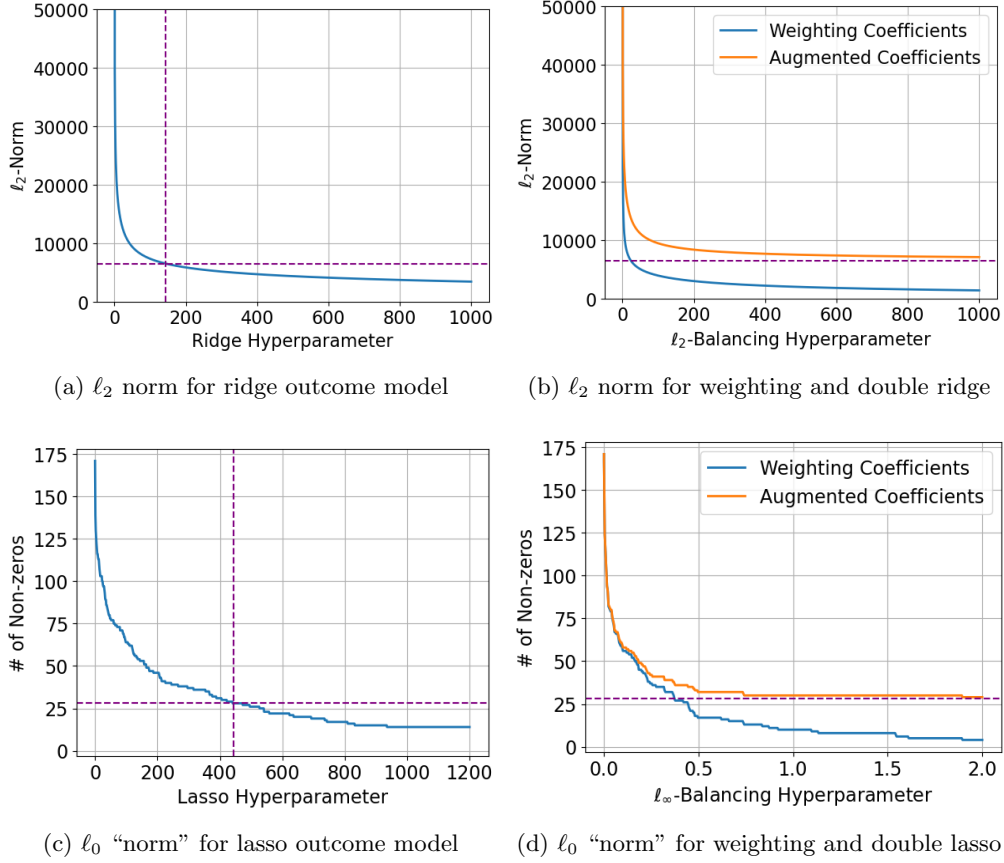


Figure I.10: Undersmoothing in norms for augmented balancing weights applied to the “high dimensional” version of the [LaLonde \(1986\)](#) data set. Panels (a) and (c) show the ℓ_2 norm and the number of non-zero covariates (the ℓ_0 “norm”) for the ridge and lasso regression, respectively, of Y_p on Φ_p among control units. Panels (b) and (d) show the ℓ_2 and number of non-zero covariates for the corresponding unaugmented and augmented balancing weights estimators. The dotted purple line is the outcome model hyperparameter chosen via cross validation. The norms for the augmented estimators are always at least as large as for the outcome model alone.

κ_j is increasing δ and λ — i.e., as the hyperparameters increase, both the outcome and weighting models move closer to uniform weights and greater shrinkage.

Connection to Student t shrinkage. If we drop the hyperprior on ξ^2 and set $\xi_j^2 = 1$, this reduces to:

$$\beta_j \mid \tau \sim N(0, \tau^2)$$

$$\frac{1}{\tau^2} \sim \text{Gamma}(\delta\lambda, 1)$$

This yields a student t posterior for β_j .

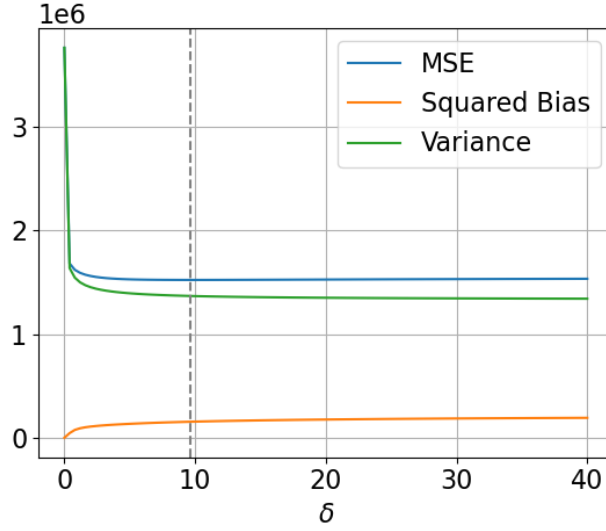


Figure I.11: ...

Connection to Normal-Gamma prior. If we instead drop the hyperprior on τ^2 and set $\tau^2 = 1$, this reduces to:

$$\begin{aligned}\beta_j | \xi_j, \tau &\sim N(0, \xi_j^2) \\ \xi_j^2 &\sim \text{Gamma}(\sigma_j^2 + \lambda + \delta, 1)\end{aligned}$$

which is a Normal-Gamma prior, where the hyperparameter depends on σ_j^2 . Here the prior mean for ξ_j^2 is simply $\sigma_j^2 + \delta + \lambda$, which is increasing in ξ_j^2 .

J.3 Connection to Zellner's g prior

Finally, we can connect this approach to generalization of Zellner's g prior known as *adaptive powered correlation prior* (Krishna et al., 2009), which has the form:

$$\beta_j | g \sim N\left(0, \frac{1}{g}(X'X)^\nu\right)$$

with additional hyperparameter ν . Zellner's g prior corresponds to $\nu = -1$, and standard ridge regression corresponds to $\nu = 0$. We are interested in the "inverted g prior" with $\nu = +1$. Since we focus on diagonal covariance, we can re-write the prior as:

$$\beta_j | g \sim N\left(0, \frac{1}{g}\sigma_j^{2\nu}\right)$$

Then the posterior mean is:

$$\begin{aligned}\tilde{\beta} &= \left(\frac{\frac{1}{g\sigma_j^{2\nu}}}{\frac{1}{g\sigma_j^{2\nu}} + \frac{1}{\sigma_j^2}}\right) \hat{\beta}_j \\ &= \left(\frac{\sigma_j^{(2\nu+2)}}{\sigma_j^{(2\nu+2)} + g}\right) \hat{\beta}_j\end{aligned}$$

Special cases include:

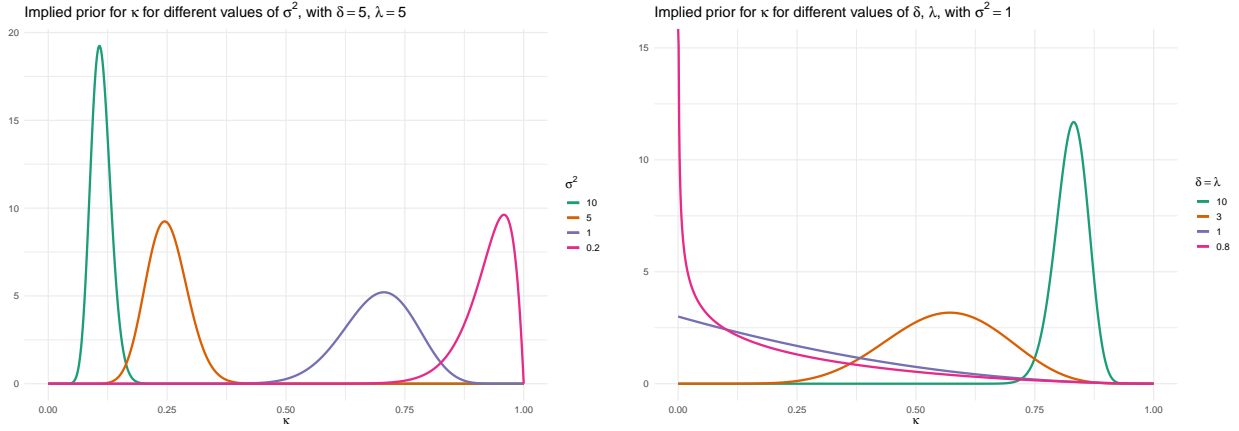


Figure J.12: Implied prior on κ for: (left) varying σ_j^2 , with $\delta = 5$, $\lambda = 5$; (right) varying $\delta = \lambda$, with $\sigma_j^2 = 1$.

- **Zellner's g prior:** ($\nu = -1$)

$$\tilde{\beta} = \left(\frac{1}{1 + g} \right) \hat{\beta}_j$$

- **Ridge regression:** ($\nu = 0$)

$$\tilde{\beta} = \left(\frac{\sigma_j^2}{\sigma_j^2 + g} \right) \hat{\beta}_j$$

- **Inverted g prior:** ($\nu = +1$)

$$\tilde{\beta} = \left(\frac{\sigma_j^4}{\sigma_j^4 + g} \right) \hat{\beta}_j$$

We can view the double ridge as a regularized form of this inverted g prior, with $\nu = +1$ and $g = \delta\lambda$.

K Additional Proofs

Closed forms for ℓ_2 and exact balancing weights. We derive the closed form for ℓ_2 balancing weights with parameter δ (with exact balance following as a special case). The optimization problem:

$$\min_{w \in \mathbb{R}^n} \|w^\top \Phi_p - \bar{\Phi}_q\|_2^2 + \delta \|w\|_2^2 = w^\top \Phi_p \Phi_p^\top w - 2w^\top \Phi_p \bar{\Phi}_q + \delta w^\top w$$

has first order condition:

$$2(\Phi_p \Phi_p^\top + \delta I_n)w - 2\Phi_p \bar{\Phi}_q = 0,$$

which gives the solution:

$$\begin{aligned} w^* &= (\Phi_p \Phi_p^\top + \delta I_n)^\dagger \Phi_p \bar{\Phi}_q \\ &= \Phi_p (\Phi_p^\top \Phi_p + \delta I_d)^\dagger \bar{\Phi}_q. \end{aligned}$$

□

Proof of Proposition 4.1. We apply Proposition 3.2. We have $a_j^\delta = \hat{\Phi}_{q,j}^\delta / \bar{\Phi}_{q,j}^\delta$. Then:

$$\hat{\Phi}_q^\delta = \hat{w}_{\ell_2}^\delta \Phi_p = \bar{\Phi}_q (\Phi_p^\top \Phi_p + \delta I)^{-1} \Phi_p^\top \Phi_p.$$

Since we have assumed that $\Phi_p^\top \Phi_p$ is diagonal, with j th diagonal entry, σ_j^2 , we have:

$$\hat{\Phi}_{q,j}^\delta = \left(\frac{\sigma_j^2}{\sigma_j^2 + \delta} \right) \bar{\Phi}_{q,j}.$$

Plugging this back into a_j^δ completes the proof.

□

Proof of Proposition 4.3. Applying Proposition Proposition 4.1:

$$\begin{aligned}
\hat{\beta}_{\ell_2,j} &= \left(\frac{\sigma_j^2}{\sigma_j^2 + \delta} \right) \hat{\beta}_{\text{ols},j} + \left(\frac{\delta}{\sigma_j^2 + \delta} \right) \hat{\beta}_{\text{ridge},j}^\lambda \\
&= \left(\frac{\sigma_j^2}{\sigma_j^2 + \delta} \right) \hat{\beta}_{\text{ols},j} + \left(\frac{\delta}{\sigma_j^2 + \delta} \right) \left(\frac{\sigma_j^2}{\sigma_j^2 + \lambda} \right) \hat{\beta}_{\text{ols},j} \\
&= \frac{\sigma_j^2(\sigma_j^2 + \lambda + \delta)}{(\sigma_j^2 + \delta)(\sigma_j^2 + \lambda)} \hat{\beta}_{\text{ols},j}
\end{aligned}$$

Then taking:

$$\frac{\sigma_j^2(\sigma_j^2 + \lambda + \delta)}{(\sigma_j^2 + \delta)(\sigma_j^2 + \lambda)} = \frac{\sigma_j^2}{\sigma_j^2 + \gamma_j}$$

and solving for γ_j gives:

$$\gamma_j := \frac{\delta\lambda}{\sigma_j^2 + \lambda + \delta}$$

which completes the proof. \square

Proof of Proposition 5.1. We begin with the constrained form of the balancing problem:

$$\begin{aligned}
&\min_{w \in \mathbb{R}^n} \|w\|_2^2 \\
&\text{such that } \|w\Phi_p - \bar{\Phi}_q\|_\infty \leq \delta.
\end{aligned}$$

Note that we can rewrite the norm constraint as two vector-valued linear constraints:

$$\begin{aligned}
w\Phi_p &\preceq \bar{\Phi}_q + \delta \\
-w\Phi_p &\preceq -\bar{\Phi}_q + \delta,
\end{aligned}$$

which results in the Lagrangian,

$$\mathcal{L}(w, \mu, \nu) = \|w\|_2^2 + \mu^\top (w\Phi_p - \bar{\Phi}_q - \delta) - \nu^\top (w\Phi_p - \bar{\Phi}_q + \delta).$$

The first-order conditions for the optimal w^*, μ^*, ν^* are:

$$\begin{aligned}
w^* &= -\frac{1}{2} (\Phi_p \mu^* - \Phi_p \nu^*) \\
\mu_j^* (w^* \Phi_{p,j} - \bar{\Phi}_{q,j} - \delta) &= 0, \forall j \\
\nu_j^* (w^* \Phi_{p,j} - \bar{\Phi}_{q,j} + \delta) &= 0, \forall j \\
\mu_j^*, \nu_j^* &\geq 0, \forall j
\end{aligned}$$

plus the linear constraints on $w^* \Phi_p$. Note that the linear constraints plus the complimentary slackness conditions imply that one of three mutually-exclusive cases holds for each covariate. Case 1: $w^* \Phi_{p,j} = \bar{\Phi}_{q,j} - \delta$, in which case $\mu_j^* = 0$. Case 2: $w^* \Phi_{p,j} = \bar{\Phi}_{q,j} + \delta$, in which case $\nu_j^* = 0$. Or Case 3: $w^* \Phi_{p,j} \in (\bar{\Phi}_{q,j} - \delta, \bar{\Phi}_{q,j} + \delta)$, in which case $\mu_j^* = \nu_j^* = 0$.

Define:

$$\theta_j^* := \begin{cases} 0 & \text{if } w^* \Phi_{p,j} \in (\bar{\Phi}_{q,j} - \delta, \bar{\Phi}_{q,j} + \delta) \\ -\mu_j^*/2 & \text{if } w^* \Phi_{p,j} = \bar{\Phi}_{q,j} + \delta \\ \nu_j^*/2 & \text{if } w^* \Phi_{p,j} = \bar{\Phi}_{q,j} - \delta. \end{cases}$$

Then we have $w^* = \Phi_p \theta^*$ from the first-order condition, and thus $w^* \Phi_p = (\Phi_p^\top \Phi_p) \theta^*$. Using the fact that $(\Phi_p^\top \Phi_p)$ is diagonal, we get $w^* \Phi_{p,j} = \sigma_j^2 \theta_j^*$.

Finally, we can plug this into the three cases that define θ^* . First, $\theta_j^* = 0$ when

$$\begin{aligned} \sigma_j^2 \theta_j^* &\in (\bar{\Phi}_q - \delta, \bar{\Phi}_q + \delta) \\ \implies 0 &\in (\bar{\Phi}_q - \delta, \bar{\Phi}_q + \delta) \\ \implies \bar{\Phi}_q &\in (-\delta, \delta). \end{aligned}$$

Second, $\theta_j^* = -\mu_j^*/2$ when $\sigma_j^2 \theta_j^* = \bar{\Phi}_{q,j} + \delta$, which implies $\mu_j^* = -2(\bar{\Phi}_{q,j} + \delta)/\sigma_j^2$. We then apply the dual variable constraint:

$$\begin{aligned} \mu_j^* &\geq 0 \\ \implies -2(\bar{\Phi}_{q,j} + \delta)/\sigma_j^2 &\geq 0 \\ \implies \bar{\Phi}_{q,j} &\leq -\delta. \end{aligned}$$

Third, $\theta_j^* = \nu_j^*/2$ when $\sigma_j^2 \theta_j^* = \bar{\Phi}_{q,j} - \delta$, which implies $\nu_j^* = 2(\bar{\Phi}_{q,j} - \delta)/\sigma_j^2$. We then apply the dual variable constraint:

$$\begin{aligned} \nu_j^* &\geq 0 \\ \implies 2(\bar{\Phi}_{q,j} - \delta)/\sigma_j^2 &\geq 0 \\ \implies \bar{\Phi}_{q,j} &\geq \delta. \end{aligned}$$

Putting the cases together we get:

$$\theta_j^* := \begin{cases} 0 & \text{if } \bar{\Phi}_q \in (-\delta, \delta) \\ (\bar{\Phi}_{q,j} + \delta)/\sigma_j^2 & \text{if } \bar{\Phi}_{q,j} \leq -\delta. \\ (\bar{\Phi}_{q,j} - \delta)/\sigma_j^2 & \text{if } \bar{\Phi}_{q,j} \geq \delta. \end{cases}$$

This is exactly the soft-thresholding operator, which completes the proof. \square

Proof of Proposition 5.2. To obtain this result from the general form of $a_j^\delta = \widehat{\Delta}_j/\Delta_j$ in Proposition 3.2, notice that the implied feature shift, $\widehat{\Delta}_j = \widehat{\Phi}_{q,j}^\delta - \bar{\Phi}_{p,j} = \mathcal{T}_\delta(\bar{\Phi}_{q,j} - \bar{\Phi}_{p,j})$ is:

$$\widehat{\Delta}_j = \begin{cases} 0 & \text{if } |\Delta_j| < \delta \\ \Delta_j - \delta & \text{if } \Delta_j > \delta \\ \Delta_j + \delta & \text{if } \Delta_j < -\delta \end{cases}.$$

Thus, for instance, $\frac{\widehat{\Delta}_j}{\Delta_j} = \frac{\Delta_j - \delta}{\Delta_j} = 1 - \frac{\delta}{\Delta_j}$ when $\Delta_j > \delta$. \square

Proof of Proposition 5.3. The result follows immediately from Proposition 5.2. \square

Proof of Proposition L.1. Rewriting the definition of γ_n with $\lambda_n = \delta_n$, we have

$$\gamma_n = \frac{\lambda_n^2}{\sigma^2 + 2\lambda_n^2} = \frac{1}{\sigma^2 \lambda_n^{-2} + 2\lambda_n^{-1}}.$$

Because $\sigma^2 x^2 + 2x = O(x^2)$ as a function of x , and because λ_n^{-1} is monotonically increasing, $\sigma^2 \lambda_n^{-2} + 2\lambda_n^{-1} = O(\lambda_n^{-2})$. And $\lambda_n^{-2} = O(\sigma^2 \lambda_n^{-2} + 2\lambda_n^{-1})$ because $\sigma^2 \geq 0$ and $\lambda_n^{-1} > 0$. Thus $\sigma^2 \lambda_n^{-2} + 2\lambda_n^{-1} \asymp \lambda_n^{-2}$.

Finally, note that for any two functions of n , f_n and g_n ,

$$f_n \asymp g_n \iff f_n^{-1} \asymp g_n^{-1},$$

and therefore,

$$\gamma_n \asymp \lambda_n^2.$$

□

L Additional Details for Asymptotic Results

Our setup for the RKHS follows [Singh \(2021\)](#). First, assume that the space $\mathcal{X} \times \mathcal{Z}$ is Polish. Let \mathcal{H} be an RKHS on $\mathcal{X} \times \mathcal{Z}$ with corresponding kernel k satisfying standard regularity conditions ([Singh, 2021](#), Assumption 5.2) and let η_j, φ_j denote the eigenvalues and eigenfunctions respectively of its kernel integral operator under p . Next, assume that the eigenvalues satisfy the decay condition $\eta_j \leq Cj^{-b}$ for some $b > 1$ and a constant C . The parameter b encodes information on the effective dimension of \mathcal{H} . For a bounded kernel, $b > 1$ ([Fischer and Steinwart, 2020](#)): the case where $b = \infty$ corresponds to a finite-dimensional RKHS; for the case with $1 < b < \infty$, the η_j must decay at a polynomial rate.

We then assume that for some $c \in [1, 2]$, the outcome function $m(x, z)$ belongs to the set:

$$\mathcal{H}^c := \left\{ f = \sum_{j=1}^{\infty} a_j \varphi_j : \sum_{j=1}^{\infty} \frac{a_j^2}{\eta_j^c} < \infty \right\} \subset \mathcal{H}, \quad (28)$$

where c encodes additional *smoothness* of the conditional expectation. If $c = 1$, then by the spectral decomposition of the RKHS, Equation (28) is equivalent to requiring $m \in \mathcal{H}$; choosing larger values of c corresponds to m being a smoother element of \mathcal{H} , with a “saturation effect” kicking in for $c > 2$ ([Bauer et al., 2007](#)). Varying b (the effective dimension of the RKHS) and c (the additional smoothness of the outcome function) changes the optimal rates for regression, with larger values of both corresponding to faster rates of convergence.

Finally, we assume that the Riesz representer, $\alpha(x, z)$, of our linear functional estimand also belongs to \mathcal{H}^c . Under these conditions, [Singh \(2021\)](#) demonstrates that an augmented estimator combining kernel balancing weights and a kernel ridge regression base learner is root- n consistent and asymptotically normal.

Following [Caponnetto and De Vito \(2007\)](#), Theorems 5.1 and 5.2 of [Singh \(2021\)](#) use hyperparameter schedules for λ and δ , which depend on the effective dimension b and smoothness c :

$$\lambda_n = \delta_n = \begin{cases} n^{-1/2} & \text{if } b = \infty \\ n^{-\frac{b}{bc+1}} & \text{if } b \in (1, \infty), \quad c \in (1, 2] \\ (n/\log(n))^{-b/(b+1)} & \text{if } b \in (1, \infty), \quad c = 1 \end{cases}$$

We can compute the implied augmented hyperparameter sequence γ_n using the following proposition.

Proposition L.1. *Let $\lambda_n > 0$ be any monotonically decreasing function of n and let $\delta_n = \lambda_n$. Then:*

$$\gamma_n := \frac{\lambda_n \delta_n}{\sigma^2 + \lambda_n + \delta_n} \asymp \lambda_n^2.$$

The standard ridge regression case corresponds to the finite-dimensional setting with $b = \infty$. When $c > 1$, the optimal rate for λ_n is $n^{-\frac{b}{bc+1}}$; the implied hyperparameter is then order $n^{-2b/bc+1} \in (n^{-2}, n^{-2/3})$ for $c \in (1, 2]$ and $b \in (1, \infty)$. Whether or not this smooths more than n^{-1} therefore depends on the relationship between the effective dimension b and the smoothness c . In particular, the implied hyperparameter goes to zero at a slower rate than n^{-1} whenever $c \geq 2 - \frac{1}{b}$. It is unclear whether the rates we find here are the only undersmoothed rates that will yield efficiency for fixed b and c ; we leave a thorough investigation to future work.